NTNU – Trondheim
Norwegian University of
Science and Technology

Production Allocation of Oil and Gas: A case Study of the Skarv Field

Simen Sæten

Petroleum Geoscience and Engineering
Submission date: June 2015
Supervisor: Curtis Hays Whitson, IPT

Norwegian University of Science and Technology
Department of Petroleum Engineering and Applied Geophysics

Abstract

Oil and gas production will typically involve wellstreams from numerous sources being brought and processed at a common facility. Allocation of hydrocarbons has an important part in the petroleum industry, and it can be defined as the procedure of assigning the portions of the commingled stream to the contributing wells. This is done by using all the measurement equipment available at the field, which might include pressure-gauges, multiphase meters, test separators, and fiscal meters. The operating conditions at which the measurements were obtained will be different for every instrument, depending on the location of that instrument. This thesis will investigate how the allocation procedure is currently done at Skarv (offshore field operated by BP), and propose an alternative allocation procedure.

Implementing a proper solution for the allocation system can be difficult, as it requires a vast amount of information to be connected and manipulated. One of the most important things to consider is how the measurements are brought from the local line-conditions to standard conditions, as this is a vital part in determining what the surface rates actually are. At Skarv, the individual well rates are periodically measured with subsea multiphase meters, and these rates are converted to standard conditions by using simplified black-oil models on a volumetric basis. One of the challenges found by using this current method is that the calculated total oil rates out of the facility are systematically underestimated, compared to the measured oil rates into storage.

The proposed alternative allocation is an automatic procedure created in Pipe-It and is based on compositional streams. The main advantage by using compositional streams instead of the simplified black-oil models, it that the compositions can be sent through any defined topside process. This allows us to do sensitivities of the process train and

investigate its influence on surface rates. It was found in this thesis that using a detailed surface process, which includes scrubbers and recycling of the gas, would increase the calculated condensate rate by over 70% compared with using black-oil models. Doing the allocation using compositions will also allow us to investigate the effect of commingling. This effect was also found to be significant, and could result in a difference up to 6% in the calculated total oil out of the facility compared to processing the streams individually.

Sammendrag

Allokering av hydrokarboner kan bli ansett som en metode for å fordele strømningsraten fra et prosesseringsanlegg til de induviduelle brønnene. Dette gjøres ved å bruke de forskjellige måleintrumentene som er tilgjengelig på feltet, inkludert trykk-målere, flerfasemålere, test separatorer og fiskale metere. Trykk- og temperaturbetingelsene vil være forskjellige for alle de ulike instrumentene, avhengig av hvor instrumentet er plassert. Det er derfor nødvendig å konvertere ratemålingene fra de lokale betingelsene til standardbetingelser, hvor de så kan bli sammenlignet med hverandre. Denne oppgaven vil undersøke hvordan allokeringsprosedyren er gjort ved Skarv (offshore felt operert av BP), og videre foreslå en alternativ allokeringsprosedyre.

De individuelle brønnratene ved Skarv blir periodisk målt ved hjelp av subsea flerfasemålere, og disse ratene vil så bli konvertert til standardbetingelser ved å bruke black-oil modeller. En av utfordringene ved å bruke denne metoden er at de beregnede totale oljeratene blir systematisk underestimert i forhold til de oljeratene som faktisk blir målt ut fra anlegget.

Den alternative allokeringenprosedyren er laget i et program kalt Pipe-It og er basert på komposisjonsstrømmer. Den største fordele ved å bruke komposisjoner i stedet for de forenklede black-oil modellene er at komposisjonene kan bli sendt gjennom en hvilken som helst definert prosess. Dette gir oss muligheten til å undersøke hvilken innflytelse denne prosessen har på de kalkulerte oljeratene ved standardbetingelser. En av prosessene som var undersøkt i denne studien inkluderete alle de ulike separasjonsutstyrene, i tillegg til resirkulering av gass. Ved å bruke denne detaljerte prosessen økte de beregnede kondensatratene med over 70% i forhold til verdiene fra black-oil modellene. Et annet resultat fra denne studien er at effekten av "commingling" har også en betydelig inflytelse på de kalkulerte ratene. Denne effekten kan resultere i en forskjell på over 8% i de beregnede

oljeratene ut fra prosessanlegget i forhold til å prosessere strømmene individuelt.

Acknowledgments

I would like to express gratitude and appreciation to my supervisor Professor Curtis H. Whitson for his guidance throughout this work. His experience and engagement have been essential. I am also very grateful for all the help from Arnaud Hoffmann, who have acted as a co-supervisor and helped me implementing the alternative allocation system in Pipe-It.

This project was done in cooperation with the BP team, and could not have been completed without their help. I would especially like to thank Tim Griffin and Carole Ross for their assistance and support. Kareem Basha has also been of tremendous help and has showed me how the allocation system at BP is currently operated. I am of course grateful for everyone that have been of help, including Hugh Rees, Siagian David, and Ove Helge Soma.

I also wish to acknowledge all the support from friends and family. Thank you.

Trondheim, June 2015

Simen Sæten

Contents

List of Figures

Page

List of Tables

Chapter 1

Introduction

The development of a hydrocarbon field often requires a fairly complicated infrastructure, where multiple wells are scattered across a large reservoir area. The streams from the individual wells will most likely be blended together at some common point (ie. manifolds), before being sent to a production facility (such as platforms, oil terminals, onshore gas plants). The gathering-system design will be different for every field, but the commingling from individual streams to a collected stream apply for nearly all cases.

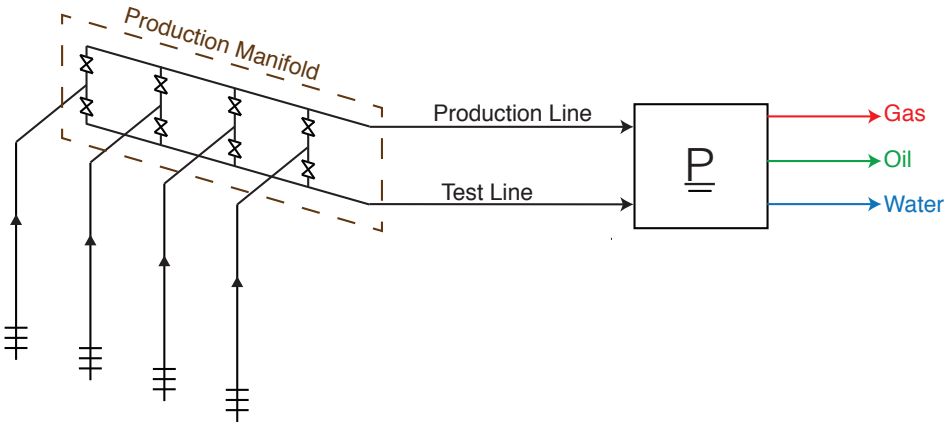

Figure 1.1: A sketch where production from multiple sources are gathered at the manifold, and transported as a commingled flow. The symbol P represent the topside process facility.

Allocation is the process for determining the individual well rates (contributing sources) that are feeding the process facility, by using the different measurement-equipments available. These measurement-equipments can for example include downhole-gauges, gauges upstream and downstream of the production chokes, multiphase flow meters (MPFM), test separators, fiscal meters. They will all be placed at different locations along the

gathering-system, and they will operate at different line-conditions depending on where in the system they are located. They will also measure a variety of different streams where; meters downstream of the process facility are measuring the commingled flow, and meters upstream of the facility will typically measure the individual flow rates. The fiscal meters, MPFM and test separators will normally measure the rates on a volumetric basis. However, if pressure-gauges are used in the allocation system, then the measured pressures need to be converted to rates by using theoretical models.

The principle of allocation might seem straightforward, but it is often considerably more complicated to implement a proper solution in practice. For example, the reservoir might be very heterogeneous with big variations in both reservoir and fluid properties. Each individual well will therefore behave very differently, with different well deliverability and fluid quality. It is also not uncommon for a single FPSO or platform to produce from several reservoirs. At every point where the streams are blended together, the fluid properties of the commingled fluid will change from the contributing sources. By the time the produced flows have gone through separation at the topside facility, the export products will be very different from what were found at the individual wellstreams.

There are three major steps to the allocation process, where the first step is to collect all the relevant measurements. The second step is to connect all of these measurements together, and bring them to a common set of conditions (typically standard conditions; 1 atm, 15°C). This is done by doing PVT (pressure/volume/temperature) calculations, which either uses black-oil (BO) tables or equation of state (EOS) method. After the measurements have been brought to a common set of conditions, then they can be compared against each other, and the different well rates can be distributed amongst the contributing wells/sources. This comparison and distribution of individual well rates is the third step of the allocation process, and is also sometimes referred to as reconciliation or back-allocation. It should be noted that allocation and hydrocarbon accounting are sometimes used interchangeably. However, hydrocarbon accounting has a wider scope, and will for example also involve the process of determining ownership of the produced hydrocarbons (if the field has multiple owners). This thesis will only focus on the process of determining the production rates of the individual wells.

1.1 Purpose of Allocation

There are different reasons why allocation is important, but it is first and foremost useful to get a clear understanding of how the field is performing. It will give an indication of how the wells behave, and how much oil and gas they are able to deliver.

Allocation will also help assist the reservoir management team, and can have an impact on future strategic planning. This is because the estimated quantities that are obtained from the allocation process are usually the most reliable production-estimates there are for the contributing wells. As a result, these quantities will typically be used as the production history, which will in turn be used for; history matching, well-testing calculations, estimation of reservoir pressure, depletion and reserves. Estimation of the remaining reserves in the reservoir (or in the different reservoir sections) is especially important because this will help determining the asset value of the field. Because the allocation is important to the reservoir management, it is also important that those involved in the allocation process are working closely together with the reservoir team.

Aside from this, most field equity partners often require reports of daily production-estimates (ie. volumes of produced fluids, export oil and gas, fuel and flare gas). In addition, regulations are likely to require a final account of the production, but they will generally allow for more time to generate these reports (often monthly basis).

1.2 Objectives

How can we use all the different measurement-equipments available at a specific field, to estimate the production from the individual wells in a fair and accurate manner? This thesis will go through the standard procedure that are involved in the allocation process, and discuss different factors that are important to consider. A big part of this discussion is on how to bring the measurements from line-conditions to a set of reference conditions. This conversion is important is because it has a significant impact on the calculated surface rates, and therefore also on overall results from the allocation process.

Another part of this thesis is to undergo a case-study of the Skarv field (which is operated by BP), and the allocation system that is implemented there. Skarv is a relative young field located in the Norwegian Sea and started production at the end of 2012. It is produced with a floating production storage and offloading (FPSO), together with subsea-templates located at the seabed. The individual streams are periodically measured with subsea multiphase meters which are placed at the different templates. This thesis will go through the allocation method that is currently used at Skarv, and discuss some of the challenges faced. The current allocation system at Skarv is done with a volumetric basis, where the surface rates are calculated with black-oil models.

Lastly, the Skarv field was also used as a basis for creating an alternative allocation system based on compositional streams and EOS calculations. This allocation system was made in Pipe-It, which is a program that was released by Petrostreamz AS in 2011, and is a useful tool for managing complex oil and gas streams. One of the motivations for creating an alternative allocation based on compositional streams is to investigate if this will have an effect on the final allocation results. Also, by doing the allocation on a componential balance it will be possible to do sensitivity of the process train, and see what influence this has on the surface rates. Allocation on a compositional basis can also account for the changing behavior of the fluid properties, and the effect of commingling.

Chapter 2

Theoretical Framework

2.1 Fundamental Aspects of Allocation

2.1.1 Typical Facilities and Interfaces

It is important to distinguish between the different types of production facilities because they have an impact on how the production system is set up. A production system (or gathering network) is referred to as the system that transport reservoir fluid to the surface, and it will consist of wells, flowlines, production manifold, separators, metering instruments, and storage tanks.

In the north sea, it is most common with offshore production facilities, which will typically imply a platform or an FPSO. At the offshore facility, the fluids that are produced will be separated into gas, oil and water phase. The oil and gas products will then generally be transported to an onshore terminal. Accurate measurements of the export products are usually available. It is more difficult to get precise measurements of the individual sources which feed the separation process. Therefore, obtaining accurate allocation of production is a common problem in offshore operation.

The characteristics of an onshore production facility are similar to the ones found offshore. It is, however, easier to obtain more accurate measurements because installation of equipment does not experience the same space or cost restrictions. The production from both offshore and onshore platforms are often further processed at an onshore liq-

uid terminal or onshore gas plant. Further processing might be required due to the sales specifications the products need to meet. At these plants, the import streams should be single phase fluids, and accurate measurements of the streams are likely to be available.

This thesis is based on the Skarv field, which is an offshore field that is produced together with an FPSO and subsea-templates. A sketch that illustrates this system is shown in **Fig. 2.1**. The streams from the individual wells will first be grouped together at the different subsea-templates. Some or all of the individual streams will then be blended together, before being transported by the shared riser to the FPSO. At the FPSO, streams from the multiple templates will be commingled, and brought through the processing facility. The commingled fluids that enter the facility will eventually be separated into different the end-products such as oil, gas, and water.

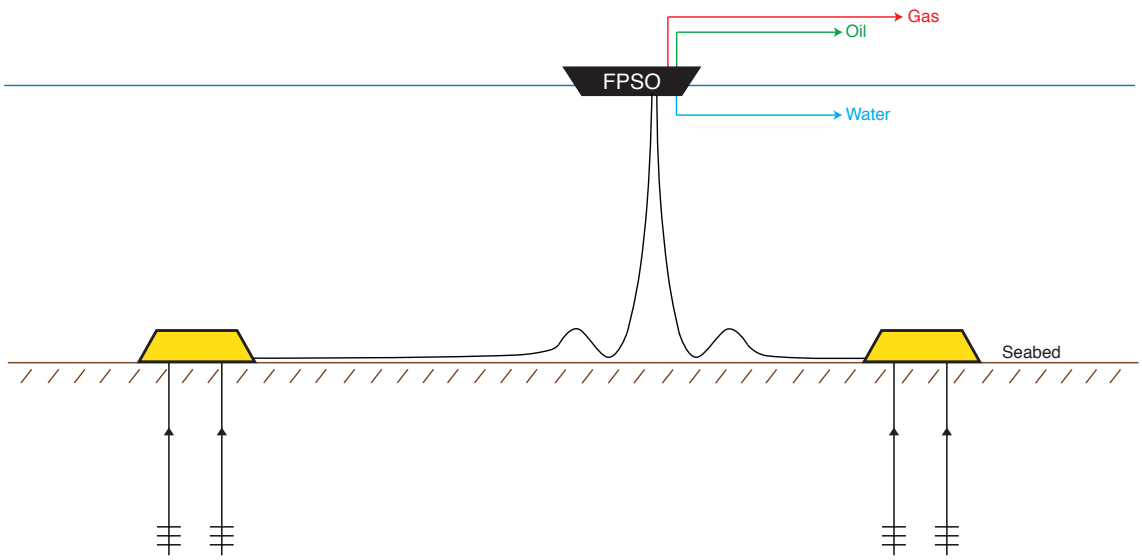

Figure 2.1: Sketch of a gathering design with subsea templates and a floating production storage and offloading (FPSO).

2.1.2 Overall Material Balance for a Production System

By looking at the system as a whole, then according to the material balance the total amount of moles or mass into the system should be the same as the total amount of moles or mass out of the system. This is when assuming that there is no leakage or accumulation, which means that production of the field needs to be in a steady state.

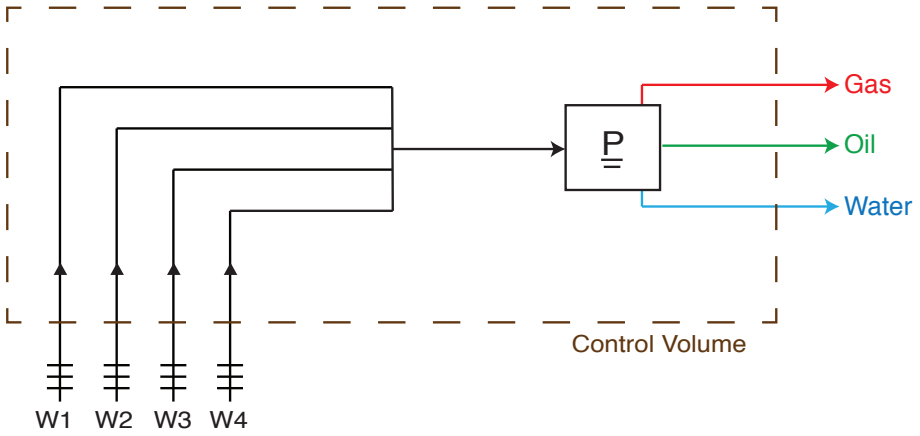

Figure 2.2: Illustration of overall material balance in the production system.

Fig. 2.2 shows an illustration where the production system is confined inside a control volume. The material balance is generally expressed in term of mass or moles, but can also indirectly be expressed in term of volume

$$\sum_{stream} \dot{n}_{upstream,\ total} = \sum_{stream} \dot{n}_{export,\ total} \quad (2.1)$$

$$\sum_{stream} \dot{m}_{upstream,\ total} = \sum_{stream} \dot{m}_{export,\ total} \quad (2.2)$$

$$\sum_{stream} (\dot{v}\rho)_{upstream,\ total} = \sum_{stream} (\dot{v}\rho)_{export,\ total} \quad (2.3)$$

where $\dot{m}$ is the mass flux, $\dot{n}$ is the molar flux, $\dot{v}$ is the volume flux, and ρ is the density. **Eqs. 2.1 through 2.3** can however not be used to keep track of the different phases, meaning that the molar rate of oil into the system will not be the same as the molar rate of oil out of facility. This is because the oil stream is not conserved throughout the system, as the composition of the oil will constantly change depending on the surrounding conditions (pressure, temperature). The reservoir fluid will, in general, prefer to stay in liquid state if the pressure is high. When the pressure is reduced as the fluid moves up to

the surface, then most of the components in the stream will prefer to stay as vapor. This means that if we were to consider the oil or gas streams into and out of the system, then we would need to account for the mass-transfer between the phases.

If we assume that there are no chemical reactions (change in the structure) of the different components (C1, C2, C3 etc.), then Eqs. 2.1 and 2.2 will also hold true on a componential basis. The equations can then be written as

$$\sum_{stream} \dot{n}_{upstream,i} = \sum_{stream} \dot{n}_{export,i} \quad (2.4)$$

$$\sum_{stream} \dot{m}_{upstream,i} = \sum_{stream} \dot{m}_{export,i} \quad (2.5)$$

Where the subscript i indicate the different components. This means that for example the total amount of methane produced from the reservoir is equal to the amount of methane out of the facility. **Eqs. 2.4 and 2.5** also suggest that the molar rate and the mass rate are additive properties. This means that for example the molar rate of the commingled stream that is feeding the process facility will simply be the sum of the streams of the individual wells.

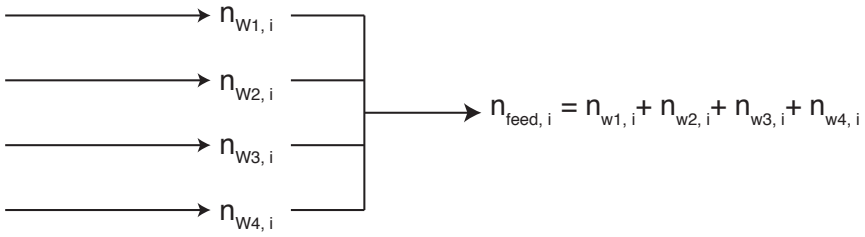

Figure 2.3: Conservation of compositional streams. Mass rate $\dot{m}_i$ and molar rate $\dot{n}$ are additive, and independent of pressure and temperature.

2.1.3 Topside Process and Calculation of Surface Rates

The fluid compositions that are produced from the different wells will be different from each other, and they will also change as the field is produced (time dependent). The commingled composition that is feeding the process $\underline{\underline{P}}$ will be a blend of all the individual wells, and will therefore also be a function of the rates from each of the wells. This implies that the composition of the commingled fluid will be very dynamic because the individual well rates are constantly changing. At the process facility, the commingled stream will go through a series of equilibrium separator (and scrubber) stages, which will split the

commingled stream into liquid and vapor phases. **Fig. 2.4** shows an illustration of how a surface process might look like. The function of these multistage separators is to gradually split the gas from the liquid, and bring the wellstream to standard condition (SC) in a way that maximize the total oil produced. Scrubbers might be used to condense liquid (remove the heavy components) out of the gas phase.

At every separator/scrubber the phases is assumed to be in equilibrium with each other, and the overall composition (z_i) will be split into an equilibrium gas composition (y_i) and an equilibrium oil composition (x_i). The equilibrium ratio (K) is typically used to describe this equilibrium condition and is defined as

$$K_i = \frac{y_i}{x_i} \qquad (2.6)$$

The K-value refers to which state the compositions prefer to be in, and it is a function of pressure, temperature, and overall composition. If $K_i > 1$ then the component favors the vapor phase, and if $K_i < 1$ then the component favors the liquid. This value is typically found by using an EOS model together with flash calculations, in addition to satisfying the equal-fugacity constraint (this will be discussed further in **Section 2.2**).

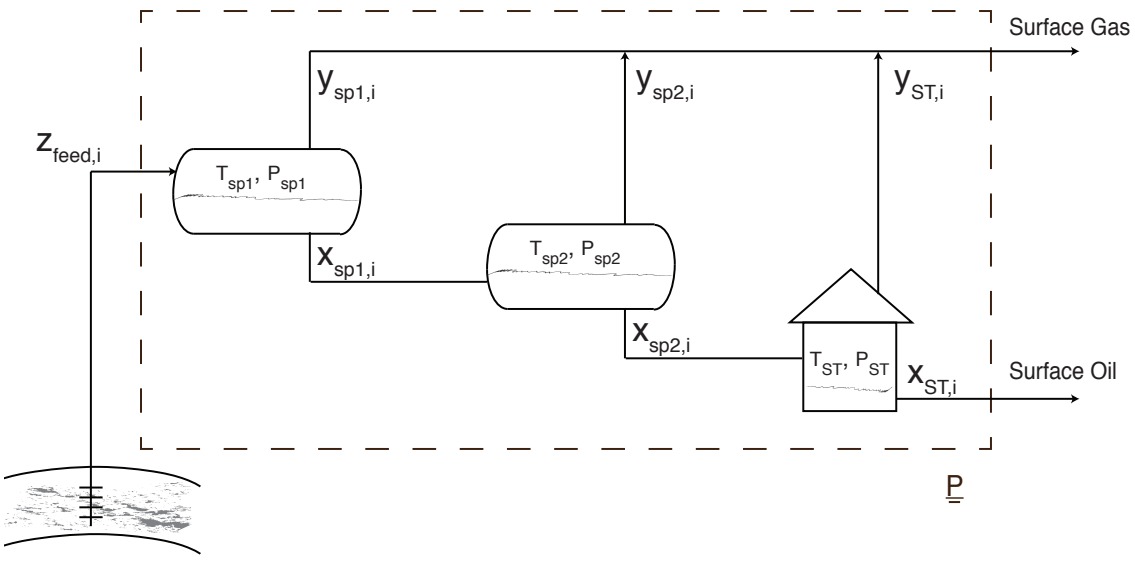

Figure 2.4: Illustration of how a surface processing facility might look like. Efficiency of the process-train depends on the rate and composition of the feed, in addition to separator conditions.

How much stock tank oil that is produced at surface conditions is dependent on; the number of separator stages and scrubbers, conditions of the different vessels, flow-rate and overall composition feeding the process. A very inefficient method for bringing the oil to standard conditions would be to have one single flash/separator, as this will leave a lot of the heavier components in the gas phase. The surface process is therefore an essential part of the allocation process because it has a significant influence on the surface rates.

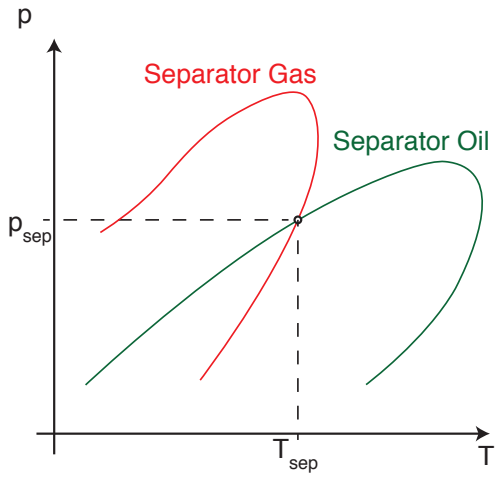

Figure 2.5: Illustration of phase-envelopes of separator gas and separator oil at equilibrium.

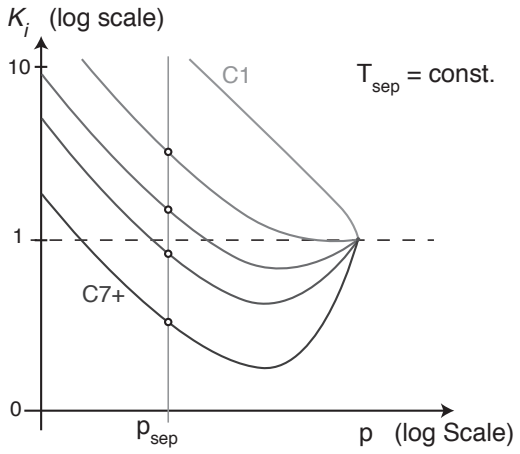

Figure 2.6: Illustration of equilibrium ratio (K) for a wellstream at separator conditions.

If the composition of the commingled stream is known, then the whole process can be simulated by using an EOS and flash calculations. This is the method that is used in most oil and gas process simulation programs (such as Aspen Hysys). Another method of predicting the behavior of the wellstream as it is brought to the surface through the processing facility is by using black-oil tables. Black-oil tables are often the preferred method because they use volumetrically units and allows us to do the whole allocation process on a volumetric basis. They are not a function of the molar rate, and do not require us to know the compositions of the streams. However, it is important to understand that a black-oil model only represents a specific fluid put through a specific surface process. This implies that we need a black-oil model for every well (if the wellstreams are significantly different from each other), and that the black-oil tables might need to be updated if the fluid properties change over time. In addition to this, the black-oil tables will not be able to capture the dynamic commingling effect of the streams, because they are not able to capture changes in fluid properties. The black-oil method will automatically assume that all the wellstreams are processed individually, which means that the stream from a single

well is brought through the facility by itself (not commingled with the other streams). How the black-oil properties is defined will be further discussed in **Section 2.2.1**.

2.1.4 Comparison of the Different Measurement Systems

As described in the previous sections, the allocation process can be done based on either a mass balance, molar balance, or volume balance. There are however some advantages and disadvantages between them, some of which are shown in given in **Table 2.1**.

Advantages

Volume balance	**Component molar balance**	**Component mass balance**
- Volume is simple and easily understood - Most meters/measurements done using volumetric flow-rates - Used for routine reporting of production and reserves	- Molar amounts are unaffected by phase change - Gas analysis are usually given in moles - Molar compositions are required to do flash calculations	- Mass of the components are not affected by phase change

Disadvantages

Volume balance	**Component molar balance**	**Component mass balance**
- Volumes are not additive, therefore are not conserved across the system because 1. change in pressures and temperatures 2. phase-change - Need accurate pressure and temperature data at all measurement points to be able to calculate the surface rates	- The compositions of the streams are seldom known - Molecular weights of non-standard components may not be known	- Direct mass-measurement is not widely used. Will therefore need to convert volume measurements to mass (which require composition, pressure and temperature data)

Table 2.1: Some of the advantages and disadvantages with different measurement systems used in the allocation process.

Doing the allocation on a volume basis (using black-oil properties) is the most common method, even though it have a number of disadvantages associated with it. One of the biggest challenges with volumes is the complexity of conserving (or even consider) the material balance constraint. Volumes are a very dynamic property, and is a function of the fluid properties, ambient conditions (pressure and temperature), and phase-change. As a result the volumes cannot simply be added together, and it is also unpractical to use on a compositional basis (as in Eqs. 2.4 and 2.5). However if the volumetric calculations are done properly, then some or all of these challenges might prove to be insignificant. Doing the calculations properly implies that the black-oil tables are truly representative of the produced streams and the process, which means that they should be updated when

1. there is a significant change in the fluid properties
2. there is a significant change in the process
3. a specified time period has passed since last update

Componential mass balance and componential molar balance is similar in the fact that they both require the compositions to be known (or assumed). It is often standard procedure to find the initial composition of a well before start of production, but besides this, well samples might be scarce. It is however possible to estimate the wellstream composition by using methods such as well-test-conversion (WTC), or black-oil to compositional (BOz). WTC is a method that allows us to convert the measured test rates to molar compositional wellstreams, and this method will be discussed in more detail in **Section 4.3**. When the composition of the wellstreams are known, then they can easily be processed through any defined $\underline{\underline{P}}$.Componential streams can consequently be used to study the effect of commingling (EOC), effect of changing the compositions (fluid properties), and do sensitivities of the process train to see the influence on surface rates. Using either mass balance and molar balance will also assure that the material balance is uphold, which again will give some confidence that the different measurements are brought to surface conditions in a fair and consistent way. Also note that it the compositional rates (either mass or moles) are known, then the volume rates can be calculated at any point in the system based on the componential properties.

2.1.5 The Allocation Process and System Imbalance

To illustrate some of the principles of allocation, lets first consider a simple made-up allocation system. This allocation system is shown in **Fig. 2.7**, and consists of a number of producing wells where each well are monitored with a multiphase meter. The flow from these wells are commingled and sent to a process facility. The product oil and gas rates out of the process facility are measured with fiscal meters.

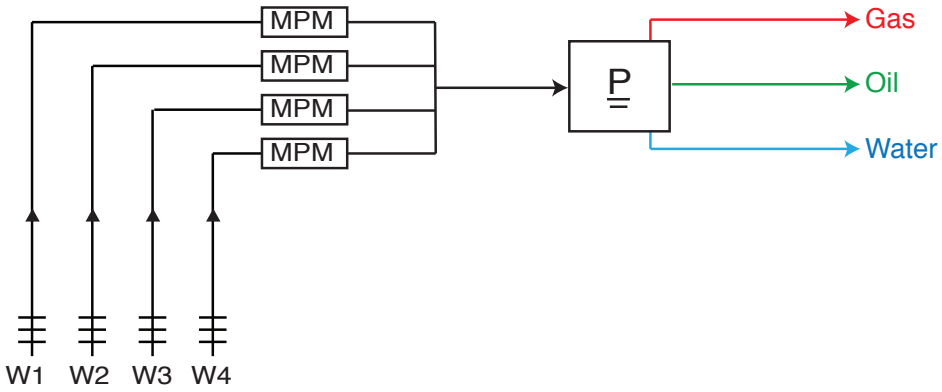

Figure 2.7: Sketch of an arbitrary allocation system with multiphase meters.

The multiphase meters are able to measure the in-situ gas and oil rates at the line-conditions, on a continuously basis. The fluid compositions that are produced from the four wells will be different from each other, and the commingled composition that is feeding the process P will be a blend of these four wells. In order to do a proper comparison of the measured rates, one need to bring all the measurements to surface conditions in a consistent way (as discussed in the previous sections).

When all the individual streams have been added together and brought to the surface, then the resulting calculated product-rates can be compared against the product-rates measured by the fiscal meters. Ideally the calculated product-rates based on the multiphase meters would be the same as the product-rates measured by the fiscal meters. However, no measurement equipments will be perfectly accurate, and the fluid model used to bring the streams from line-conditions to the surface will not be perfectly representative of the actual fluid behavior. As a consequence, there will in general be an imbalance

between a higher-accuracy meters, and the lower-accuracy meters. This system imbalance can be defined as

$$I = Q_{export} - \sum_{1}^{n} Q_{upstream} \quad . . . . . \quad (2.7)$$

where I is the system imbalance, Q_{export} is the rate measure out of facility, and $Q_{upstream}$ represents the measured rates from the individual sources (after being converted to surface conditions). Note that the rates in **Eq. 2.7** do not have to be volumetric, but can also be based on mass or molar rates. The higher-accuracy meters will in general be the fiscal meters (measuring the export products), and all other measurements will typically be compared up against these. The reason why the export meters have are higher accuracy is because the export products are more important, as they have a direct impact on the revenue of the operator(s). The export products are also single phase flow, which are easier to measure than the unprocessed, multiphase mixtures. The lower-accuracy meters are usually the ones reading the flowrate of the individual streams (for example the multiphase meters in Fig. 2.7).

The rates used in Eq. 2.7 should be measured over the same time interval/frequency. For example, if the fiscal rates are available on a daily basis, then this should be the specified time interval used (ie. STB/say or Sm^3/day). The rates can be defined as

$$Q = \int_{\Delta t \cdot (i-1)}^{\Delta t \cdot (i)} q(t)dt \quad . . . . . \quad (2.8)$$

where Δt is the time period. The parameter $q(t)$ can for example represent the continuously measured well-rates from the multiphase meters.

Figs. 2.8a and 2.8b shows example of how the system imbalance might look like, and the relative deviation between the higher-accuracy and lower-accuracy meters. The imbalance I should optimally fluctuate in a random pattern, on both sides (positive and negative) of the relative deviation curve. Fig. 2.8b shows an example of a on-going trend of under predicted surface oil rates ($\sum_1^n Q_{upstream}$), and this type of systematic error does not reflect the random uncertainty of the meters.

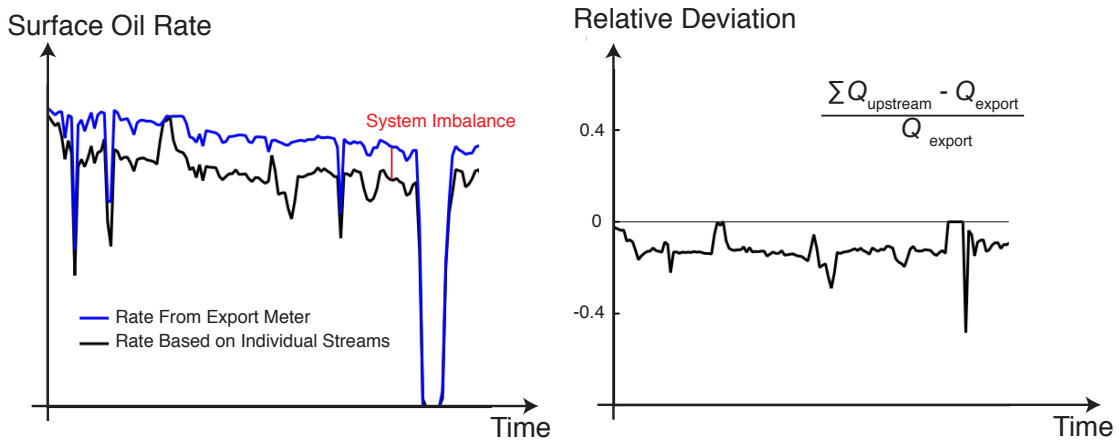

(a) System imbalance for surface oil rates.

(b) Relative deviation and systematic error.

Figure 2.8: Illustration of system imbalance between higher-accuracy and lower-accuracy meters.

There are different methods that can be used to distribute the system imbalance amongst the individual wellstreams. The most common method is to use proportional-based allocation factors, and this is the method that is currently used for the Skarv field. Another method is called uncertainty-based allocation factors, which can be applied if the uncertainties of the different measurement equipments are known.

Proportional-Based Allocation Factors

When all the measurements are at common conditions, then the new allocated production rates can be found as

$$Q_i^{allocated} = Q_{total} \cdot \left(\frac{Q_i^{calculated}}{\sum_{j=1}^{N} Q_j^{calculated}} \right) \quad (2.9)$$

where $Q_i^{allocated}$ is the allocated or adjusted rate for well i, Q_{total} is the measured total production rate (ie. with fiscal meter), $Q_i^{calculated}$ is the measured or calculated rate for the individual well i. The values for Q may be in any units (volume, mass, moles), but is usually in volume rates. The equation can also be written as

$$Q_i^{allocated} = Q_i^{calculated} \cdot \alpha_i \quad (2.10)$$

where α_i is the allocation factor or the reconciliation factor. If we are looking at the oil rates, then this factor describes the difference in the total export oil (ie. measured with

fiscal meters), and the sum of the individual oil rated for the wells ($Q_i^{calculated}$).

Two underlying assumptions with this method is that the fiscal meter is perfectly accurate, and that there is an equal uncertainty among the lower-accuracy meters (for the individual wells). If the reconciliation factor for a period is significantly different from one, then this will indicate that at least one of the predicted well-rates ($Q_i^{calculated}$) deviates from the true value. This deviation will then be evenly distributed between all of the individual wells during the allocation process. This evenly distribution might be a disadvantages, especially if there is a wide variation between the accuracies of the individual meters (which is for example often the case with subsea measurements).

Uncertainty-Based Allocation Factor

This method incorporates the random uncertainties of each meter, in addition to the relative throughput (amount of material flowing through). The system imbalance will therefore be assigned to those meters that are most likely to have caused the difference. For example, if a specific meter has a large throughput in addition to a high uncertainty (above the average), then this meter will be assigned the largest portion of the imbalance.

The method was proposed by API recommended practice in 2003, and was developed primarily for allocation systems using subsea flowmeters. The uncertainties in subsea multiphase meters can be high, they can vary significantly from meter to meter, and they are likely to change (creep) over time due to drift in sensor readings or changes in operating conditions and fluid properties. Implicit in this discussion is that the accuracy of the meters are known or can be quantified. The allocation factor for each stream can be defined as

$$\alpha_i = \frac{\sigma_i^2}{\sigma_z^2 + \sum_{j=1}^{N} \sigma_j^2} + \frac{Q_i}{\sum_{j=1}^{N} Q_j} \cdot \frac{\sigma_z^2}{\sigma_z^2 + \sum_{j=1}^{N} \sigma_j^2} \qquad (2.11)$$

where the σ_j^2 is the variance of the j^{th} meter, the subscript z represents the reference meter (ie. fiscal), and the allocation factors sum to one $\left(\sum_i^N \alpha_i = 1\right)$. The allocation factor is defined in a way that will minimize the error in a stochastic sense. Because this method is based on random uncertainties, it assumes that the entire imbalance is created in a random

fashion. This means that one should get rid of all non-random, systematic error before performing this type of allocation. An brief example of how to use the uncertainty-based allocation method is given in **Appendix A**.

2.1.6 Fields Using Periodic Well-Tests

Most fields do not have multiphase meters installed on every well because of economical constraints. Another allocation system is shown in **Fig. 2.9**, where the producing wells are monitored with downhole gauges. The field also has a test separator which is shared amongst all the wells, and can be used to get periodic tests for the individual wells.

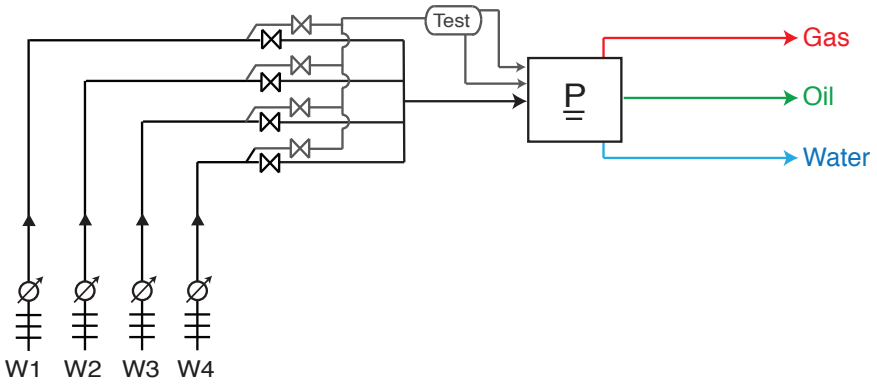

Figure 2.9: Sketch of an allocation system with test separator and bottomhole gauges.

The accuracy of a test separator will usually be higher than that for multiphase meters. This is because the test separator will physically separate the well stream into an oil phase and a gas phase, and measure these rates independently. However, because a test separator only allows for periodic tests, it will have problems capturing the dynamic behavior of the well. The rate of a well might for example change considerably in-between test, for example due to change in back-pressure at flowline, change in choke position, or unexpected shut-downs. **Fig. 2.10a** shown an illustration of how the rates measured with a test separator might look like. The number of tests and the frequency of the measurements will depend on the number of wells that is sharing the test separator.

Installation of permanent pressure gauges is increasingly common in the industry, and they can be used to get high frequency pressure measurements. These measurements can be used together with theoretical models to calculate the flow-rates. However, for the

theoretical models to be representative of the the flow-rates in the well, it is required the they are updated and corrected on a regular basis. This correction is typically done based on the periodic measurements from the test separator. How the pressure measurements can be used to estimate the rates will be discussed further in **Section 2.3**.

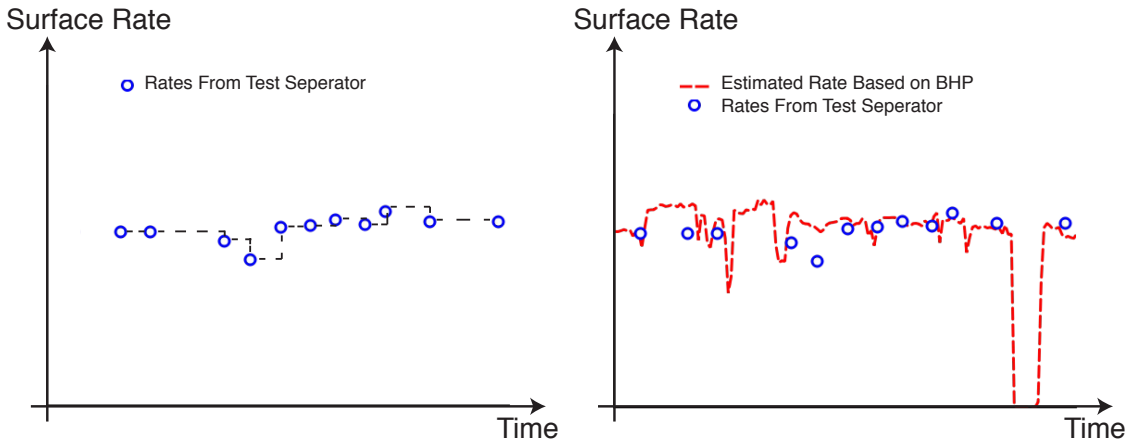

(a) Illustration of periodic well tests using a test separator.

(b) Estimated rates from pressure gauges together with test separator.

Figure 2.10: Shows the test measurements, along with rates calculated from pressure-gauges. The test measurements are plotted as points, whereas the theoretical rates have a continuous function.

Fig. 2.10b show an illustration where the bottomhole-pressures (BHP) have been used together with the test separator. It can be seen from this figure that the estimated rates from the BHP (shown with red dashed line), do not perfectly align the rates from the separator. There are different reasons for why this discrepancy might occur; for example the theoretical models are not up to date. In order to force the rates in Fig. 2.10b to match, one can define a set of correction factors (CF)

$$Q_{o,\ adjusted} = Q_{o,\ calculated} \cdot \left(\frac{Q_{o,m}}{Q_{o,\ calculated}} \right) = Q_{o,\ calculated} \cdot CF_o \quad . \quad . \quad . \tag{2.12a}$$

$$Q_{g,\ adjusted} = Q_{g,\ calculated} \cdot \left(\frac{Q_{g,m}}{Q_{g,\ calculated}} \right) = Q_{g,\ calculated} \cdot CF_g \quad . \quad . \quad . \tag{2.12b}$$

where $Q_{adjusted}$ is the corrected rate, $Q_{calculated}$ is the rate estimated based on bottomhole pressure, and Q_m is the measured pressure at the test separator. **Figs. 2.11a and 2.11b** show how the adjusted rates, and the corresponding correction factors might look like. It can be seen from Fig. 2.11b that the correction factors in-between tests are found by

assuming a constant value from the latest test. Another method that could be used to find the correction factors in-between test is with for example linear interpolation.

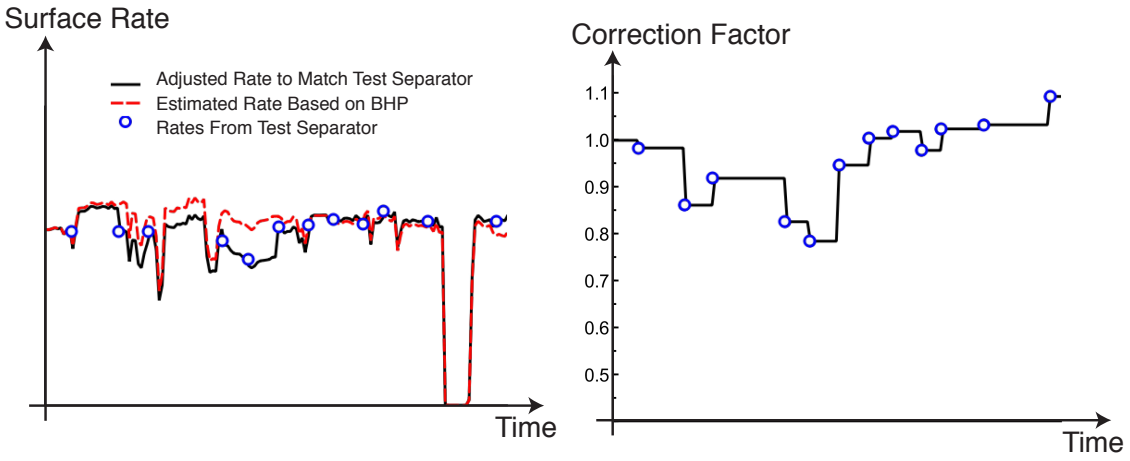

(a) Adjusting the rates based on BHP, in order to match the test separator rates.

(b) Correction factors used to adjust the rates.

Figure 2.11: Illustration of how correction factors can be used to adjust the theoretical rates, so that these rates are consistent with what is measured at the well tests.

2.2 Phase Behavior

The composition of petroleum fluids are in general a very complex, and can consist of hundreds of different hydrocarbons (in addition to non-hydrocarbons). When describing the phase behavior of these complex fluids, there are two fundamental approaches; black-oil models and compositional models. The black-oil approach uses a set of black-oil properties, whereas the compositional approach will be based a thermodynamic consistent model such as an equation of state. Both of these models are extensively used in the industry.

2.2.1 Modified Black-Oil Formulation

Black-Oil formulation is a simplified way to predict the behavior of reservoir fluids, with only using two different pseudo-components to describe the gas and the oil phases. This type of PVT formulation is often a preferred method, because it is not as complex (and computationally intensive) as accounting for all the components (ie. N_2, CO_2, C_1, C_2 ... C_{35+}). The two pseudo-components are defined as

$$\bar{g} = \text{Surface gas} \quad (2.13a)$$

$$\bar{o} = \text{Surface oil} \quad (2.13b)$$

and they are measured in volume (instead of moles). We can then use these two pseudo-components to define the quantity $V_{\bar{o}}$ and $V_{\bar{g}}$, which will refer to the volume of surface oil and surface gas respectively. The four different properties that are used in the black-oil formulation can then be written

$$R_s = \frac{V_{\bar{g}o}}{V_{\bar{o}o}} = \frac{\textit{surface gas dissolved in reservoir oil}}{\textit{stock-tank oil from reservoir oil}} \quad (2.14)$$

$$r_s = \frac{V_{\bar{o}g}}{V_{\bar{g}g}} = \frac{\textit{condensate produced from the reservoir gas}}{\textit{surface gas produced from the reservoir gas}} \quad (2.15)$$

$$B_{gd} = \frac{V_g(T,p)}{V_{\bar{g}g}} = \frac{\textit{volume of reservoir gas}}{\textit{surface gas from the reservoir gas}} \quad (2.16)$$

$$B_o = \frac{V_o(T,p)}{V_{\bar{o}o}} = \frac{\textit{volume of reservoir oil}}{\textit{stock-tank oil from the reservoir oil}} \quad (2.17)$$

Where **Eqs. 2.14 and 2.15** are the surface volume ratios (solution GOR, and solution OGR respectively), and **Eqs. 2.16 and 2.17** are the Formation-Volume-Factors (FVF). The second letter in the subscript is used to clarify where the surface fluid originates from (ie. $\bar{o}g$ indicate surface oil from reservoir gas). The solution OGR is a relatively new term which represents the liquid carrying capacity of the reservoir gas. The reciprocal of the oil FVF is also commonly known as the shrinkage factor*, and is denoted by b_o. As the oil moves from the reservoir to the surface, the gas will evaporate out of the solution due to pressure reduction, and this will result in a shrinkage of the oil volume. In a similar way, the reciprocal of the gas FVF is also known as the gas expansion factor.

Furthermore, it is important to understand that the surface gas ($\bar{g}$) and surface oil ($\bar{o}$) are found as a result of a specific surface process ($\underline{\underline{P}}$). This implies that if the underlying process is changed, then the surface properties would also be somewhat altered. The dependence of these black-oil properties on the process, will again vary with what type of reservoir fluid we have. In general, the dependency is stronger for fluids with high GOR.

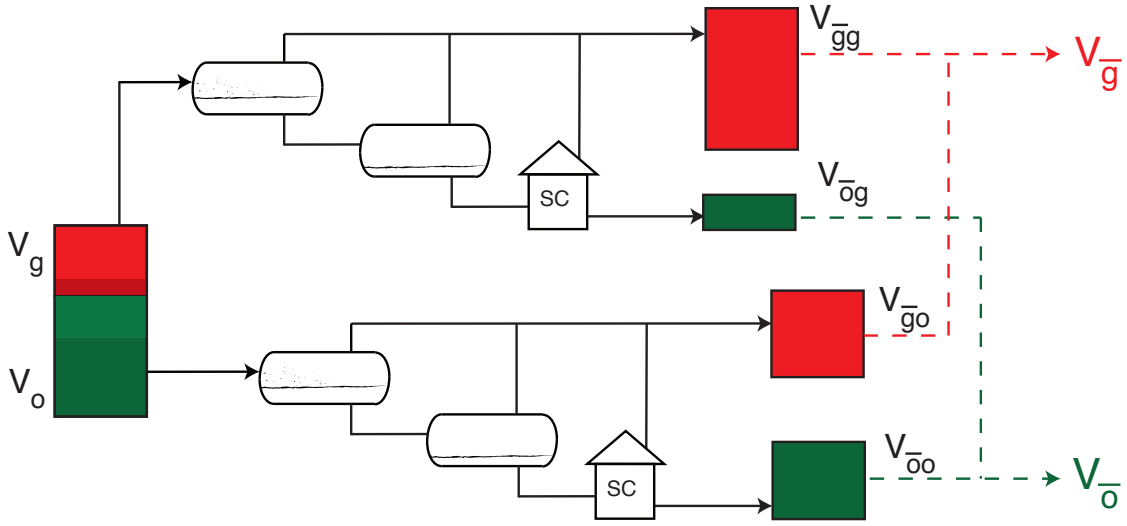

Figure 2.12: Sketch of a surface process, and surface properties. Adapted from

It should be noted that in Eqs. 2.14 through 2.17, the reservoir has been used as a

*The term "shrinkage factor" can be regarded as a misrepresentative term, because it does not represent the actual shrinkage. The actual shrinkage of a oil can be found as $SF = 100\% \cdot (1 - b_o)$

reference/starting-point. This do not always have to be the case, and it would for example be possible to use the wellhead, multiphase meter, test separator, or any other arbitrary point as a reference. Furthermore, the black-oil model do not differentiate between the properties of $V_{\bar{o}g}$ (condensate from gas phase) and $V_{\bar{o}o}$ (surface oil from reservoir oil). This means that for example the density of the surface oil from the oil phase ($\rho_{\bar{o}o}$) is assumed to be the same the density of condensate oil ($\rho_{\bar{o}g}$). In a similar way, the black-oil model do not differentiate between the properties of $V_{\bar{g}o}$ (surface gas from the reservoir oil) and $V_{\bar{o}o}$ (produced reservoir gas).

The black-oil properties are typically found today based on PVT-programs that use EOS models, which are tuned to match experimental data (from ie. Constant-Volume-Depletion tests). **Fig. 2.13** shows some illustrations of how the different black-oil properties depends on the pressure. The p_{bi} refers to the initial bubblepoint pressure, whereas p_{di} refers to the initial dewpoint pressure.

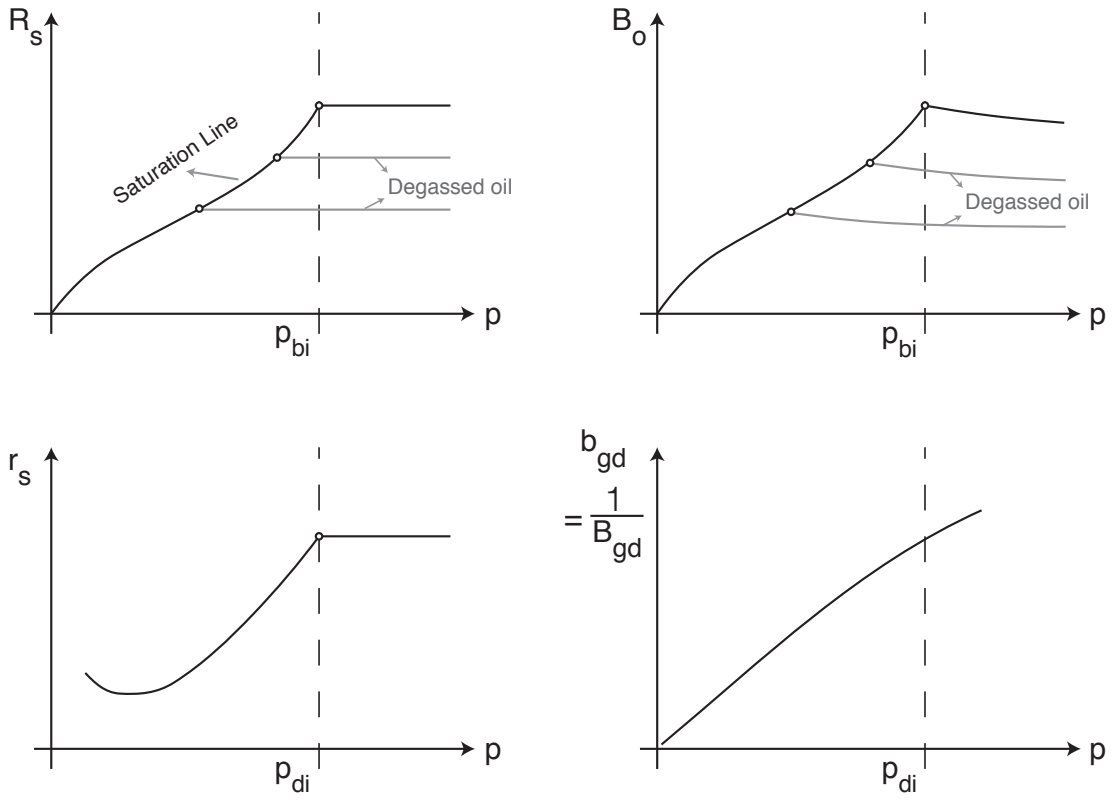

Figure 2.13: The dependency of black-oil properties on pressure. The behavior of the oil is typically very different when the oil is undersaturated, and when it is saturated (pressure below bubblepoint). Adapted from

2.2.2 Cubic Equations-of-State

An equations of state is a method that tries to describe how a fluid will thermodynamically behave, given a certain composition of a fluid. Some EOSs are phase dependent, and should only be applied to a specific phase (vapor or liquid). Examples of phase specific EOSs are the ideal gas law which should only be used for gases, or the Costald EOS which should only be used for liquids. Another group of EOS are termed cubic equations, which tries to describe the behavior of any phase. A cubic EOS can therefore be used to describe both gases and liquids, in addition to fluids near critical conditions (where the phases coexist).

The first proposed cubic EOS was by Van der Waals in 1873. This equation is a modification of the ideal gas law, and includes correction parameters for the attraction and repulsive forces between the molecules in the fluid. Most of the equations that have been developed since, are derived based on this equation from Van der Waals. The two most widespread and commonly used EOS in the petroleum industry are the Soave-Redlich-Kwong (SRK) and the Peng-Robinson (PR). This section will further discuss the PR, as this is the EOS that is used in the Skrav field. It should however be noted that the computation of both SRK and PR are similar, and for most simulations, either of these methods are adequate. The PR is a two-constant equation, and is defined as

$$p = \frac{RT}{v-b} - \frac{a(T)}{v(v+b)+b(v-b)} \qquad (2.18)$$

where R is the universal gas constant, v is molar volume, T is temperature, p it pressure. The two constants a and b can be found using the component properties of the fluid, together with **Eqs. 2.19 through 2.22**

$$a = \Omega_a \frac{R^2 T_c^2}{p_c} \cdot \alpha \; ; \qquad \text{where } \Omega_a = 0.45724 \qquad (2.19)$$

$$b = \Omega_b \frac{RT_c}{p_c} \; ; \qquad \text{where } \Omega_b = 0.07780 \qquad (2.20)$$

$$\alpha = \left[1 + m\left(1 - \sqrt{T_r}\right)\right]^2 \qquad (2.21)$$

where T_c is the critical temperature, p_c are the critical pressure. There are two different equations for finding the m-coefficient. Peng and Robinson initially proposed an equation (Eq. 2.22a below) in 1976, and later proposed a modified version (Eq. 2.22b) which is better suited for heavier components ($\omega > 0.49$)

$$m = 0.37464 + 1.54226\,\omega - 0.26992\,\omega^2 \quad . . . . . \quad (2.22a)$$

$$m = 0.3796 + 1.485\,\omega - 0.1644\,\omega^2 + 0.01667\,\omega^3 \quad . . . . . \quad (2.22b)$$

where ω is the acentric factor. The PR equation can also be written in terms of the compressibility factor ($Z = pv/RT$), in which case it will become a cubic expressing

$$Z^3 - (1-B)\cdot Z^2 + (A - 3B^2 - 2B)\cdot Z - (AB - B^2 - B^3) = 0 \quad . . . . \quad (2.23)$$

$$A = a \cdot \frac{p}{(RT)^2} = \Omega_a \cdot \frac{p_r}{T_r^2} \cdot \alpha \quad . . . . . \quad (2.24)$$

$$B = b \cdot \frac{p}{RT} = \Omega_b \cdot \frac{p_r}{T_r} \quad . . . . . \quad (2.25)$$

where $T_r = T/T_c$ is the reduced temperature, and $p_r = p/p_c$ is the reduced pressure. **Eq. 2.23** can be solved both analytically, or by using trial-and-error approach. If we are dealing with a pure component fluid, then we can use the component properties of this single component directly into the equations above. It is however more likely that we are dealing with a mixture of multiple components, in which case we would need to use average values for the properties. The average values for the A and B constants (for a vapor phase) should be found as

$$A = \sum_{i=1}^{N}\sum_{j=1}^{N} y_i y_j \sqrt{A_i A_j}\cdot(1-k_{ij}) \quad . . . . . \quad (2.26)$$

$$B = \sum_{i=1}^{N} y_i B_i \quad . . . . . \quad (2.27)$$

where i and j represents the individual components, N is the total number of components, z is the mole fraction, k is the binary-interaction parameters (BIPs). The BIPs can be though of as a set of correction numbers, which is often used to tune the EOS to fit experimental data. These values will have a significant effect on the predicted K-values when the pressure is high (above 50 bar).

One of the most important thermodynamic property that the EOS are able to predict, is the fugacity (f). This is because the fugacities of the components are used together with flash calculations to generate the K-values (discussed further in **Section 2.2.3**). The fugacity for pure components (vapor phase) can then be found as

$$\ln\ \phi = \ln \frac{f}{p} = Z - 1 - \ln(Z - B) - \frac{A}{2\sqrt{2}B} \ln \left[\frac{Z + \left(1 + \sqrt{2}\right) B}{Z - \left(1 - \sqrt{2}\right) B} \right] \quad . \ . \ . \quad (2.28)$$

or expressed for multicomponent systems (vapor phase)

$$\begin{aligned} \ln\ \phi_i = \ln \frac{f_i}{y_i p} &= \frac{B_i}{B}(Z - 1) - \ln(Z - B) \\ &+ \frac{A}{2\sqrt{2}B} \left(\frac{B_i}{B} - \frac{2}{A} \sum_{j=1}^{N} y_j A_{ij} \right) \ln \left[\frac{Z + \left(1 + \sqrt{2}\right) B}{Z - \left(1 - \sqrt{2}\right) B} \right] \quad . \ . \ . \quad (2.29) \end{aligned}$$

where ϕ is called the fugacity coefficient. The componential fugacities for the liquid phase are found the same way, but with replacing y_i with x_i.

Table 2.2 shows an example of how a fluid characterization with the corresponding compositional properties might look like. Critical temperature, critical pressure and acentric factor in this table are properties that are needed to solve the Eqs. 2.19 through 2.27. The molecular weight can be used to convert between moles and mass. The dimensionless volume-shift factor (s) is a correction factor that was defined by Peneloux et al. (1982) as

$$v = v^{EOS} - c \quad . \quad (2.30)$$

$$s = c/b \quad . \quad (2.31)$$

where v is the corrected molar volume, v^{EOS} is the molar volume predicted by the EOS, and c is the volume translation. The need for a shift factor is because the predicted molar volume for the liquid phase (both SRK and PR) will generally have a systematic deviation compared with experimental data. This deviation can be subtracted away by this constant, without significantly affecting the molar volumes for the vapor phase.

Components	Molecular Weight M (kg/kmol)	Critical Constants T_C (F)	P_C (psia)	Z_C	Acentric Factor ω	Volume Shift s
C_1-N_2	16.19	-118.3	664.643	0.28626	0.0112	-0.1502
CO_2	44.01	87.746	1069.51	0.27433	0.2250	0.00191
C_2	30.07	89.906	706.624	0.27924	0.0990	-0.0628
C_3C_4	49.29	241.01	586.276	0.27619	0.1688	-0.0605
C_5C_6	77.57	415.76	483.865	0.27751	0.2457	-0.0302
C_7C_{10}	117.5	578.33	390.121	0.27324	0.3430	-0.0132
$C_{11}C_{15}$	178.6	754.51	289.302	0.26121	0.5047	0.05963
$C_{16}C_{30}$	296.0	952.29	205.961	0.25845	0.7440	0.08266
C_{31+}	567.3	1218.4	133.773	0.28622	1.2031	0.08815

Table 2.2: Component properties for the Skarv Field EOS (when modeling the reservoir). The volume shift factors used when modeling the reservoir is a little different for those used when modeling the topside process.

For gas stream, where most of the components are lower than heptane (C_7), the default EOS parameters are usually sufficient for most allocation predictions. For the liquid stream, where there are significant amounts of components above heptanes, the heavy end will need to be characterized and tuned to match measured data.

Table 2.3 shows an example of how a BIPs might be defined. The binary interaction number is usually zero ($k_{ij} = 0$) for hydrocarbon-hydrocarbon pairs, and non-zero for nonhydrocarbons-hydrocarbon pairs. The table only shows the non-zero BIPs used.

Components	C_1-N_2	CO_2
CO_2	0.10401	—
C_2	-0.00012	0.13
C_3C_4	0.00052	0.1213
C_5C_6	0.00065	0.115
C_7C_{10}	0.05579	0.115
$C_{11}C_{15}$	0.08091	0.115
$C_{16}C_{30}$	0.10726	0.115
C_{31+}	0.11793	0.115

Table 2.3: Binary interaction parameters for the Skarv Field EOS model.

2.2.3 Two-Phase Flash Calculation

Lets assume that we have a stream with a known overall composition (z_i), that is produced into the first stage separator. How much of the mixture will go into the liquid phase, and what is the composition of this liquid (x_i)? How much of the mixture will go into vapor phase, and what is the corresponding composition of this vapor (y_i)?

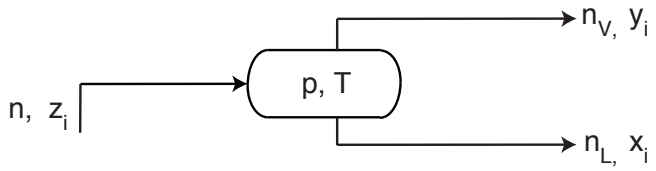

Figure 2.14: Separation of an overall z_i composition into vapor y_i and liquid x_i.

The two-phase flash calculations finds the composition of the liquid phase and vapor phase, at a given pressure, temperature, and overall composition. This is typically done by using a component material balance constraint, together with the equal fugacities constraint. The component material balance constraint can be used to derive the Rachford-Rice equation, which is given as

$$h(F_v) = \sum_{i=1}^{N} \frac{z_i(K_i - 1)}{1 + F_v(K_i - 1)} = 0 \quad \ldots\ldots\ldots\ldots\ldots\ldots \quad (2.32)$$

where F_v is the vapor mole fraction, and K_i is the equilibrium ratio. How this equation is derived is shown in **Appendix B**. If we have the feed composition, and we assume that the K_i-values are known, then this equation can be solved for the vapor mole fraction (F_v). If can have the vapor mole fraction, this can which in turn be used to find the compositions of the phases

$$x_i = \frac{z_i}{1 + F_v(K_i - 1)} \quad \ldots\ldots\ldots\ldots\ldots\ldots \quad (2.33a)$$

$$y_i = K_i x_i \quad \ldots\ldots\ldots\ldots\ldots\ldots \quad (2.33b)$$

The "assumed" (or first approximation) of the K-value can be found using the equation proposed by Wilson

$$K_i = \frac{\exp\left[5.37(1 + \omega_i)\left(1 - T_{ri}^{-1}\right)\right]}{p_{ri}} \quad \ldots\ldots\ldots\ldots\ldots\ldots \quad (2.34)$$

where $T_r = T/T_c$ is the reduced temperature, and $p_r = p/p_c$ is the reduced pressure. Given the K-values, the predicted phase compositions (x_i and y_i) from **Eq. 2.33** can then be used to find the fugacities (f_{Li} and f_{vi}) from our EOS, and check the fugacity constraint defined as

$$f_{Li} = f_{vi} \quad . . . . . (2.35)$$

$$\sum_{i=1}^{N} \left(\frac{f_{Li}}{f_{vi}} - 1 \right)^2 < \epsilon \quad . . . . . (2.36)$$

where ϵ represent an error threshold. If the initial K-values estimated by **Eq. 2.34** are not accurate enough to satisfy **Eq. 2.36**, then the K-values should to be updated. A method for updating the equilibrium ratio can be done with

$$K_i^{(n+1)} = K_i^{(n)} \frac{f_{Li}^{(n)}}{f_{vi}^{(n)}} \quad . . . . . (2.37)$$

where the superscript $(n+1)$ indicate the updated value, based on the old value (n). The procedure for finding the K-values will therefore be an iterative process, and might require some computation time. When the K-values converges, then we will end up with the final equilibrium streams for the liquid phase and vapor phase (at the separator conditions). Following the same methodology, it will be possible to simulate the whole topside process with all of its different separator stages.

2.3 Well Performance

When the reservoir fluids flows from the subsurface to the process facility, there will be an associated pressure drop along the path. If we were to regard the separator as the end-point in the production system, then the difference in the pressure between the reservoir and the separator can be expressed as

$$\begin{aligned} p_e - p_{sep} &= \Delta p^{reservoir} + \Delta p^{completion} \\ &+ \Delta p^{tubing} + \Delta p^{choke} + \Delta p^{flowline} \end{aligned} \quad \ldots\ldots\ldots\ldots\ldots\ldots \quad (2.38)$$

where the notation Δp represents the different pressure losses in the system, and p_e is the reservoir pressure at the reservoir boundary. **Fig. 2.16** shows an illustration of how a pressure for a well might look like, going from the subsurface to the separator. Note that the pressure profile will always be a continuous function along the path. In addition, the pressure at one specific component (or node) will be dependent on all the other components in the system. The bottomhole pressure (p_{wf} or BHP) will for example be dependent on the separator pressure, the choke position, the wellhead pressure, the friction loss in the tubing etc. This means that if the wellhead conditions changes, then there will be an associated change in the bottomhole conditions.

The most common way to describe how the different components (reservoir, tubing, choke etc.) in the system interact with each other, is to consider the inflow performance relationship (IPR) together with the vertical flow performance* (VFP).

*Vertical flow performance is also commonly referred to as wellbore performance, or tubing performance relationship

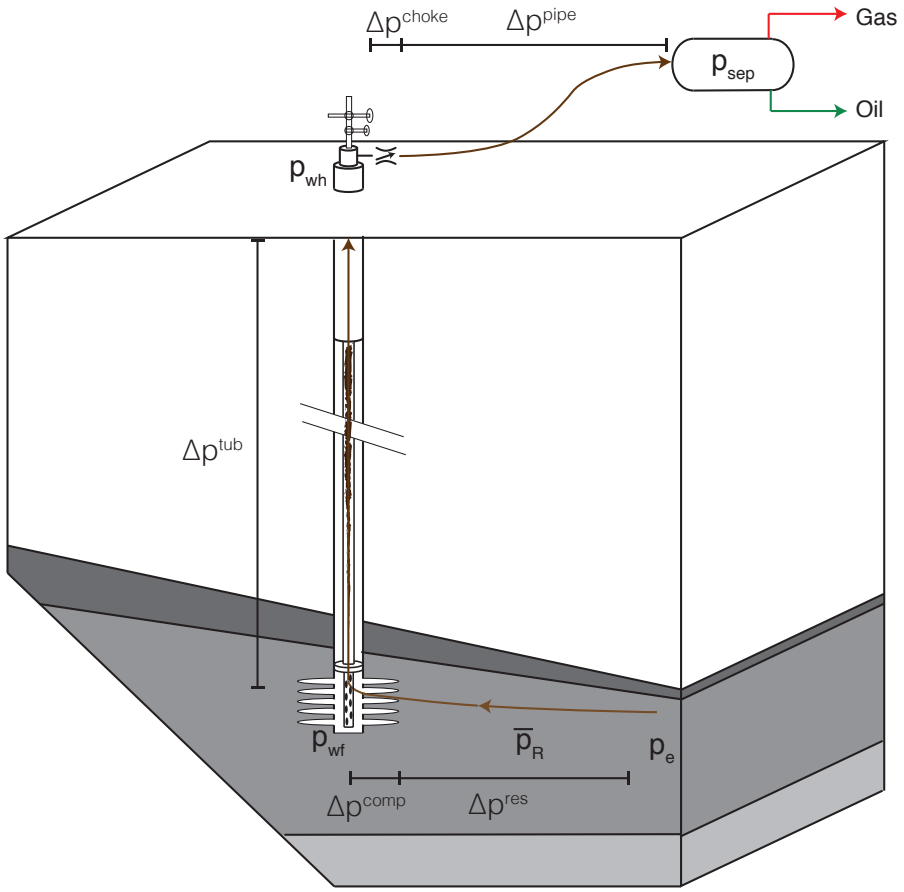

Figure 2.15: Sketch of production system (with pressure drops). Analysis the performance of a system involving a set of different interacting components are also termed nodal analysis. Adapted from

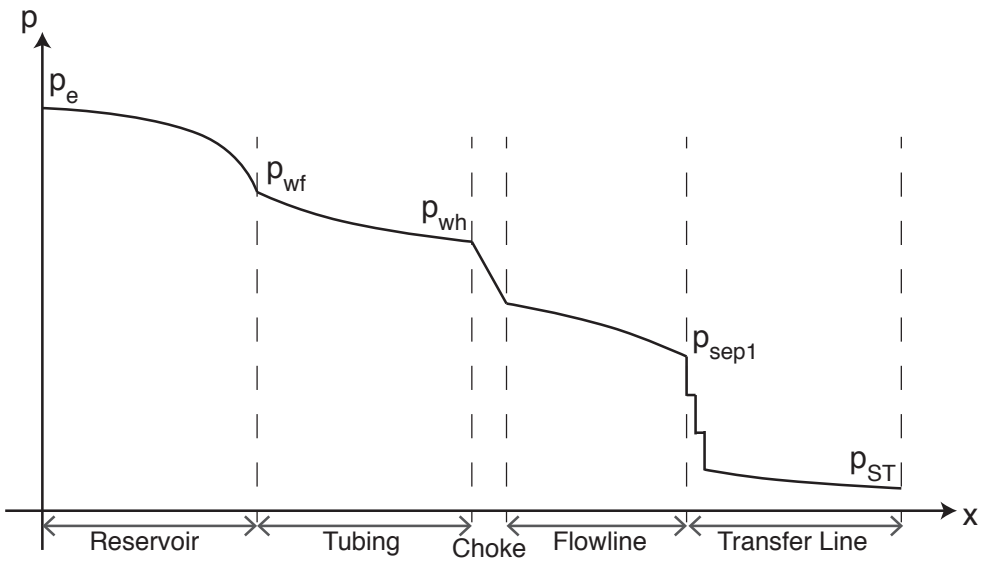

Figure 2.16: Sketch of pressure profile along the production system for a well. Adapted from

2.3.1 Inflow Performance Relationship

The IPR is a relationship that express how much the reservoir is able to deliver (surface rates), given a specific bottomhole pressure. For example if the well is producing from an undersaturated oil reservoir with p_{wf} above bubblepoint pressure (p_b), then the IPR can be written as

$$q_o = J \cdot (\bar{p}_R - p_{wf}) \quad . . . . . \quad (2.39)$$

where J is the productivity index, and the differential pressure ($\Delta p = \bar{p}_R - p_{wf}$) is the drawdown. The bottomhole pressure is defined as the pressure at the point opposite the producing formation. The productivity index is a value that describes all the different rock and fluid properties, whereas the drawdown pressure represents the pulling effect that the wellbore have on the reservoir. **Eq. 2.39** is a relatively simple equation, and will plot as a straight line with productivity index as the slope. However, different types of equations are used to describe the reservoir inflow performance for different types of situations, some of these are discussed in **Appendix C**. Two different sketches that show how the IPR curves might look like are illustrated below, where **Fig. 2.17a** represents an incompressible fluid and **Fig. 2.17b** represents a more compressible fluid. Fig. 2.17b also shows some of the different effects that will influence the IPR curve.

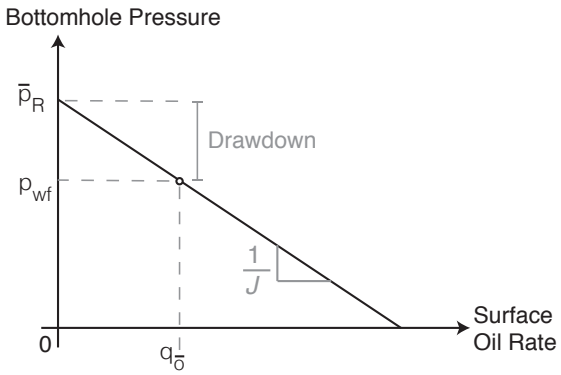

(a) IPR curve for incompressible fluids, used for undersaturated oil reservoir with bottomhole pressure above bubblepoint.

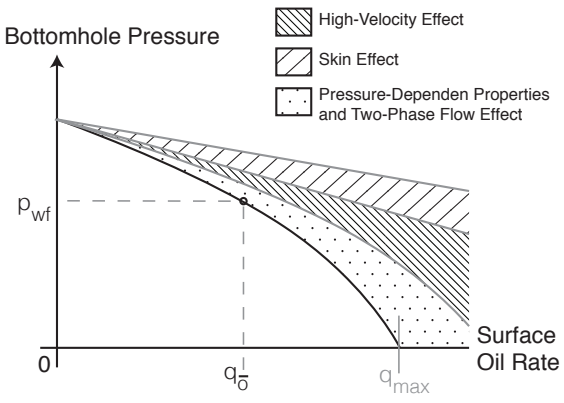

(b) IPR curve used for natural gas reservoirs or saturated oil reservoirs (two-phase). Pressure-dependent fluid properties include viscosities and formation volume factors.

Figure 2.17: Illustration of IPR curves used for compressible and incompressible fluids. The IPR curve for compressible mixtures will typically have some curvature due to skin effects, pressure dependency, and two-phase effects. Adapted from

2.3.2 Vertical Flow Performance

In contrast to the the reservoir inflow performance, the vertical flow performance is typically regarded as a relationship that describes how much the well is able to deliver. More specifically VFP represents how the bottomhole pressure for a given well changes with the surface production rate, given a certain wellhead pressure. An illustration of how this curve might look like for a two-phase flow in shown in **Fig. 2.18**. The pressure drop required to lift the reservoir fluid from the bottomhole through the tubing, can be written

$$\Delta p^{tubing} \simeq \Delta p_{PE} + \Delta p_{KE} + \Delta p_F \quad . \quad . \quad . \quad . \quad . \quad . \quad . \quad . \quad . \quad . \quad . \quad . \quad . \quad . \quad . \quad . \quad . \quad (2.40)$$

where Δp_{PE} is the loss due to change in potential energy, Δp_{KE} is the loss due to change in kinetic energy (often ignored), and Δp_F is the loss due to friction. The friction-loss term in this equation is not always easy to solve, because it dependents on various factors such as; flow rates, well geometry (diameter and trajectory), fluid properties, gas-liquid ratio, and two-phase flow regime. Different empirical correlations have been proposed in order to try and calculate this friction-term, including the Hagedorn and Brown (1965) method or the Beggs and Brill (1973) method. The method proposed by Beggs and Brill is briefly discussed in **Appendix D**.

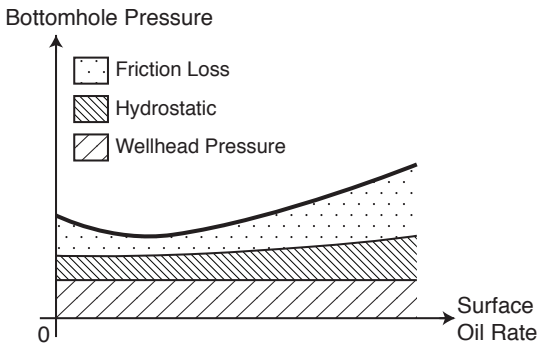

Figure 2.18: Illustration of the VFP curve for two-phase flow, showing the three major pressure losses. Adapted from

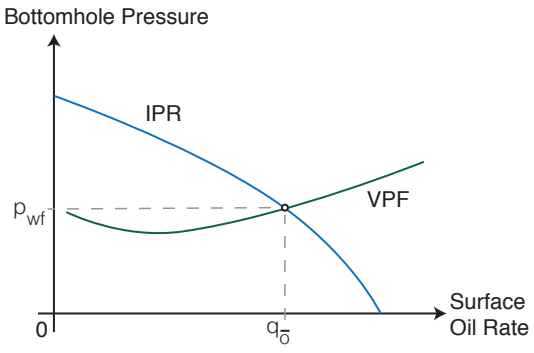

Figure 2.19: The IPR curve plotted together with VFP curve. The intersection point of the two curves shows where the flow is stable. Adapted from

2.3.3 Natural Flow

The VFP curve and the IPR curve is often used together because they are co-dependent. The bottomhole pressure (and therefore the production rates from the reservoir) are dependent on the total pressure drop in the production system. Whereas the total pressure drop is in return dependent on the flowrate of the fluid being lifted. **Fig. 2.19** shows an illustration where the IPR and the VFP are plotted together. At the point where the curves intersect, the production rate from the IPR (given a specific P_{wf}) will be the same as the P_{wf} from the VFP (given a specific rate). The system will therefore be in equilibrium, and the flowrate will be stable.

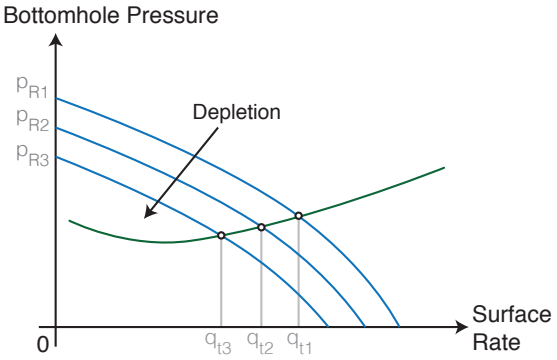

(a) The reservoir pressure will decline with production, which leads to a reduced drawdown.

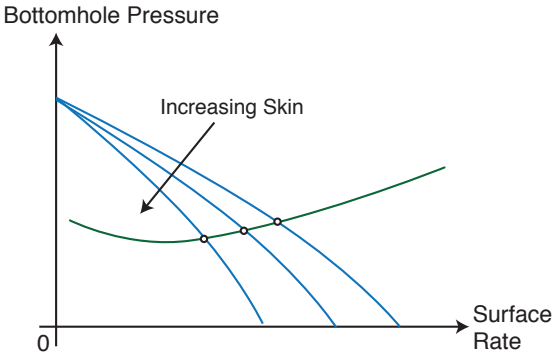

(b) The skin factor will influence the productivity index, which will change the IPR slope.

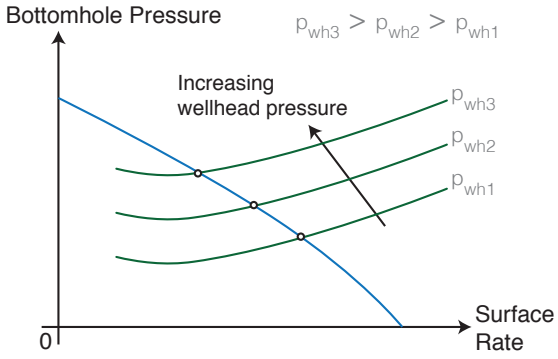

(c) Change with increasing wellhead pressure. Increased p_{wh} can for example be a result of increased backpressure in the flowline, or a change in choke position.

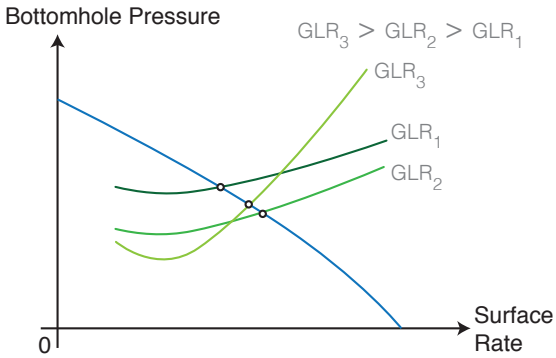

(d) Change with gas-liquid ratio. Can be a result of natural increase in GOR, gas injection, increased water cut, and similar.

Figure 2.20: Illustrations that show the change in the equilibrium point between the IPR and VFP curves, as a function of different factors. Adopted from

Figs. 2.20a through 2.20d shows how the equilibrium between the IPR and VFP changes with different factors. Other factors that is not shown, but which also will have an impact is the tubing diameter, well trajectory, emulsion, sand production, reservoir compaction.

2.3.4 Estimating Rates Using Pressure Measurements

In order for the flow to be stable, it needs to move along the IPR curve. This means that if we have an estimate of the bottom hole pressure, then we can use this together with a know IPR curve to estimate the production rate. Most wells are monitored with a pressure gauge at the wellhead and/or downhole. The measurements from either of these can be used together with the VFP relationship to find the BHP. The downhole gauge would predict the BHP more accurately, as this is much closer to the formation depth (around mid-perf). If we have pressure gauges at both places, then they can be used together to tune the VFP correlation.

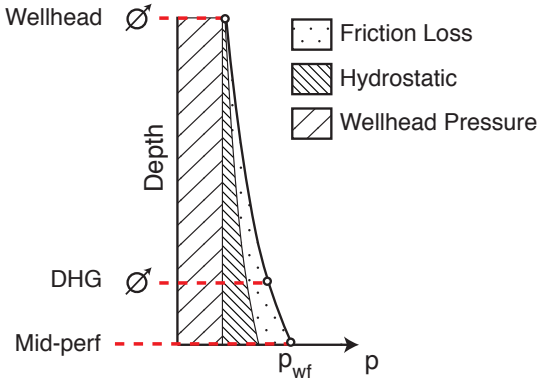

Figure 2.21: Pressure traverse for multiphase mixture. DHG stands for the downhole gauge. Adapted from

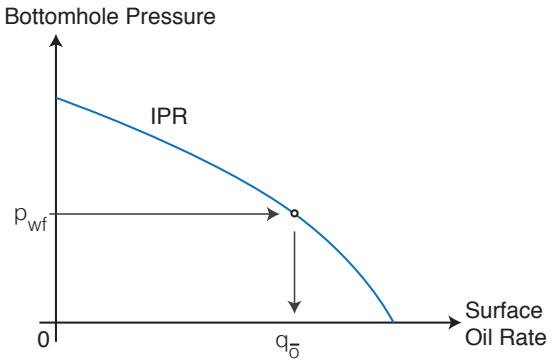

Figure 2.22: Estimation of surface rate using IPR curve and BHP.

The IPR curve is in general difficult to predict, because of the uncertainties in reservoir parameters (ie. skin effect) and reservoir pressure. If the reservoir pressure is know, and we have a periodic well-test of the production rate (from for example a test separator or MPFM), then it is possible to estimate the productivity index (from Eq. 2.39). The reservoir pressure is however seldom known, and it will constantly change as the field is being produced. One method that could be used to predict how the reservoir pressure

evolve, is by using a reservoir material balance. The productivity index will also change with time, because both the reservoir and fluid properties are time dependent.

Given that we have a well test, then this test can be plotted on the well deliverability diagram as shown in **Figs. 2.23a and 2.23b**. If this test lies on the IPR curve, then this is an indication that our IPR is representative of the reservoir. If there is an inconsistency in the match (as shown in the figures below), then the IPR can be updated by for example adjusting the reservoir pressure (Fig. 2.23a), or by adjusting the productivity index (Fig. 2.23b). In reality however, it may be a combination of factors that need to be adjusted, so some precaution should be taken.

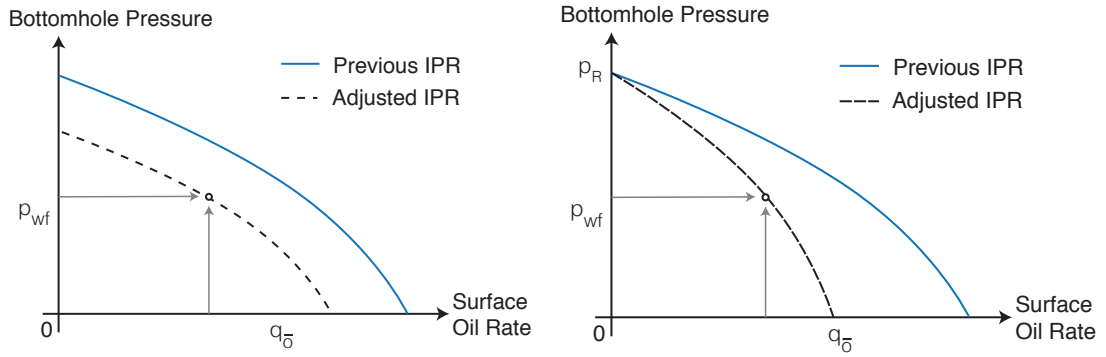

(a) Adjusting the reservoir pressure.

(b) Adjusting the productivity index.

Figure 2.23: Two different methods that can be used to update the IPR curve. Some other tests that can be done to assist the prediction of the IPR relationship is for example with build-up tests (and transient well analysis) or multi-rate flow tests.

Another very different method that can be used to predict the production rates, is by using choke models. Almost all wells are controlled by an adjustable choke, which places a restrict on the flow rate. The pressure drop through the choke is often though to be a function of the flow rate, and numerous correlations have therefore been proposed to predict this relationship. In order to use these types of models it is requires that the pressures both upstream and downstream of the production choke are known. Different choke models are briefly discussed in **Appendix E**.

Chapter 3

Allocation at the Skarv Field

3.1 Production System at Skarv

The Skarv field is produced with a FPSO and five subsea-templates, but only four templates are currently used for production. The different templates are producing from different reservoir sections, as shown in **Fig. 3.1**. The separator and process facility is situated on deck of the floating vessel, and is connected to the templates (located at seabed) with flexible flowlines and risers.

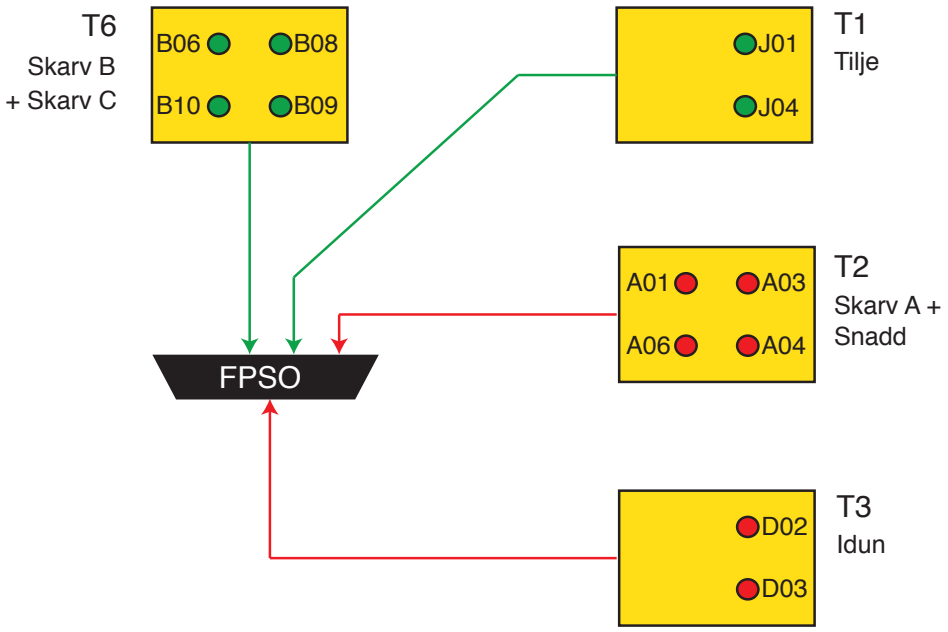

Figure 3.1: There are four subsea-templates at the Skarv field that is used for production, with a total number of six oil producers and six gas producers. Oil wells shown with green color, while gas wells are shown with red color.

Since the start-up of the field, subsea multiphase flow meters (MPFM) have actively been used to measure the individual flow-rates for the different oil and gas-condensate wells. There is one MPFM installed at every subsea-template, and every meter is shared by a number of wells. The wells are measured on a periodic basis, in rotation with the other wells in the same subsea-template. As shown in **Fig. 3.2** the flow from a well can either be directed through the MPFM, or directly to the first stage separator by a riser. The intervals and duration for which an individual well is measured with the MPFM, will depend on the template, and the total number of wells that need to be measured in that template. For example template T3 which consists of two active wells (see Fig. 3.1), will measure the production of these single wells more frequently than for those situated on a template with ie. four wells.

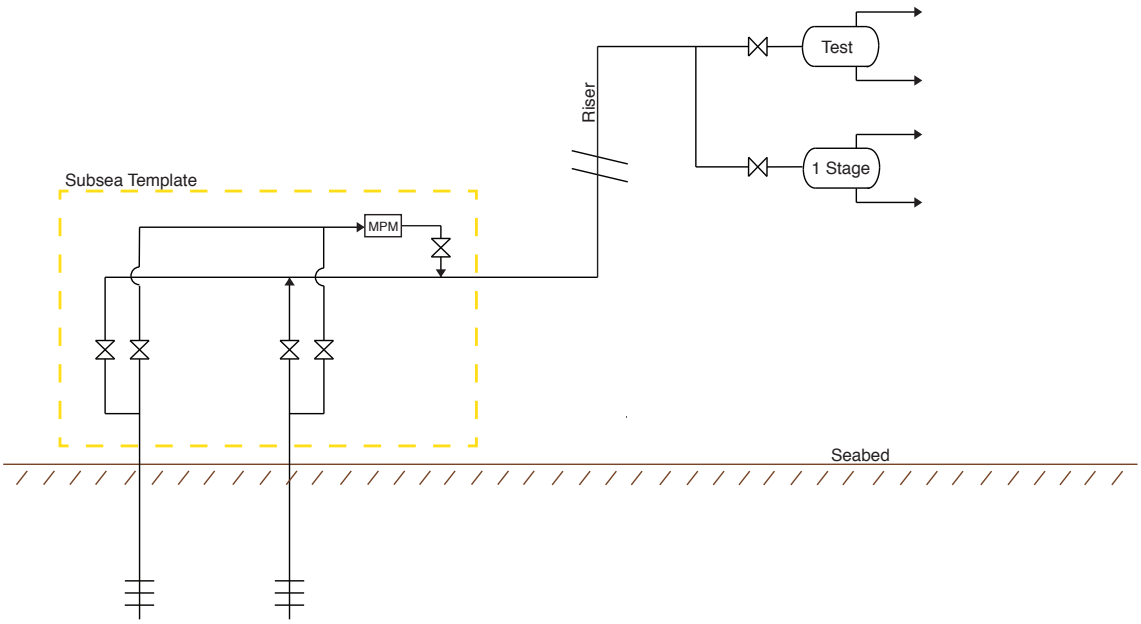

Figure 3.2: Sketch of flow diagram from the well to process facility. In this figure there are two producing wells active in the subsea-template, sharing one multiphase flow meter.

In addition to the periodic MPFM-tests, the production rates can also be estimated with pressure gauges. The pressures and temperatures for every well are measured both upstream and downstream of the wellhead choke, in addition to downhole (with permanent downhole gauges). The continuously measured pressures from these instruments can therefore be used together with assumed IPR and VFP (or with a choke model) to estimate the individual production rates in-between the periodic tests.

Furthermore, the streams can occasionally be routed through a test separator located at the FPSO. The test separator can therefore function as a reference instrument, which can can be used to validate/invalidate the rates measured by the MPFM. This means that if any discrepancies are spotted between the measurements, then one should start to investigate PVT properties, MPFM measurements or the reference instrument. One complicating factor however is that the test separator can only measure multiple wells at the same time, and not the individual rates as for the multiphase meters. The streams that are measured by the multiphase meter will therefore need to be added together to match the total stream that is measured by the separator.

3.2 Processing Unit at the FPSO

The production from the wells are sent to the process train given in **Fig. 3.3**. A high-pressure (HP) manifold leads to the first stage separator, whereas a low-pressure (LP) manifold leads into the second stage.

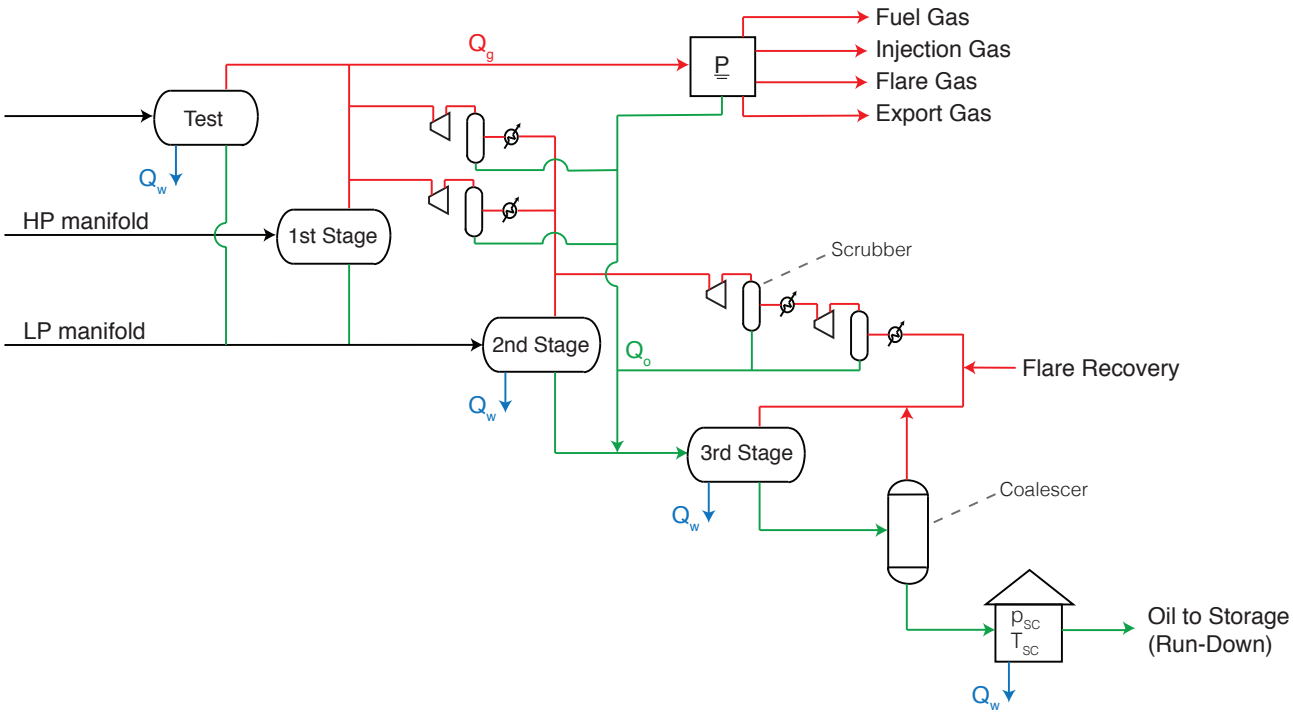

Figure 3.3: Sketch of the flow diagram for the separation process at the Skarv Field. There are four stages, where the first the first stage is connected to a high pressure manifold, and the second stage is connected to a lower pressure manifold.

The purpose of the LP manifold is the have the opportunity to redirect the wells that are producing with very small pressures away from the first stage separator. If a well is mature and are producing with low reservoir pressure, then the high pressure in the first stage separator might be enough to kill the well. Therefore, by redirecting these wells to the second stage separator, the production from these wells might be maintained for longer. This can also be seen by looking back at Fig 2.16, where a smaller separator pressure will lead to higher drawdown (lower p_{wf}).

It can be seen from Fig. 3.3 that the processing unit consists of four separators, in addition to a number of scrubbers. The condensate oil from the scrubbers are recycles into the third stage separator. The conditions of the different separators are in the reservoir simulator as shown in **Table 3.1**. It can be seen from this table that the pressure for the first stage separator is considerably higher then that for the second stage separator.

	Temperature [°C]	**Pressure** [**Bara**]
1st stage	92.2	80.0
2nd stage	82.8	25.0
3rd stage	98.9	3.00
4th stage	15.6	1.0135

Table 3.1: The conditions of the surface process train as defined in the Nexus reservoir simulator (for the Skarv field).

After the process train, the single-phase surface oil is lead into storage tank, whereas the surface gas is used for fuel, re-injected to reservoir, flared, or exported (as shown in Fig. 3.3). The surface rates of oil and gas out of process are continuously measured. The surface oil out of the facility are transported into a storage tank, before it can further be pumped into cargo tankers (from shipping). The export oil out of FPSO storage tank (into cargo tankers), is also measured with fiscal meters. Some of the produced gas are re-injected into the reservoir, in order to maintain the reservoir pressure. The composition of the injected gas will depend on the produced well stream, and might change somewhat as the field is produced. When the gas is re-injecting, it might also interact with the reservoir fluid, making it leaner.

3.3 Current Allocation Methodology

The allocation at Skarv is done based on volumetric balance, where the rates measured at the MPFM (or the test separaor) are converted from line-conditions to surface conditions by using black-oil tables. Because the MPFM tests are done periodically for the individual wells, the pressure gauges are needed to estimate the rates in between the tests. The allocation system at Skarv is therefore similar to the example given in Fig. 2.9 (on page 17), but with the periodic measurements done with MPFM instead of a test separator. The different steps involved in the allocation procedure at Skarv

- Estimation of the daily production rates from the individual wells, based on downhole pressure-measurements. The calculation of these daily rates are done automatically with Integrated-Surveillance-Information-System (an internal software at BP). This software will automatically generate the theoretical oil rates for the oil wells, and the gas rates for the gas wells. It does these calculations based on the same principals that was discussed in Section 2.3 (on page 29), using the IPR and VFP curves together with measurements from the downhole gauges. If for some reason the downhole gauge is not operative, then the daily rates are estimated using Perkins Choke model.

- Collect the periodic MPFM tests at line conditions, and convert these rates to surface conditions using black-oil tables. A description of how the black-oil properties are generated is given in **Section 3.3.1**.

- Correct the daily rates to match the individual MPFM tests, by using the Eq. 2.12 (on page 18). Then add all the corrected surface rates from all the production wells together, on a daily basis. Compare the resulting total surface rates against meters measuring the flow out of facility. The oil rates are also allocation on a monthly basis, where the calculated total production is compared against the fiscal measurements of oil into crude tankers. All allocation factors are found using the proportional-based method discussed in Section 2.1.5.

3.3.1 Black-Oil Properties Used in the Allocation Process

The black-oil tables are generated based on different virtual constant-composition-expansion (CCE) tests, using the commercial software called PVTp. A virtual single-cell CCE experiment is based on a specific fluid composition, which is brought from a set of conditions to surface conditions through subsequent steps. A schematic of these subsequent steps are shown in **Fig. 3.4**.

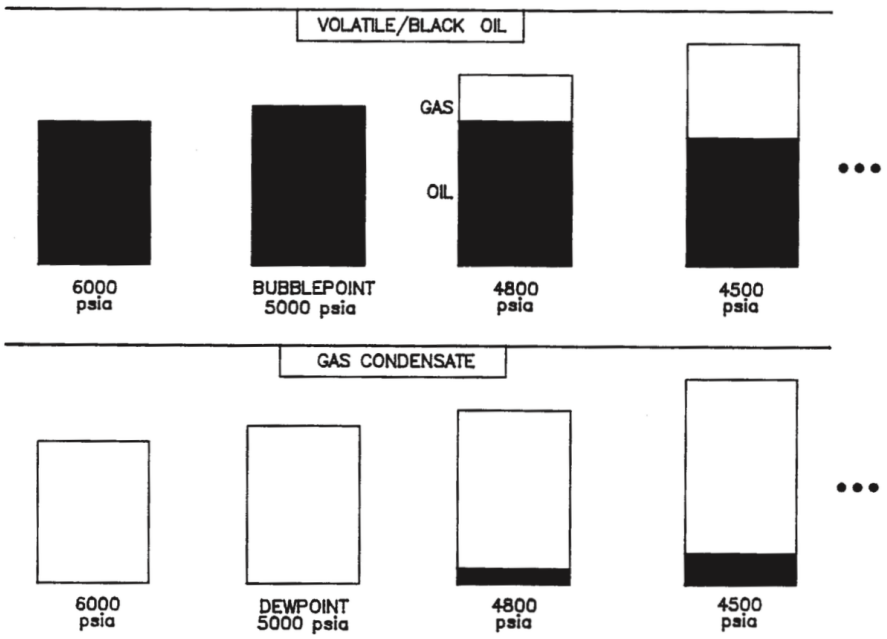

Figure 3.4: Schematic of a CCE experiment for an oil and a gas condensate. From

At every step the volumes of the phases are reported, and compared with the volumes produced when the phases are brought to surface condition (through a specific surface process). A virtual experiment is based on an EOS, and there is no restriction (except computational time) on how many steps that can be simulated.

The black-oil tables used at Skarv are generated for the pressure-range of 20-150 bara, and temperature range 1-130°C, resulting in 1156 different steps for each single-cell CCE. There is however five different CCE experiments (using five different compositions), one for each reservoir section; Tilje, Snadd, Idun, Skarv A, and Skarv BC.

The process that was chosen in the CCE experiments, to convert the volumes of the phases at the different stages to SC, was assumed to be a single-stage-flash. This simplified process is illustrated in **Fig. 3.5**.

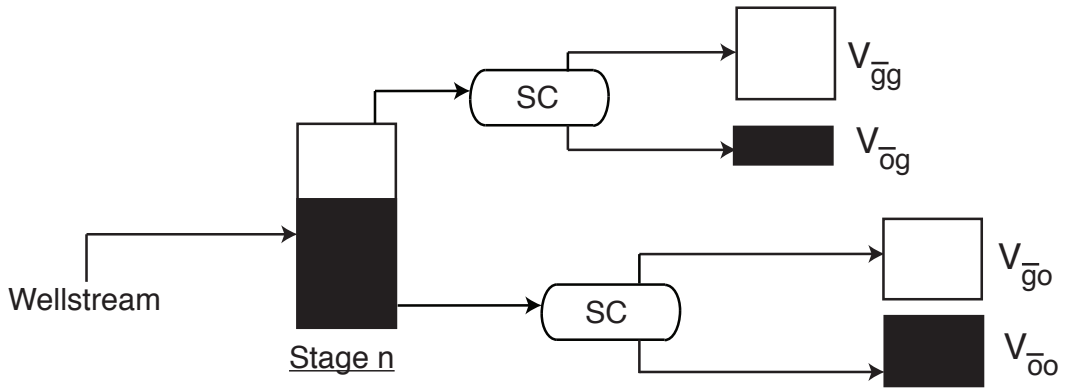

Figure 3.5: Surface process assumed in the CCE experiments. When using the black-oil tables to convert measured rates, then the *Stage n* are meant to represent MPFM or test separator. The BO-properties calculated from the stage with the conditions closest to the meter is then used for the conversion.

It is also important to understand that when the black-oil tables are used to convert MPFM rates, then the black-oil model will automatically assume two separate phases at the MPFM. This assumption is a consequence of how the black-oil properties are defined, and can be seen by looking at Fig. 3.5. This is however not representative of what actually happens, because the multiphase will not be in equilibrium state. At the MPFM the phases will not actually separate from each other as is the case for the test separator.

Figs. 3.6a through 3.6d on the next page show some of the resulting black-oil properties for Tilje and Idun formation, when the temperature is held at $T = 130°C$. Tilje is a oil formation, whereas Idun is a gas formation.

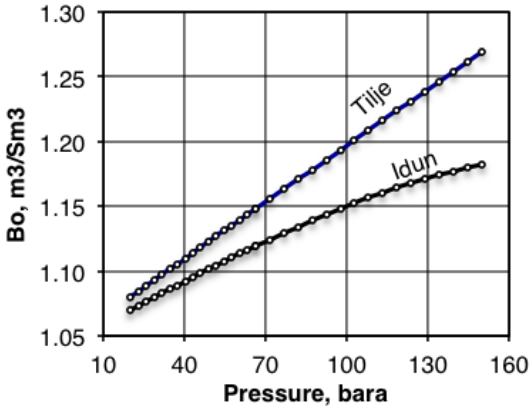

(a) CCE data for oil FVF (B_o) at $T = 130°C$.

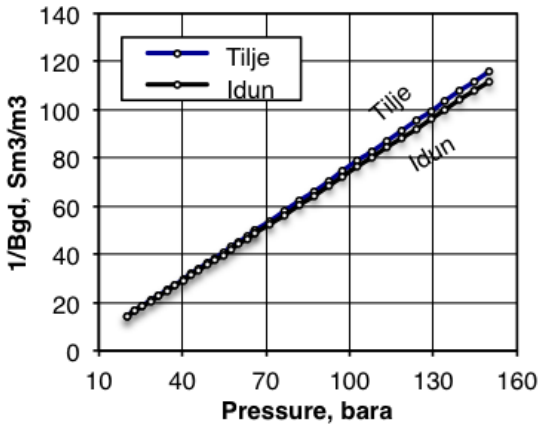

(b) CCE data for gas expansion factor ($b_{gd} = 1/B_{gd}$).

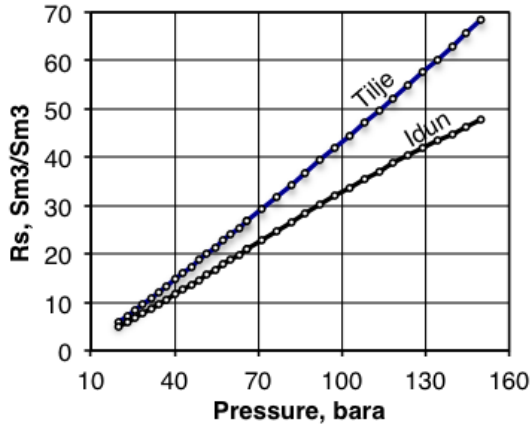

(c) CCE data for Gas-Oil-Ratio (R_s).

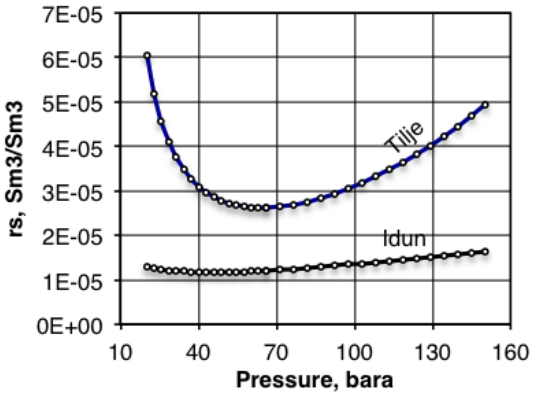

(d) CCE data for Condensate-Gas-Ratio (r_s).

Figure 3.6: Different black-oil properties generated by the PVTp software. All values found from CCE experiment at $T = 130°C$. The blue line used for Tilje, and the black line for Idun.

If we are for example considering the MPFM-tests, then the black-oil properties can be used to calculate the surface-rates as

$$Q_{o,SC} = \frac{Q_{o,MPFM}}{B_{o,MPFM}} + CGR_{MPFM} \cdot \frac{Q_{g,MPFM}}{B_{gd,MPFM}} \quad \ldots\ldots\ldots\ldots\ldots\ldots (3.1)$$

$$Q_{g,SC} = \frac{Q_{g,MPFM}}{B_{gd,MPFM}} + GOR_{MPFM} \cdot \frac{Q_{o,MPFM}}{B_{o,MPFM}} \quad \ldots\ldots\ldots\ldots\ldots\ldots (3.2)$$

where the subscript MPFM are used to specify that the the properties are at line conditions.

3.3.2 Results From the Current Allocation Process

This section will be based around **Figs. 3.8 and 3.10**, which show some of the results when using the current allocation process at Skarv. Fig. 3.8 illustrates the process used to estimate the daily production-rates from the individual wells, and this figure is based on two different wells; B08 and A06. Well B08 is an oil producer located in the Skarv B section, while A06 is a gas well producing from the Skarv A section. The calculated individual rates (from the current allocation method) for all of the other wells can be found in **Appendix G**. Fig. 3.10 compares the resulting total production from the Skarv field, with the meters measuring the rates out of facility.

If we first consider an oil well, then the theoretical oil rates are found based on the pressure gauges (Integrated-Surveillance-Information-System). These rates are then corrected by using the appropriate corrections factors, which are found by comparing the theoretical oil rates against the oil rates measured at the MPFM. When the oil rates have been adjusted, then the corresponding gas rates are calculated by R_p (the producing GOR), which are found from the MPFM tests. The producing GOR ($R_p = V_{\bar{g}}/V_{\bar{o}}$) is defined as the ratio of total surface gas divided by the total surface oil, and is not to be confused with the solution GOR (R_s) which was discussed in Section 2.2.1 (on page 20).

Fig. 3.7a shows an example where the initial theoretical oil rates, the adjusted rates, and the rates from MPFM are plotted together for B08. All the rates are given in standard conditions, which are found using the appropriate BO-properties for the well. As can be seen from this figure, the adjusted daily oil rates do not always match the rates measured at the MPFM. In fact, the daily rates are typically adjusted too high compared to the MPFM data point, and this trend is also seen for most other oil wells (see Appendix G). The reason for this offset might be due to the way that the correction factors are currently found in the allocation process. The engineer who is responsible for determining these factors needs to do this manually for every individual wells, and for every MPFM test. In addition, if the engineer determines that a specific MPFM test is unreliable, then this test might be disregarded. The factors from the different tests might also be averaged over a specific time-interval (for example over a month). The correction factors that is used for B08 is shown in **Fig. 3.7c**, and it can be seen that these factors are relatively high at the start, and is gradually reduces to around 1 through 2014. Note that if the factors are significantly different from one, then this means that the model used to estimate the theoretical rates are not very representative of the well.

The producing GOR that is used for B08 to find the gas rates produced are shown in **Fig. 3.7e**. Is can be seen that this well have a steep upward trend, and the value of the producing GOR doubles from start till end of 2014. This change in GOR will consequently mean that the fluid properties from this well might be significantly altered as the well is produced. The initial BO-table used at the start of 2014 might therefore no longer be representative of the fluid at the end of the year. It can also be seen that the GOR used are generally consistent with what is actually measured at the multiphase meter. The resulting gas rates by using the producing GOR are shown in **Fig. 3.7g**. These rates are slightly over predicted compared with the measured rates at the MPFM, which is mainly a result of the over prediction in the oil rates (compared with the MPFM tests).

The process for calculating the daily rates from gas wells is similar to that of the oil wells. However, for the gas producers the adjusted theoretical gas rates (from the Integrated-Surveillance-Information-System) are used together with the producing CGR to find the daily oil rates. It can also be seen from **Fig. 3.7b** that theoretical rates from A06 are largely in accordance with the multiphase meter. This agreement between theoretical rates and MPFM is also the case for the other gas producers (see Appendix G). The correction factors needed for the gas wells are therefore closer to unity, than what was the case for most oil wells. Furthermore, the producing CGR for the gas wells are fairly constant over the time period, which might in turn indicate that the fluid compositions for these wells are stable. The predicted oil rates from the gas wells are also consistent with the MPFM measurements.

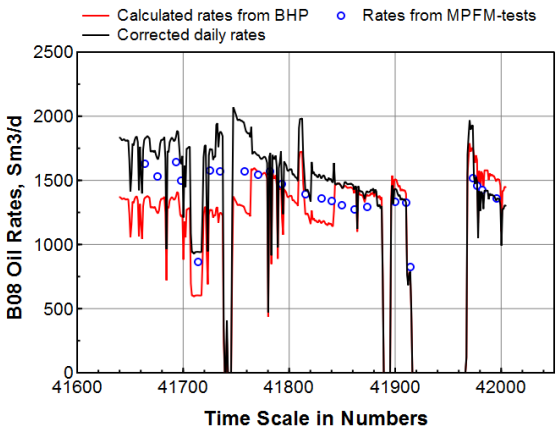

(a) Daily oil-rates for B08 (Skarv B field).

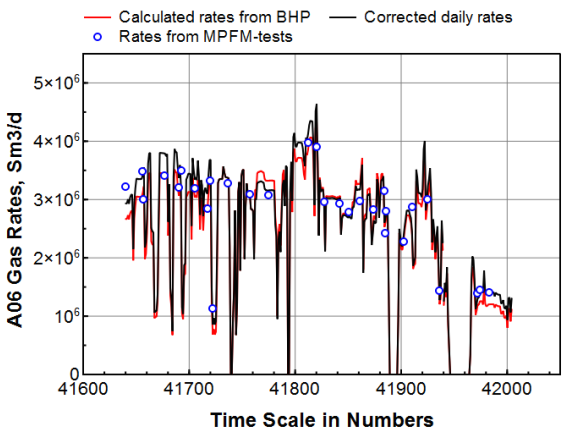

(b) Daily gas rates for A06 (Skarv A field).

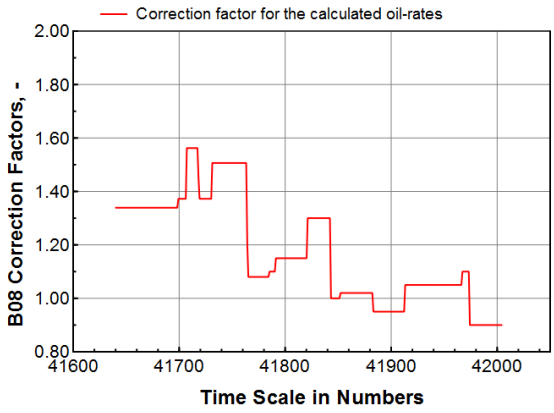

(c) Correction Factors for B08 (Skarv B field).

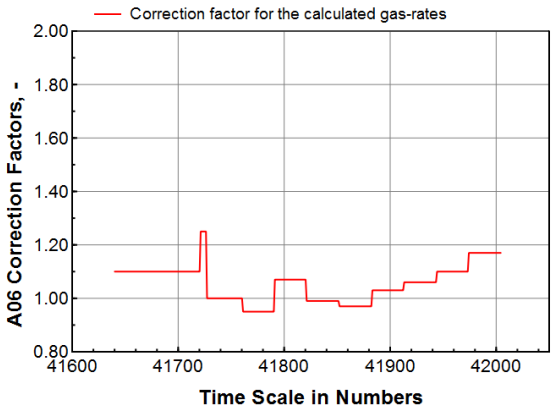

(d) Correction factors for A06 (Skarv A field).

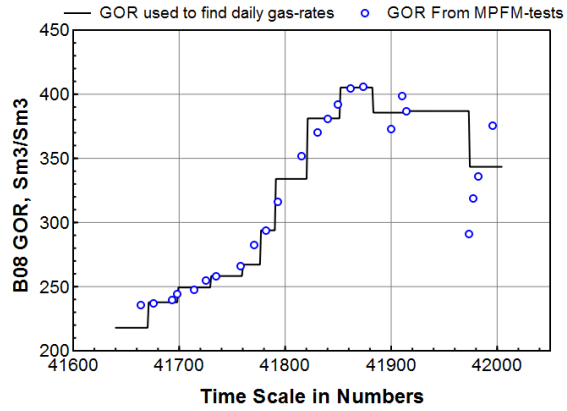

(e) Producing *GOR* used to find gas rate from B08.

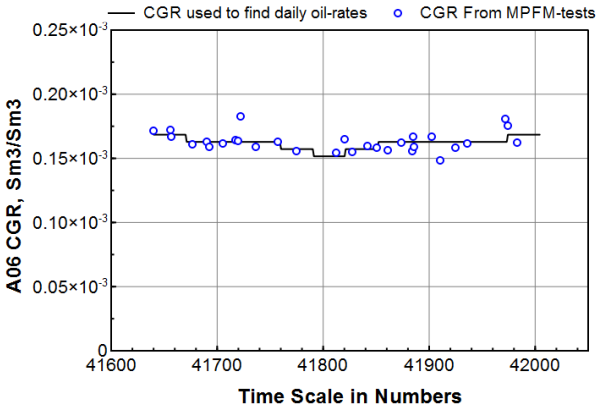

(f) Producing *CGR* used to find oil rate from A06.

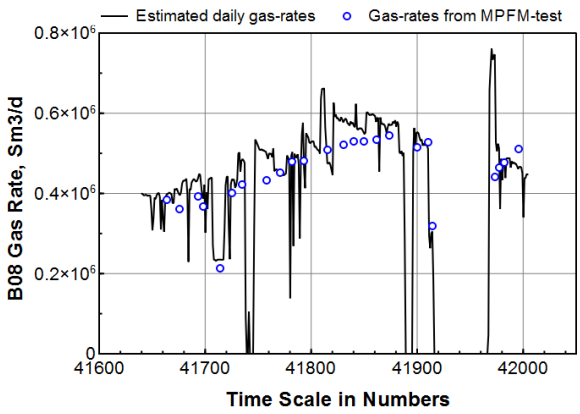

(g) Measured and calculated gas rates from B08.

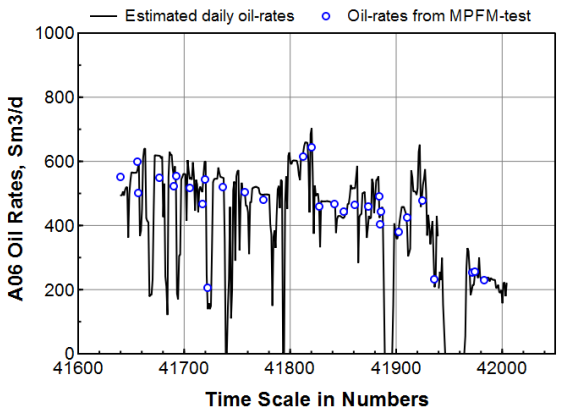

(h) Measured and calculated oil rates for A06.

Figure 3.8: These plots illustrate the process for estimating the daily production rates for the individual wells, using the current allocation method. The process for oil wells are slightly different from gas wells. For oil wells, the gas rates are found from the adjusted theoretical oil-rates, used together with the producing GOR. Similarly for gas, the adjusted theoretical gas rates, used together with the producing CGR. The time scale for all the plots are in numbers, where one digit represent one day, and the time-interval (41640−42005) represents year 2014.

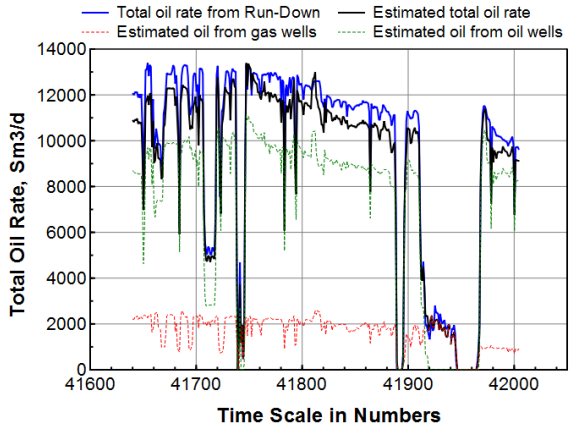

(a) Comparison of total oil rates out of facility.

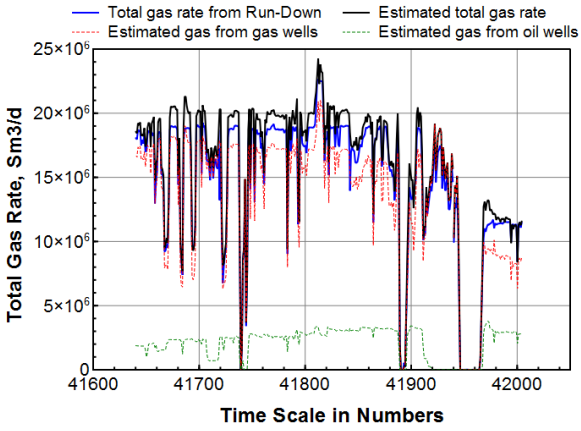

(b) Comparison of total gas rates out of facility.

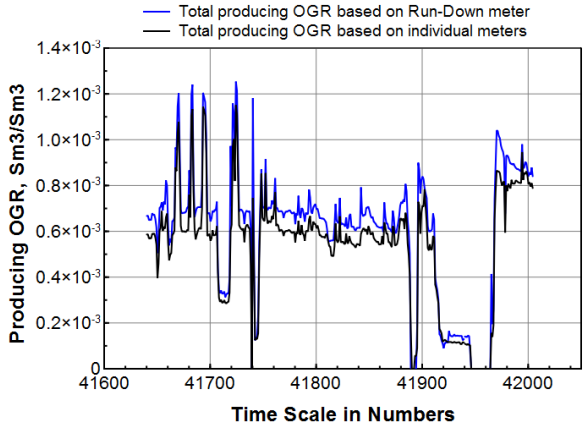

(c) Comparison of total producing OGR (r_p) out of facility.

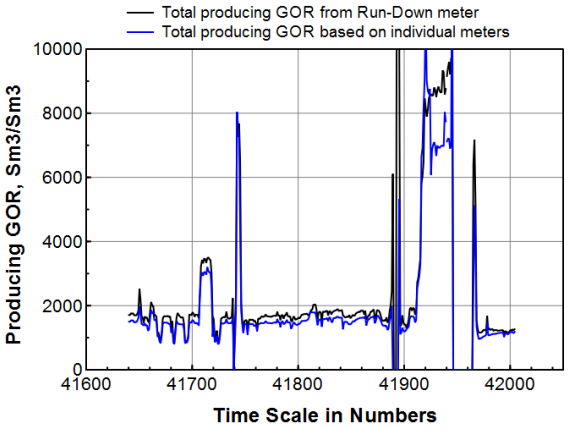

(d) Comparison of total producing GOR (R_p).

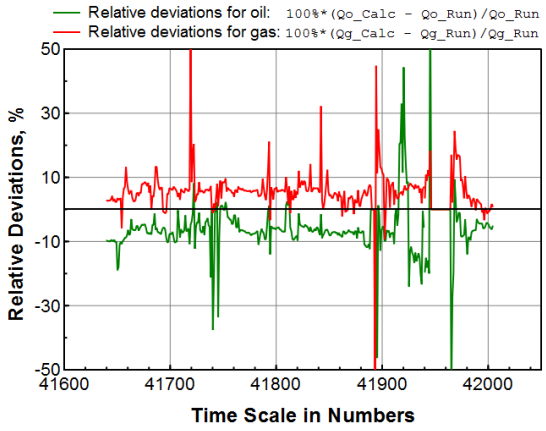

(e) Relative deviations of oil and gas rates.

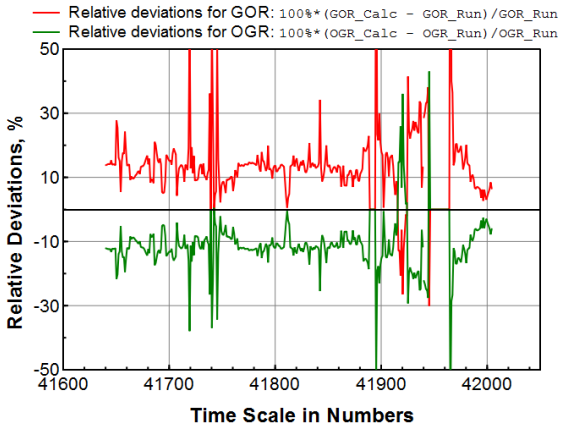

(f) Relative deviations of r_p and R_p.

Figure 3.10: Comparison of total product rates out of facility, when using current allocation method. Blue lines represent the rates from meters measuring the total streams out of facility. The time scale for all the plots are in numbers, where one digit represent one day, and the time-interval (41640−42005) represents year 2014.

Note that the surface rates that are compared in Figs. 3.7a through 3.7h are dependent on the fluid model and the process used to bring them to surface conditions. Even if there is a good match between the predicted daily rates and the MPFM rates, this will not imply that the predicted rates are representative of the actual rates.

Figs. 3.9a and 3.9b compares the total rates that are found when adding the calculated rates for all the individual wells, against the measured rates out of the facility. It can be seen from Fig. 3.9a that the estimated total oil production is systematic underestimated compared with what is measured. This under prediction seems to be relatively constant across the time-interval. The figure also suggest that a large portion ($\sim 20\%$) of the produced oil is from gas condensate. The oil coming from the gas phase will typically range from 1% to 15% for most gas condensate reservoirs*. Fig. 3.9a shows that the total gas rate is generally over predicted for most of the interval, which is opposite to what was seen for the oil.

Figs. 3.9c and 3.9d compares the total surface ratios, namely the producing OGR and the producing GOR. Because the oil is under predicted whereas the gas is overestimated, the deviation in the surface ratios are amplified. The producing OGR is estimated to be too low compared with the measured, while the producing GOR is estimated to be too high. One interesting observation in Fig. 3.9c is the behavior at time interval 41920 to 41940 (month of September). In this interval none of the oil wells are producing (can be seen from Figs. 3.9a and 3.9b), and the producing OGR therefore represents the condensate from the gas wells. In this interval the producing OGR is still underestimated with what is measured by the meters, which might indicate that the condensate from the gas wells too low. One reason for this might be due to the way that the black-oil tables are found; single-stage flash to standard conditions instead of recycled processing unit (as was shown in Fig. 3.3).

Figs. 3.9e and 3.9f compares the relative deviations (RD), which are calculated as

$$RD_o = 100\% \cdot \frac{(Q_{o,calculated} - Q_{o,measured})}{Q_{o,measured}} \quad (3.3)$$

$$RD_g = 100\% \cdot \frac{(Q_{g,calculated} - Q_{g,measured})}{Q_{g,measured}} \quad (3.4)$$

$$RD_{GOR} = 100\% \cdot \frac{(R_{p,calculated} - R_{p,measured})}{R_{p,measured}} \quad (3.5)$$

$$RD_{OGR} = 100\% \cdot \frac{(r_{p,calculated} - r_{p,measured})}{r_{p,measured}} \quad (3.6)$$

These values are in general safer to compare than the rates, because they are normalized. The relative deviation for the total oil looks like a reflection the relative deviation for the total gas.

*Personal discussion with Whitson, C.H. (2015).

Both of the deviations seems fairly systematic, and they fluctuates randomly around the ±6%-lines. The relative deviations for the surface ratios also looks systematic, and these are even higher than for the rate-deviations. **Table 3.2** gives a summary of the different deviations. The RMS (root mean square error) in this table is defined as

$$\delta_{RMS} = \sqrt{\frac{1}{N}\sum_{n=1}^{N}(RD_n)^2} \quad . . . . . (3.7)$$

where RD_n represent the residual between predicted and measured value of a specific production day.

	Total oil	**Total gas**	**GOR**	**OGR**
Average RD (%)	-6.0	5.5	13.2	-10.7
Maximum RD (%)	69	54	166	43
Minimum RD (%)	-56	-61	-30	-62
RMS (%)	10	8	19	14

Table 3.2: Overall deviations in predicted total rates and surface ratios, when using the current allocation method.

Figs. 3.11a and 3.11b shows the calculated oil rate over the month, the monthly oil rate from the Run-Down meter, and the rate measured into cargo tankers. The term Run-Down meter is used for the meter measuring the oil rates out of the facility and into storage. The oil rate that is measured into cargo is done on a fiscal basis. Total rate oil into cargo is calculated once a month, and found with

$$Q_{oil}^{total} = \sum Q_{oil}^{lifted} + \Delta Q^{storage} + Q_{oil}^{not\ lifted} \quad . . . . . (3.8)$$

where $\sum Q_{oil}^{lifted}$ is the net sum of oil rate that have been lifted with cargo tankers, and $\Delta Q^{storage}$ is the change in storage level. The volume $Q_{oil}^{not\ lifted}$ is an amount that occurs if a cargo is in the process of being lifted at month end.

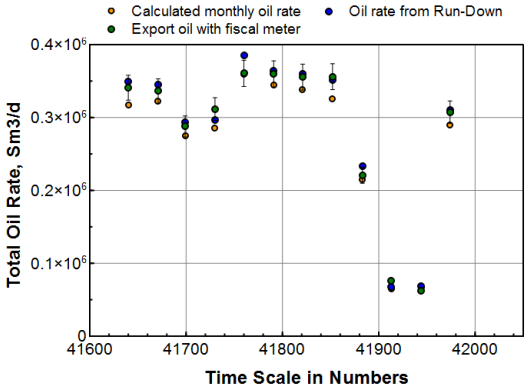

(a) Comparison of monthly oil rates. The error bars represents 5% deviation from fiscal.

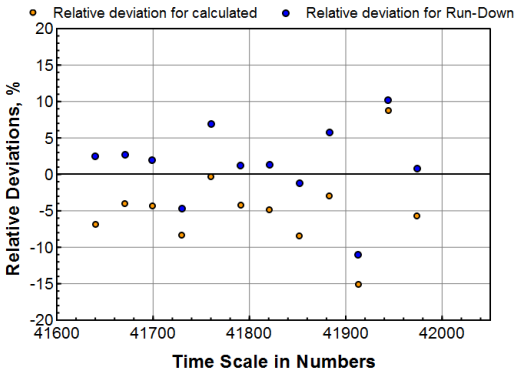

(b) Comparison with relative deviations, when calculated using Eqs. 3.9 and 3.10.

Figure 3.11: Comparisons of calculated monthly rates, when compared against the measured oil from storage into cargo.

The relative deviations that is found in Fig. 3.11b is calculated as

$$RD_o^{Calc.-fiscal} = 100\% \cdot \frac{(Q_{o,calculated} - Q_{o,fiscal})}{Q_{o,fiscal}} \quad . . . . . (3.9)$$

$$RD_o^{Rundown-fiscal} = 100\% \cdot \frac{(Q_{g,Rundown} - Q_{g,fiscal})}{Q_{g,fiscal}} \quad . . . . . (3.10)$$

These figures show that measured oil into storage, and the measured oil out of storage are not the same. This means that there is also an uncertainty in the measurement done out of facility. However, there is no clear systematic pattern in the deviation between the Run-Down meter and the cargo liftings, as is the case for the calculated oil rates.

Chapter 4

Alternative Allocation Method Using Compositional Streams

One of the motivations for developing an alternative allocation based on compositional streams, is to see if this will have an effect on the allocation results. The results from the current allocation system at Skarv seem to have a systematic deviation (as discussed in **Section 3.3**). This systematic deviation might occur as a consequence of using the defined black-oil tables with a single-stage flash to standard conditions. By doing the allocation on a componential balance it will be possible to do sensitivity of the process train, and see what influence it has on the surface rates. Doing the allocation on a compositinal basis can also account for the changing behavior of the fluid properties, and the effect of commingling.

4.1 Pipe-It Software

The adjusted allocation method was made in Pipe-It, which is a program released by Petrostreamz AS in 2011. This section is meant to give a brief introduction to this program, and how it is used in this work.

The main purpose of Pipe-It is to do integrated modeling across programs. It is more specifically a platform that enables different programs (such as PhazeComp, Hysys, Excel etc.) to be launched, perform some action based on an input, and report the resulting output from those actions. The output and the input from the different programs can be linked together, given a certain flow of information. For example, the production estimates from a reservoir simulator software (ie. Eclipse) can be used as an input into a process simulator software (ie. Aspen Hysys). Pipe-It can be a useful tool when doing repetitive work, sensitivities, or optimization.

The graphical interface in Pipe-It is very basic, and consists of a canvas (flow diagram) and four main elements. The four elements are Resources, Connectors, Processes, and composites. The resource represents an input file or an output file, and the process represent a program or an operation that is performed on the resource. The connectors link the resources and the process together, and they determine the flow of information. The fourth element is the composite, which can be used to create sub-levels. The composite do not have any function except sort or categorize the resources and processes into local groups. **Fig. 4.1** shows how the canvas looks like, together with the four of the main elements.

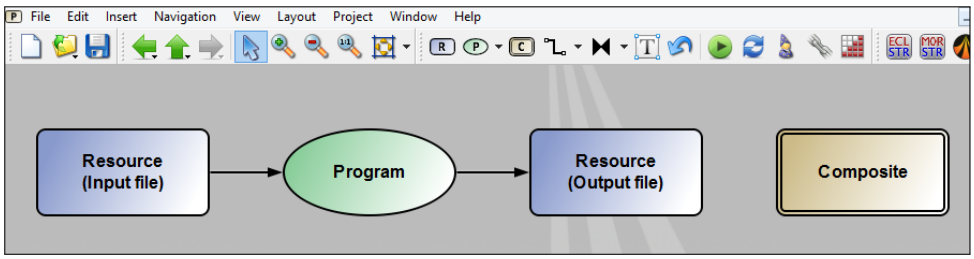

Figure 4.1: Shows the canvas in Pipe-It, with the four main elements (resources, connectors, process, composites).

In this work, Pipe-It have mainly been used together with the program called Streamz*, which is an equation-of-state phase behavior modeling software (comparable with other programs such as PhazeComp or Hysys). This software can therefore be used to manage compositional streams, and do EOS based calculations (for example flash calculations, which was discussed in Section 2.2.3). An important reason that Pipe-it might be useful is because all the twelve wells producing at Skarv will have an unique wellstream (oil rate, gas rate, and composition) every single day. This will in turn result in hundreds of different streams and EOS calculations over the period of one year. Managing and manipulating this vast amount of fluid information would be difficult if one were to use a phase behavior modeling software (like Hysys) by itself.

A simple example of how Streamz and Pipe-It are used together is shown in **Fig. 4.2**. The Streamz operation (green oval) in this figure can be regarded as a virtual separator, which calculates the compositions of the equilibrium phases at a set of given conditions. Streamz can do EOS based calculations on any number of streams, but it is required that the compositions, conditions, and the fluid characteristics (EOS properties) are known. The compositional properties that is used for this alternative allocation method is given in **Appendix F**, which is the same EOS table that is used in the reservoir simulator (Nexus). How the different compositions are estimated will

*Was developed in 2001 by Dr. Aaron A. Zick in partnership with Petrostreamz. Is an integrated part of the Pipe-It program.

be discussed in **Section 4.3**.

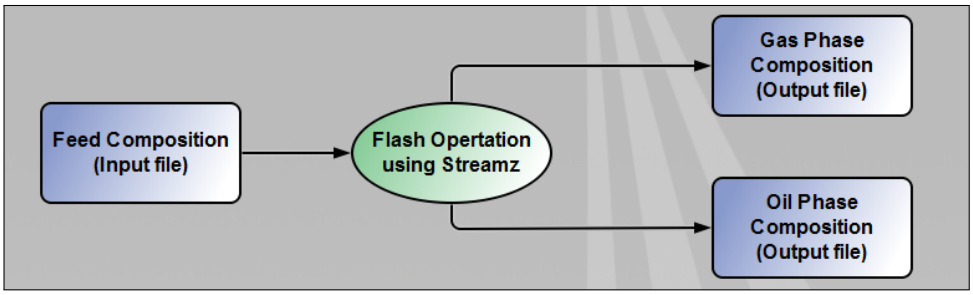

Figure 4.2: Illustration where an input file (containing compositional streams) is linked to the Streamz software. Streamz will do a EOS based flash calculation to estimate the composition of the gas phase and the oil phase at some given pressure- and temperature condition. The flash operation results in two different output files, one for the gas compositions and another for the oil compositions.

Fig. 4.3 shown an example of how an input file that is linked into the Streamz operation might look like. Every row in this file represents a unique stream, at for example a specific well test.

Template | Contains | Select a column header to create/edit a formula...

	Name	Start	End	QoAC	QgAC	MPMP (bar)	MPMT (C)	Moles CO2	Moles C1N2	Moles C2	Moles C3C4	Moles C5(
1	J01	41657.3	41658.3	992.693	1328.81	108.085	93.5873	0.0252204	0.536239	0.0639199	0.0682556	0.02826
2	J01	41663.6	41664.6	870.508	1218.99	111.47	92.8047	0.0254026	0.550824	0.0637864	0.0672843	0.02752
3	J01	41671.3	41672.6	787.534	1166.88	109.799	91.8424	0.0254727	0.556432	0.0637351	0.0669108	0.02723
4	J01	41682.3	41682.9	803.771	1268.06	108.948	92.8725	0.0255889	0.565736	0.0636499	0.0662912	0.02676
5	J01	41696.3	41696.9	858.016	1788.82	106.555	94.5081	0.0260199	0.600232	0.0633341	0.0639938	0.02500
6	J01	41700	41700.6	812.832	1696.57	107.808	93.7156	0.0260554	0.603077	0.0633081	0.0638043	0.02485
7	J01	41702.3	41702.6	801.383	1646.17	109.349	93.6436	0.026093	0.606081	0.0632806	0.0636043	0.02470

Figure 4.3: Example of how an input file used by Streamz might look like. Each row will represent a different stream, at for example a specific well test. The row can contain any amount of information, but in order to do phase behavior calculations, then the composition and some conditions need to be specified. In this file the composition is shown with green-colored cells. The Streamz software will regard each row separately, and do EOS calculations based on the information in this row alone.

Note that when using a process simulator as part of the allocation system, then the simulator is only needed to determine how hydrocarbons are distributed amongst the different product-streams leaving the facility. Stream enthalpies and equipment performance are therefore not important, and equipment such as pumps and control values should not be included (consumes computation time and might lead to instabilities). The allocation system can be designed by only using a series of flashes, mixers and splitters. The fact that there are equiptments between these flashes will not affect the vapor-liquid equilibrium in the vessels.

4.2 Reproducing Surface Rates Predicted by the Reservoir Simulator

The EOS model used in Pipe-It is chosen to be the same as the one used in the reservoir simulator at Skarv. It is therefore interesting to see if both softwares generates the same estimates of the surface rates, when sending a given composition through the same surface process.

This analysis is done by using the output file from a compositional reservoir simulation, which will have predictions of the compositional streams ($z_{res,i}$) for every well over a given period of time. In addition to the composition, the reservoir simulator will also have an estimate of the surface rates, and the surface ratios. By using the same compositional streams and surface process as the reservoir simulator, then Pipe-It should essentially estimate the same producing GOR. How the surface process is defined in the reservoir simulator was given in Table 3.2 (on page 50), and is implemented in Pipe-It as shown in **Fig. 4.4**. The figure shows in total four separators, where each flash operation done by Streamz is shown as a green round-edged rectangle.

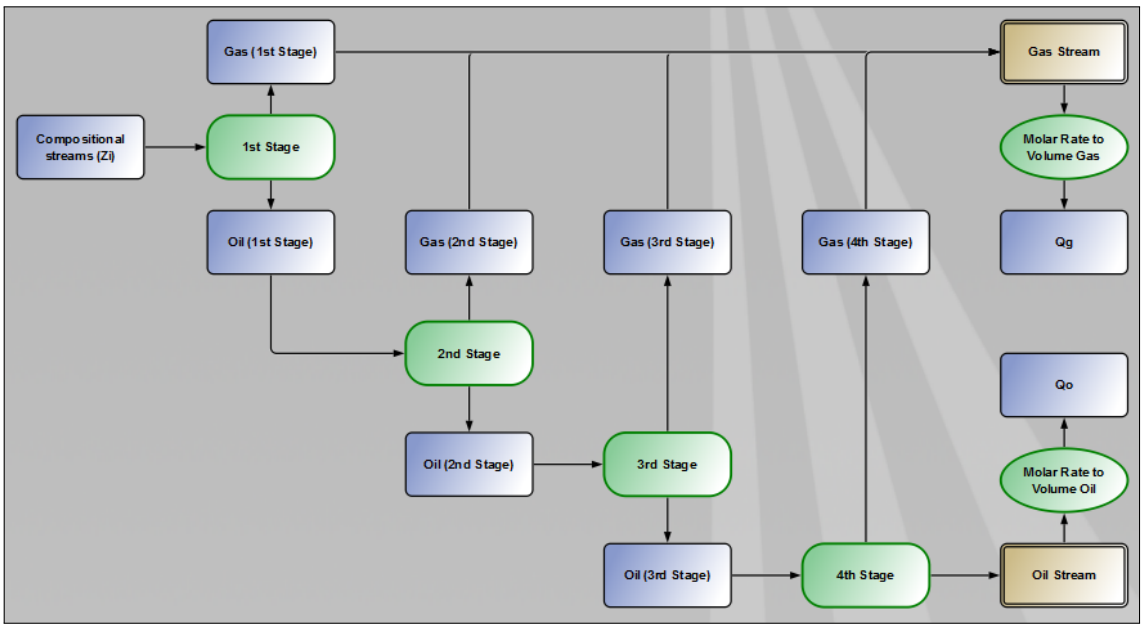

Figure 4.4: Implementation of surface process as defined in the reservoir simulator. Every green oval in this figure represents a flash operation done by Streamz.

The resulting comparisons between the producing GOR generated from Pipe-It and the GOR from Nexus are shown in **Fig. 4.5**. It can be seen that the producing GOR predicted from Pipe-It are generally consistent with those from the reservoir simulator, with the only exception being the producing GOR from well A01 (deviation highlighted in **Fig. 4.5a**). This well is producing from the Snadd field, which is a separate reservoir that the other wells (with its own Nexus file). Because

this is the only well that have a deviation, it can be assumed that either the surface process or EOS properties for this well is defined differently in the reservoir simulator than the other wells. However, for the purpose of this study, both the EOS model and the surface process of all the wells will be assumed to be the same.

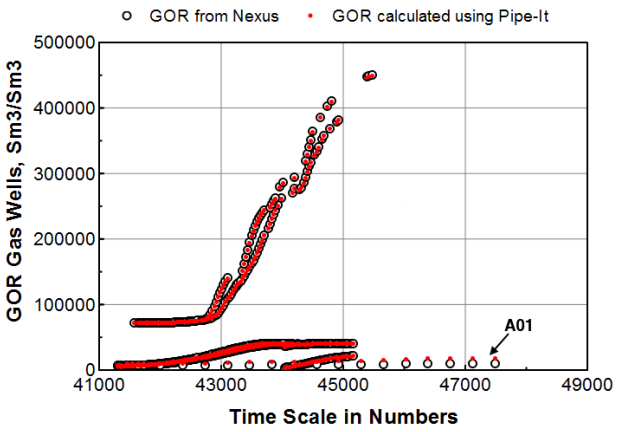

(a) Producing GOR for gas wells.

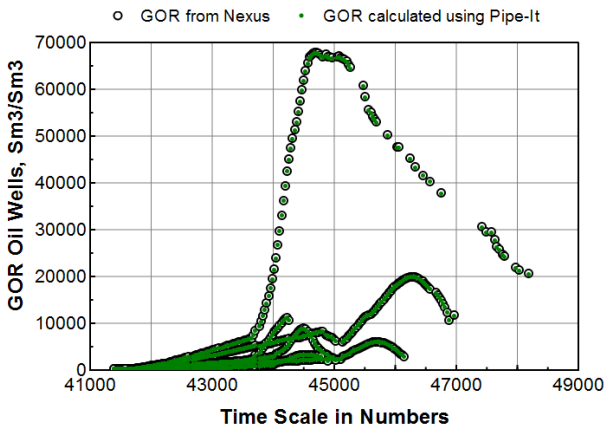

(b) Producing GOR for oil wells.

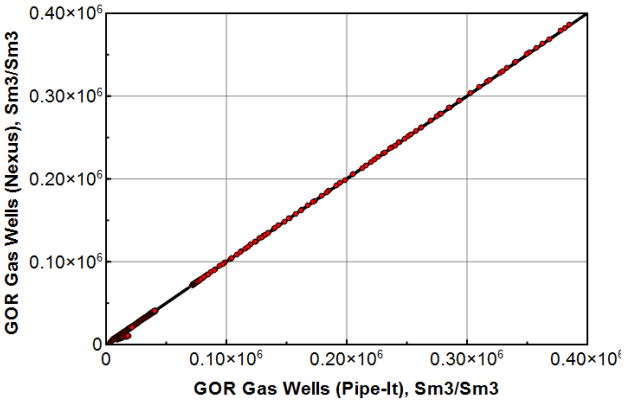

(c) Diagonal error-plot comparing R_p for gas wells.

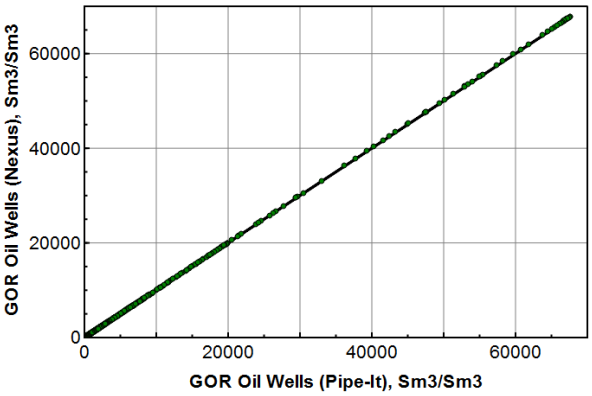

(d) Diagonal error-plot comparing R_p for oil wells.

Figure 4.5: Comparison between the estimated R_p from Pipe-It against R_p from reservoir output file. The time scale goes from 2013 to 2030, and represents the period for which the reservoir simulation have estimations of the well rates.

4.3 Well-Test-Conversion to Compositional Molar Wellstreams

One of the main challenges with doing the allocation process on a compositional basis, is that the compositions are seldom known. So how do we find the molar compositional wellstreams for all the different well tests, and the adjusted daily rates? There are primarily two methods used in the petroleum industry to find these molar compositional streams. The first method is called well-test-conversion (WTC), while the second method is called black-oil to compositional (BOz). This section will discuss well-test-conversion, as this is the method that was chosen for the alternative allocation process.

4.3.1 Description of Method

The WTC method is based on volumetric rates from the well tests, and the conditions at which these measurements were obtained. In addition, it is required that an appropriate EOS is defined, and that there is an initial estimate of the wellstream composition. This initial estimate of the composition is termed the seed feed composition ($z_{seed,i}$), and the accuracy of this composition can range from being very poor, or being very representative of the fluid. Different ways used to find the seed feed will be discussed in **Section 4.3.2**.

Given a seed feed, then this composition ($z_{seed,i}$) is brought through a flash separation at the test conditions at which the volumetric rates were measured. This flash separation will then yield an estimate of the equilibrium gas phase composition ($y_{seed,i}$), and the equilibrium oil phase composition ($x_{seed,i}$). These are in turn recombined to exactly match the volumetric rates that are measured, by using the formula

$$n_i \quad = \quad x_i \cdot n_L + y_i \cdot n_v \quad \simeq \quad x_{seed,i} \cdot \left(\frac{Q_{o,m}}{v_o} \right) + y_{seed,i} \cdot \left(\frac{Q_{g,m}}{v_g} \right) \quad . \; . \; . \; . \; . \; . \; . \; . \quad (4.1)$$

where $Q_{o,m}$ and $Q_{g,m}$ are the measured rates of oil and gas respectively, v_o and v_g are the molar volumes, and n_i is the compositional molar rate ($z_i = n_i/n$).

The procedure for implementing the WTC method into Pipe-It is shown in **Fig. 4.6**, where every process (green ovals) represents an operation done with Streamz. The resulting output files from theses Streamz operations are collected in the composite called *Calculation of WTC equation*, where the actual calculation of **Eq. 4.1** is done. The composite is used to keep the flowsheet clean, and because the mechanical procedure of exactly how Pipe-It calculates Eq. 4.1 is not important.

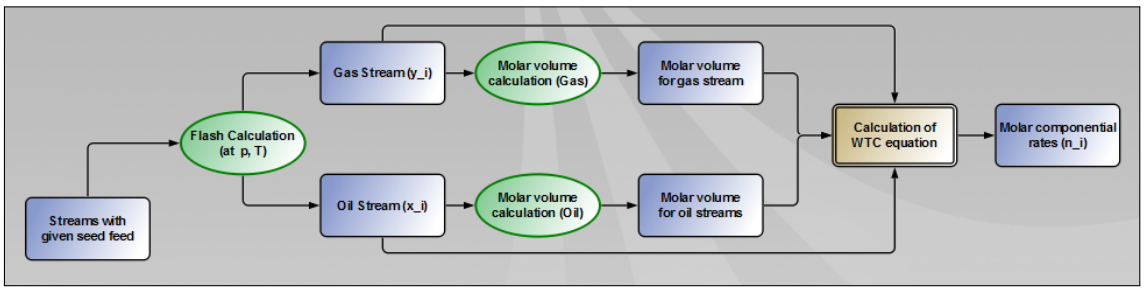

Figure 4.6: Well test conversion using Pipe-It and the Streamz software. The seed feed and the conditions of the well tests are used to find equilibrium compositions. The molar volumes of these compositions are found using the defined componential properties from the EOS model. The mechanical calculation of Eq. 4.1 is done in the composite *Calculation of WTC equation*.

4.3.2 Seed-Feed Dependency

The seed feed estimate is only an initial value used in the EOS flash calculation, to predict the equilibrium ratio (K_i) and molar volumes. The resulting wellstream compositions from this method are adjusted in order to match the measured rates. However, even if wellstream compositions are able to reproduce the volumetric rates, this does not mean that the composition will be able to give an accurate description of the fluid characterization. The seed feed is therefore still important, because it might have a significant effect on what the predicted fluid properties are.

To get a sense of the seed feed dependency on the adjusted wellstream compositions, we can use the compositions given in the reservoir output file ($z_{res,i}$). What we want to do is to assume an arbitrary seed feed, which is meant to represent a poor estimation of the known $z_{res,i}$-composition. Then, by only using the associated volumetric rates from the reservoir output to scale the seed feed with Eq. 4.1, we can see if the seed feed is able to converge towards the $z_{res,i}$-composition. A more descriptive illustration of this procedure is shown in **Fig. 4.7**. The WTC method would be independent of the seed feed if the adjusted wellstream composition are able to approximate (approach towards) the reservoir composition, no matter what the seed feed is chosen to be.

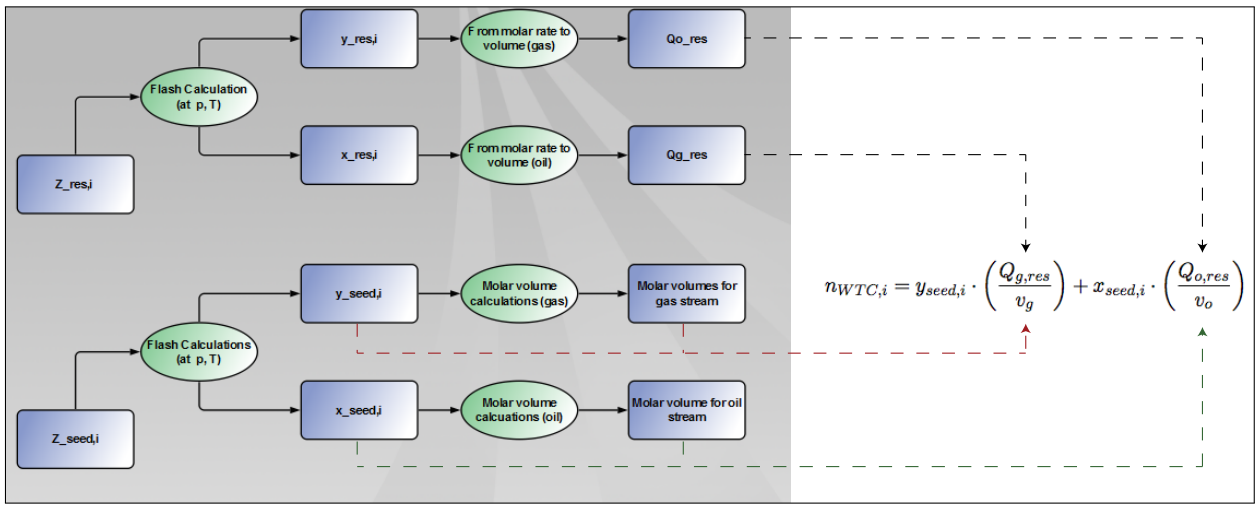

Figure 4.7: Using the reservoir output file to see the seed feed dependency on the adjusted wellstream composition from the WTC method.

In Fig. 4.7 we have a known wellstream composition ($z_{res,i}$) from the reservoir file, which can be used together with the EOS properties to find the associated volume rates ($Q_{o/g,res}$) at any set of conditions. The assigned seed feed ($z_{seed,i}$) is put through a flash operation, with the same conditions at which the Q_{res}-rates were found (could for example be SC). The resulting equilibrium phase composition ($y_{seed,i}$ and $x_{seed,i}$) and the corresponding molar volumes are then scaled with Eq. 4.1, in order to match the Q_{res}-rates. The adjusted wellstream compositions ($z_{WTC,i}$) can finally be compared with $z_{res,i}$ in reservoir file, to see if they are similar or if they have significant deviations.

This investigation was performed using two different wells, A04 (gas producer) and B06 (oil producer). To approximate the conditions seen at the multiphase meters, the flash operations of the compositions (see Fig. 4.7) were preformed at a pressure of 110 bara, and a temperature of 100°C. The arbitrary seed feed compositions used for the two well are given in **Table 4.1**, and the results from the WTC method are shown in **Fig. 4.8**.

	CO_2	C_1-N_2	C_2	C_3C_4	C_5C_6	C_7C_{10}	$C_{11}C_{15}$	$C_{16}C_{30}$	C_{31+}
A04 Seed-Feed	0.02	0.78	0.05	0.04	0.03	0.03	0.02	0.02	0.01
B06 Seed-Feed	0.02	0.78	0.05	0.04	0.03	0.03	0.02	0.02	0.01

Table 4.1: Arbitrary seed feed compositions used to investigate the seed feed dependency on WTC method.

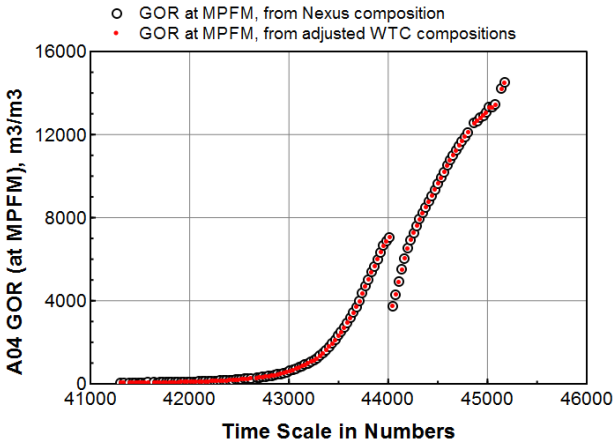

(a) Producing GOR for A04 at the proxy MPFM conditions. These volume rates should be consistent, as these are the rates used for the scaling process.

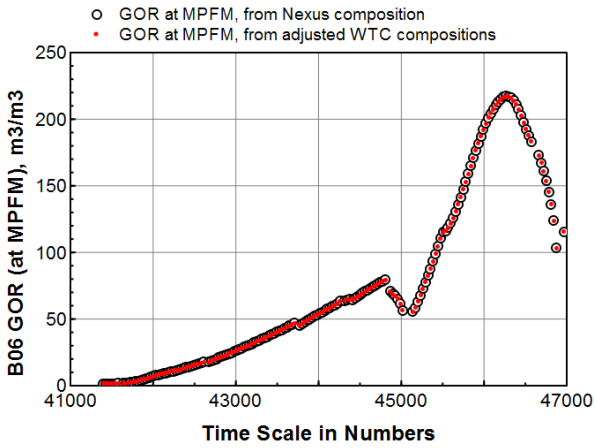

(b) Producing GOR for B06 at the proxy MPFM conditions. These values should be fairly consistent.

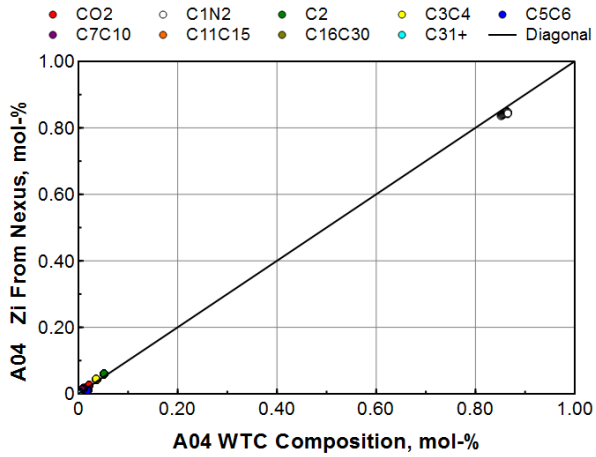

(c) A04 adjusted compositions after WTC against composition from reservoir file.

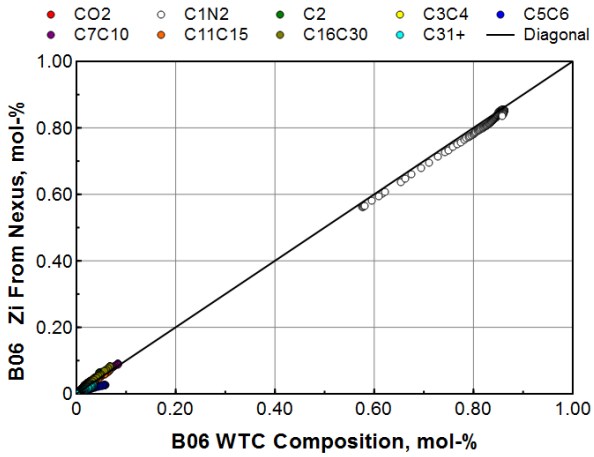

(d) B06 adjusted compositions after WTC against composition from reservoir file.

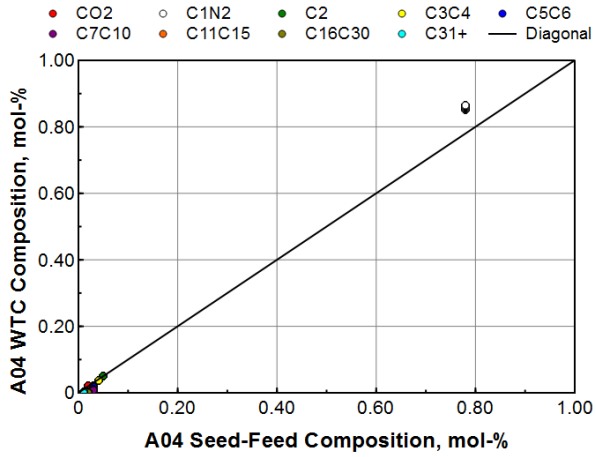

(e) Correction in seed feed for A04.

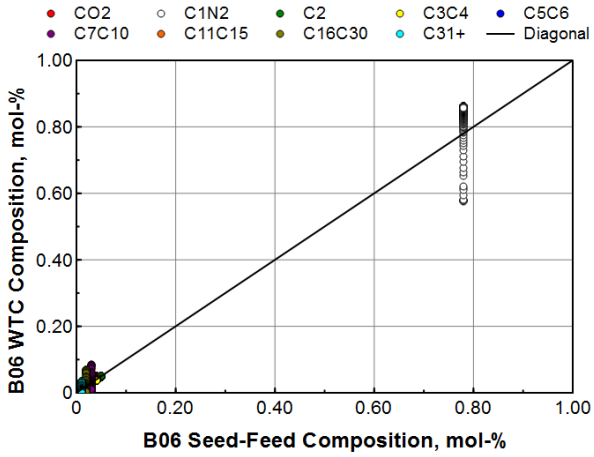

(f) Correction in seed feed for B06.

Figure 4.8: Adjusted WTC compositions generated by the WTC method. The volumetric rates should be accurate, but the compositions will have some deviations. Small deviations in heavier components might significantly alter the estimated gas condensate at surface.

It can be seen from Fig. 4.8 that the WTC method is able to correct the seed feed to a certain extent, but there is still some deviation between the adjusted wellstreams and the $z_{res,i}$-compositions. It is however difficult to relate to the significance of these deviations, as the molar components are not a very intuitive quantity. Note from **Figs. 4.8c and 4.8d** that the C_1N_2-component falls to the right of the diagonal curve, which means that this component is overestimated. This will in turn indicate that the WTC compositions are predicted to be too light, and the surface gas rates calculated using these compositions would be too high. Another observation from these figures is that the compositions for the oil well is much more dynamic then for the gas well (components span a much wider range).

It is interesting to check if the deviations of the adjusted WTC compositions have any noticeable influence on the predicted surface volume rates. To see if this is the case, we can put both the adjusted composition and the $z_{res,i}$-compositions through the same surface process, and examine if the calculated surface ratios are significantly different from each other. If they are significantly different, then this means that the adjusted WTC compositions are a poor representation of the actual compositions, as they are not able to estimate the correct volumetric rates. The surface process used in this analysis is the same as the one defined in Fig. 4.4, and all calculations are done using Pipe-It. The results from sending these compositions through the surface process is shown in **Figs. 4.9 and 4.10**.

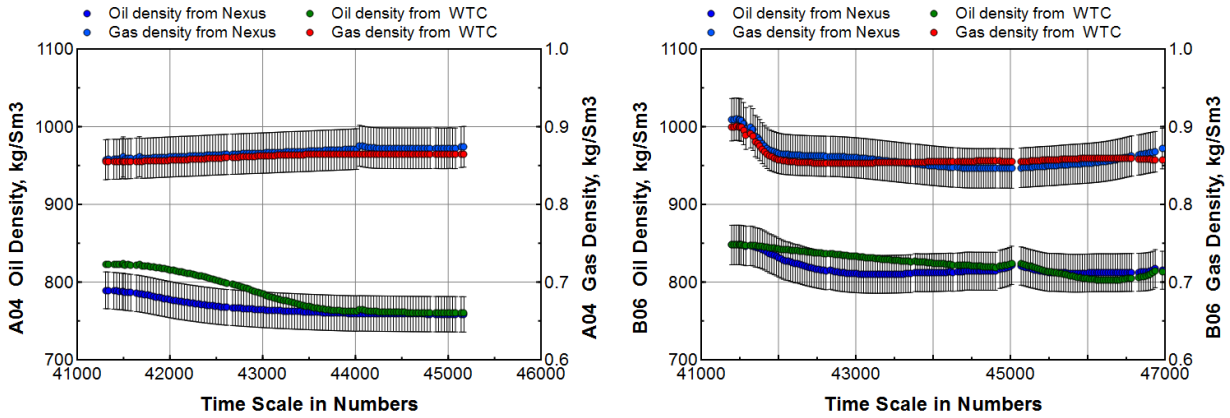

(a) Surface densities for A04.

(b) Surface densities for B06.

Figure 4.9: Comparison of surface densities, between the ones found from $z_{WTC,i}$ (adjusted WTC compositions) and those found from $z_{res,i}$ (compositions in reservoir file). All the error bars represent 3% deviation.

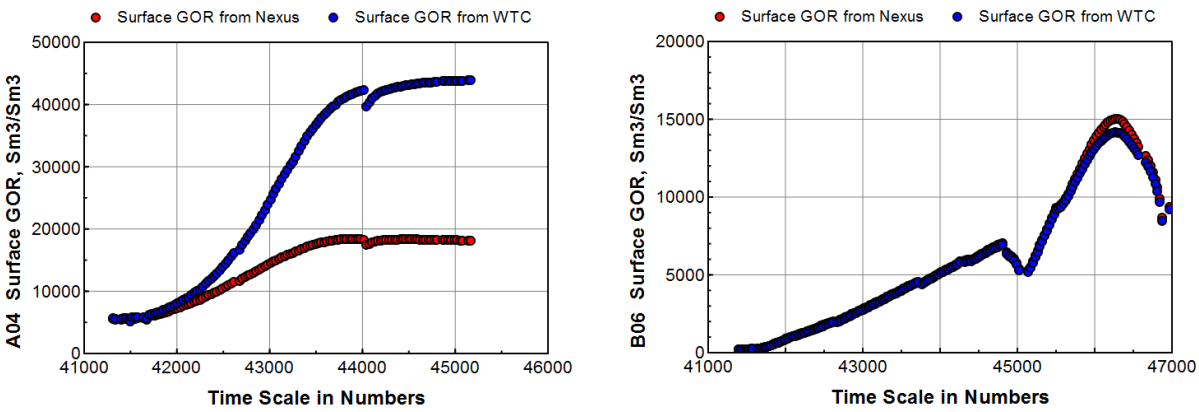

(a) Producing GOR for A04 at SC.

(b) Producing GOR for B06 at SC.

Figure 4.10: Comparison of producing GOR at surface conditions, between the ones found from $z_{WTC,i}$ and those found from $z_{res,i}$. The GOR for the gas well is especially bad, and the deviation grows with time.

The calculated surface densities that are shown in Fig. 4.9 do not seem to differ significantly from each other, and they are mostly within 3% range. However, the adjusted WTC compositions are not able to capture the producing GOR accurately, and the GOR for A04 seems to be particularly vulnerable. A possible reason for the poor GOR prediction of the gas well, might be because the condensate from the gas is very dependent on the heavy tail in the mixtures. There are usually much less of the heavier components in the gas phase than the lighter components, and small discrepancies in the tail will therefore have a considerable impact on the resulting condensate.

The main result from this simple exercise is that we cannot use an arbitrary seed feed if we want to predict the volumetric behavior of the fluid (as it moves from the multiphase meter to the surface). If we want to do the allocation process on a componential basis, then we need to have better seed feed estimates. It is common to have a laboratory test of the fluid characterization of a the initial wellstream before the well was first put on production. This is typically the characterization that is used for creating the EOS model and the black-oil tables, and this characterization would also be the reasonable choice of for the seed feed. **Fig. 4.11** shows some of the results, when doing the same exercise as before, but with using seed feed compositions as defined in **Table 4.2**.

	CO_2	C_1-N_2	C_2	C_3C_4	C_5C_6	C_7C_{10}	$C_{11}C_{15}$	$C_{16}C_{30}$	C_{31+}
A04 Seed-Feed	0.0253	0.8415	0.0603	0.0435	0.0108	0.0148	0.0032	4.94E-4	4.17E-6
B06 Seed-Feed	0.0189	0.5645	0.0632	0.0619	0.0269	0.0890	0.0681	0.0817	0.0258

Table 4.2: Seed feeds based on the compositions used in the development of the 9-component EOS model.

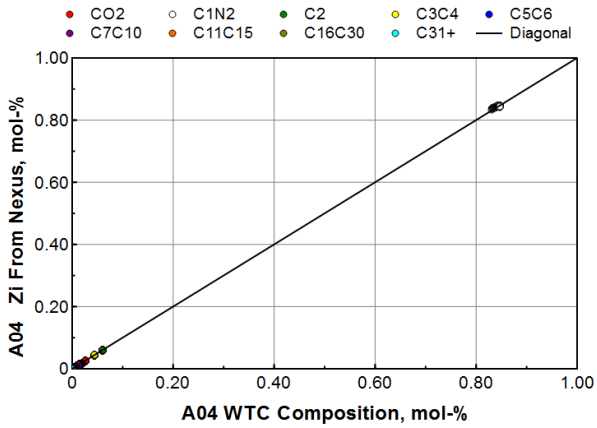

(a) A04 adjusted WTC compositions against the composition from reservoir file.

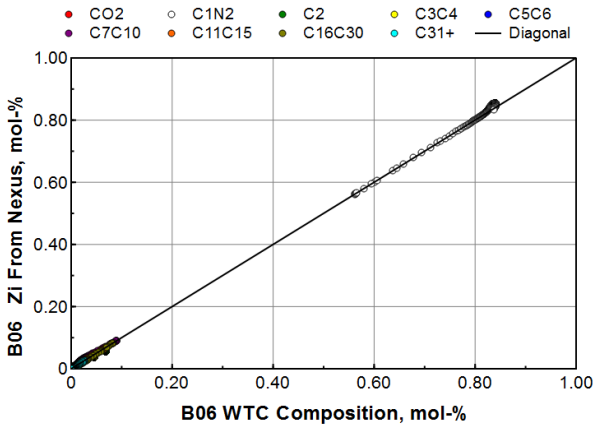

(b) B06 adjusted WTC compositions against the composition from reservoir file.

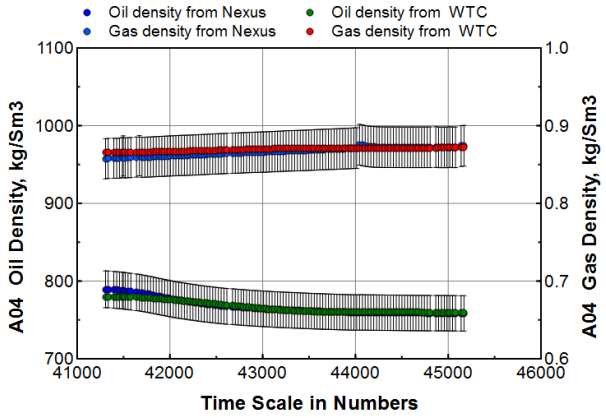

(c) Surface densities for A04.

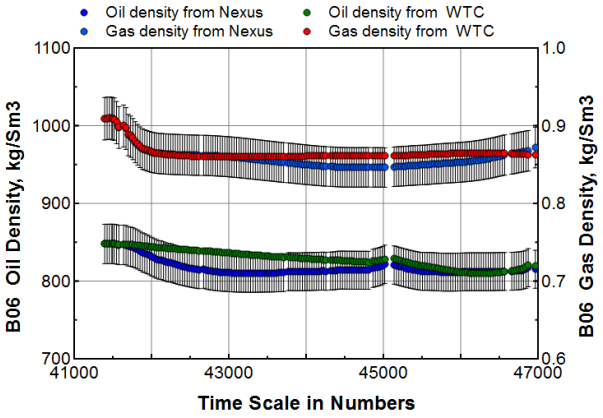

(d) Surface densities for B06.

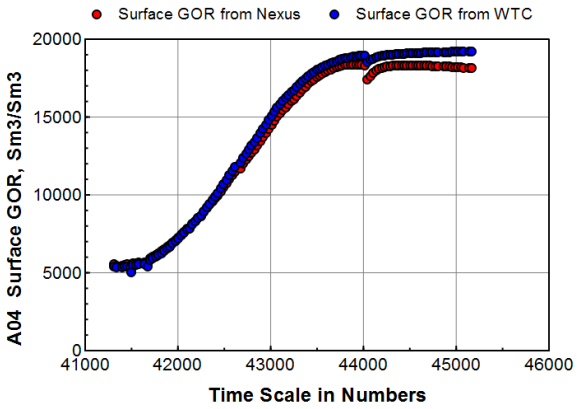

(e) Producing GOR for A04 at SC.

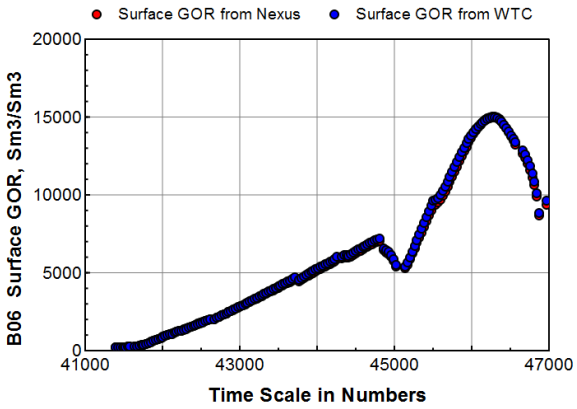

(f) Producing GOR for B06 at SC.

Figure 4.11: Results from WTC method when using more representative seed feed compositions.

The most noticeable difference in the results shown in Fig. 4.11 compared with the results from the arbitrary seed feed, is the improvement in the calculated surface GOR for the gas well. There are still some deviation between the results, however not as distinct.

So far in this discussion, the chosen seed feeds have been based on a constant composition (ie. Table 4.2). This means that for a given well, then all the wellstreams will be assigned with the same seed feed independent of the date, gas oil ratio, fluid density, or any other variable. If however the fluid properties for a specific well changes significantly as the well is produced, then this constant seed feed might start being mis-representative. A method that is more capable of capturing the dynamic effect of the well, is by using lookup tables. For a given well, then the seed feed composition can be assigned based on some control variables (time, fluid densities, volume ratios etc).

Well	measured OGR	Seed feed Zsi (CO2, C1, C2, C3 ...)			
J01	0.001	0.028	0.731	0.062	0.055 ...
J01	0.002	0.027	0.679	0.063	.....
⋮	⋮	⋮	⋮	⋮	⋮

Figure 4.12: Illustration of a lookup table for seed feed composition.

A lookup table can for example be generated by using a compositional reservoir simulation (which is often the most capable way of predicting the compositional behavior). It is however important to understand that even the reservoir simulator is only able to predict the dynamic effect to a certain extent. **Fig. 4.13** shows an illustration where the compositions from the reservoir simulator have been plotted against the volume ratios.

Notice that the compositions are almost a linear function with OGR. This means that if the OGR is used as the control variable, then the seed feed lookup table would only need a few data points, and the values in between the chosen points can be approximated using piece-wise linear interpolation. This type of OGR-based lookup table have been implemented and is used in the alternative allocation process. More about lookup tables, and how they can be automatically created in Pipe-It is discussed in **Section 4.5**.

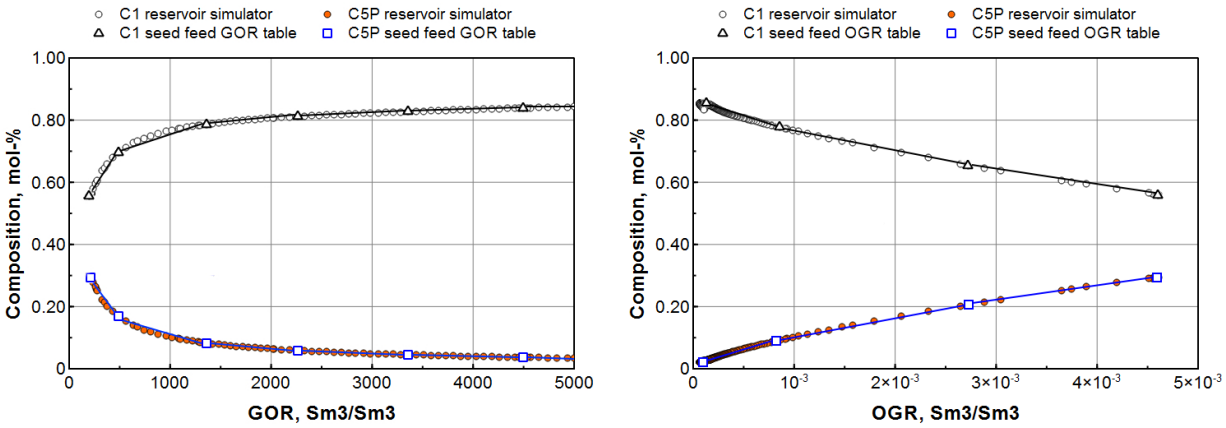

(a) Composition as function of GOR.

(b) Composition as function of OGR.

Figure 4.13: Using the reservoir simulator (compositional) output to create seed feed lookup table. This illustration only shows two components (C_1 and C_{5+}), plotted against volume ratios. GOR is usually non-linear and therefore not recommended for the linear interpolated seed feed table. Adapted from

4.4 Influence of the Topside Process on the Calculated Surface Rates

After the WTC method has used to convert the volumetric rates from the MPFM tests to compositional streams, then the resulting streams can be sent through a defined surface process. This section will focus on investigating the influence that this process has on the calculated surface rates. The way this investigation has been done, is by defining different topside processes and comparing the resulting surface rates from these processes against the surface rates based on black-oil properties.

For the purpose of this analysis, it was chosen to recalculate the black-oil propertied in Pipe-It, instead of using those already generated by BP. The procedure of finding the black-oil properties in Pipe-It is shown in **Fig. 4.14**. Every well is assigned a feed composition, which is flashed at the local MPFM conditions by assuming phase equilibrium at the meters. The resulting equilibrium phases are further flashed at standard condition to find the surface rates, which are then used to calculate the black-oil properties with Eqs. 2.14 through 2.17 (see Section 2.2.1 on page 20).

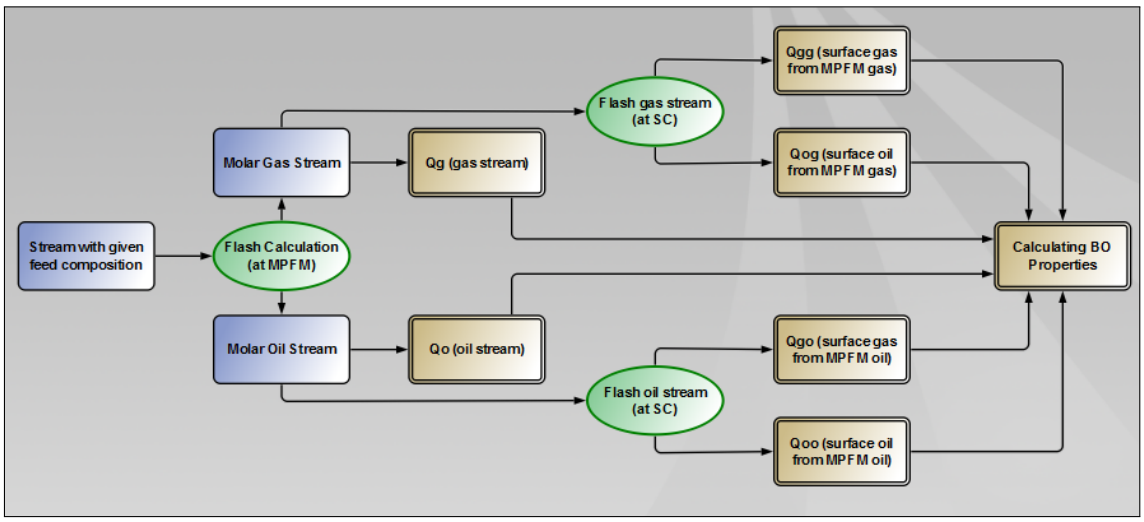

Figure 4.14: Generating black-oil properties using Pipe-It. A given feed composition is first flashed at line-conditions. The resulting equilibrium phases are then flashed at standard conditions in order to find; $Q_{\bar{g}g}$ (surface gas from MPFM gas), $Q_{\bar{o}g}$ (surface oil from MPFM gas), $Q_{\bar{g}o}$ (surface gas from MPFM oil), and $Q_{\bar{o}o}$ (surface oil from MPFM oil).

When using this method in Pipe-It, the black-oil properties are found for every individual well test at/using the local line conditions. For example if a specific well test is done at 106 bara and 98°C, then the black-oil properties are found at exactly these conditions. Consequently, the black-oil values generated in Pipe-It are not actually formulated as a table with discrete values at specific pressure and temperature steps. This is an advantage compared with the black-oil tables from the PVTp software (as currently done at BP), because that method require some form of interpolation between the discrete values. A comparison between the black-oil values generated by BP and those generated in Pipe-It can be found in **Appendix H**.

The calculated surface rates from the black-oil properties are shown in **Fig. 4.15**. In this figure the variable *well-id* is defined to be able to differentiate between the well tests. A number is assigned to every individual well, where the values below 20 represent gas wells and the values above 20 represent oil wells. The different well ids can be found in **Table 4.3**. The well test number (x-axis) seen in Fig. 4.15 is first sorted by the well ids, and then by date (from oldest to newest).

Well	Formation	Type	ID
A01	Snadd	Gas	11
A03	Skarv A	Gas	12
A04	Skarv A	Gas	13
A06	Skarv A	Gas	14
D02	Idun	Gas	15
D03	Idun	Gas	16
B06	Skarv B	Oil	21
B08	Skarv B	Oil	22
B09	Skarv C	Oil	23
B10	Skarv C	Oil	24
J01	Tilje	Oil	25
J04	Tilje	Oil	26

Table 4.3: Defined *well-ids* for the wells at Skarv.

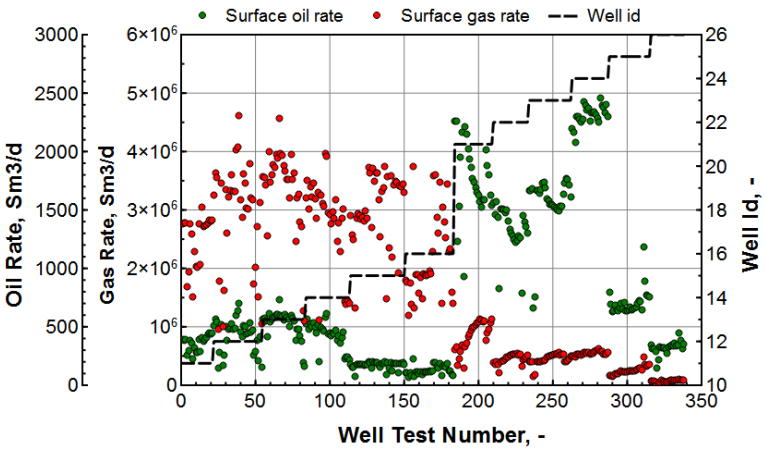

Figure 4.15: Resulting surface rates when converting MPFM tests using BO-properties. The BO-properties is generated in Pipe-It by using the procedure shown in Fig. 4.14.

There are in total four different topside process that will be compared again the surface rates from the black-oil properties. This is done by using the relative deviation, which are defined as follows

$$RD_o = 100\% \cdot \frac{(Q_{o,calculated} - Q_{o,BO})}{Q_{o,BO}} \quad . . . . . (4.2)$$

$$RD_g = 100\% \cdot \frac{(Q_{g,calculated} - Q_{g,BO})}{Q_{g,BO}} \quad . . . . . (4.3)$$

where $Q_{o,calculated}$ and $Q_{g,calculated}$ are the surface rates from the defined processes, and $Q_{o,BO}$ and $Q_{g,BO}$ are the surface rates using BO-properties. The main reason why it was decided to do the comparison using relative deviations, is because it is easier to see the difference than comparing the surface rates directly. The results from the different processes are shown in **Fig. 4.17**.

The comparison shown in **Fig. 4.17a** is based on the same four stage surface process as defined in the reservoir simulator. This surface process was shown in Fig. 4.4 (on page 56), and the corresponding separator conditions were defined in Table 3.1 (on page 40). It can be seen from this figure that the relative deviations for the surface gas rates are placed at around zero for all wells. The deviations in the surface oil rates are split in two parts; the first part is the oil rates from the oil producers, while the other part is the condensate from the gas producers. The oil coming from the oil wells lies fairly flat at around zero, whereas the condensate falls on the negative side, and have much bigger variations. The negative values for the deviations in the condensate implies that the four stage surface process predicts less condensate than the black-oil model (which is somewhat surprising). The reason for this behavior might be because the the black-oil model assumes a flash at the multiphase meters, which are generally at high pressure (promotes condensation). Furthermore, in the black-oil model the gas stream are flashed at standard conditions, which will also yield some condensate. In the four stage separation, the multistage separators are to gradually

splitting the gas from the liquid, and bring the oil stream to standard condition. However, the gas coming out of the different separators are never flashed at standard conditions the same way as in the black-oil model.

Also note that the black-oil properties are based on the initial lab-reported compositions, and do not account for any change in the fluid properties (unless they are updated). Because the wellstream usually becomes lighter as the reservoir is produced, the initial fluid compositions used in the black-oil model might be mis-representative and overestimate the heavy tail in the mixture.

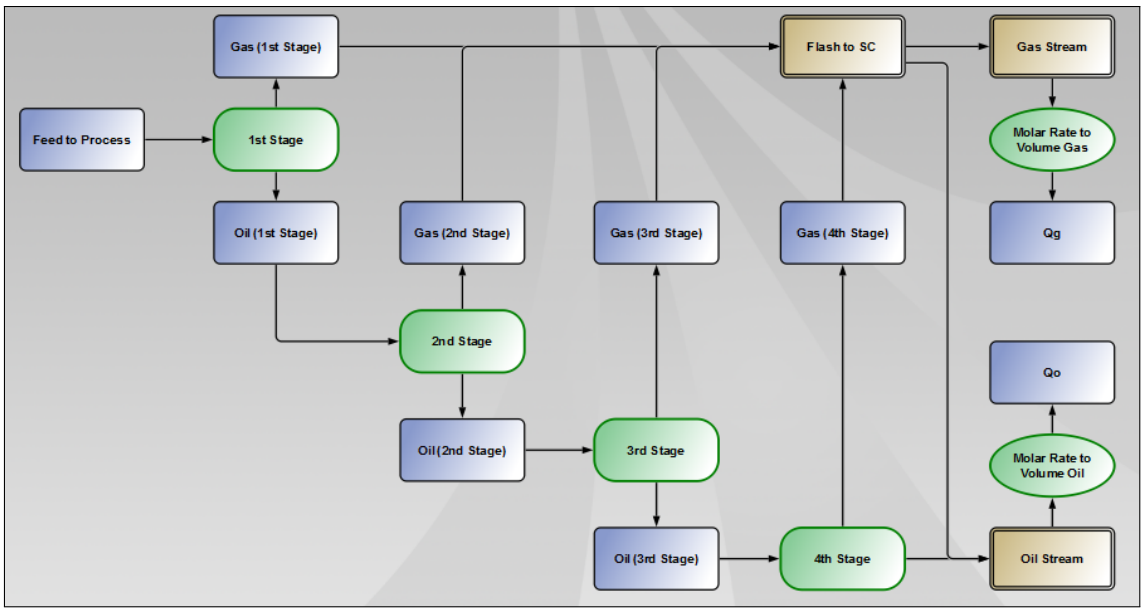

Figure 4.16: Surface process where the gas coming out of the separators are flashed to standard conditions. The condensate from this flash is commingled with the oil stream from the fourth stage separation.

The comparison shown in **Fig. 4.17b** is based on the same four stage process as before, but the gas coming out of the separators are now flashed at standard conditions. The resulting condensate from this flash is blended together with the oil stream coming out of the fourth stage separator. An illustration showing this process is given in **Fig. 4.16**. The separator conditions used for the different stages are still as defined in the reservoir simulator. It can be seen from Fig. 4.17b that the predicted condensate from the gas wells is shifted upwards, with the majority of the point right above zero. The gas rates from the gas producers, and the oil from the oil wells remain indifferent.

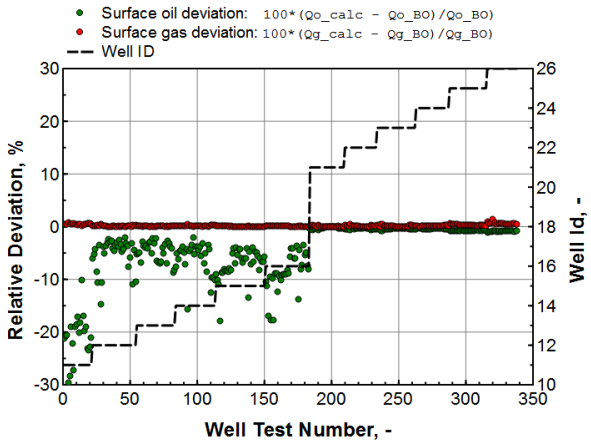

(a) Surface process is a 4 stage separation as defined in the reservoir simulator (Fig. 4.4). The separator conditions are also as defined in the reservoir simulator (Table 3.1).

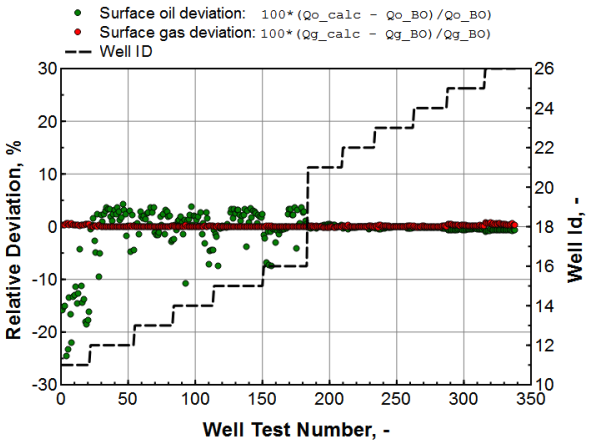

(b) Surface process is a 4 stage separation, and flash of the total gas out of the separator to standard condition (Fig. 4.16). The separator conditions as defined in reservoir simulator (Table 3.1).

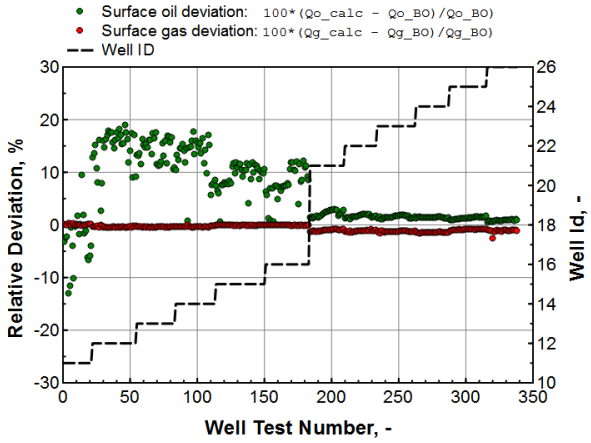

(c) Surface process is a 4 stage separation. The separator conditions are as defined in Table 4.4.

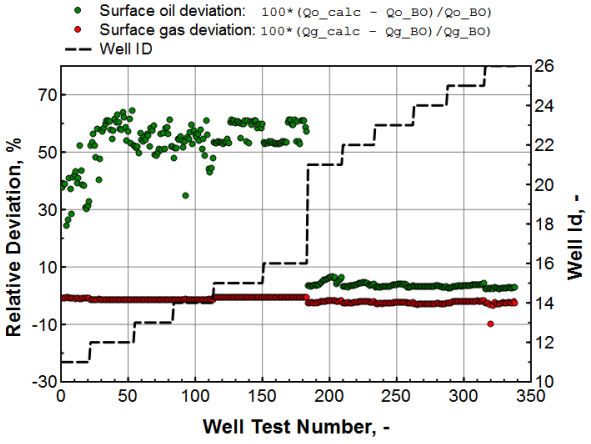

(d) Complex surface process, with scrubbers and recycling of condensate (Fig. 4.18). The separator conditions are as defined in Table 4.4.

Figure 4.17: Calculation of Surface Rates From Line Conditions, and dependency on the surface process. The relative deviations are found by comparing the surface rates from the defined process train, against the surface rates found using black-oil properties. The condensate from the gas stream are very dependent on the number and the conditions of separators (and scrubbers).

Fig. 4.17c is based on the same four stage separator process as in the reservoir simulator (same as Fig. 4.17a). The separator conditions are however different, and in this case they are defined as in **Table 4.4**. At Skarv the pressure- and temperature- conditions of the separators are measured on a continuously basis, and the conditions given in Table 4.4 are taken from a snapshot from such measurements (at 22th of April 2015). The main difference between these conditions and those defined in the reservoir simulator are the temperatures, which are around 20°C lower in this case for the 1st, 2nd and 3rd stage separator.

	Temperature [°C]	**Pressure [bara]**
1st stage	73	81
2nd stage	65	26
3rd stage	80	3.3
4th stage	15.6	1.0135
1st scrubber	26	3.1
2nd scrubber	27	8.9
3rd scrubber	26	26
Dehydrator scrubber	26	79
Export scrubber	4.4	69

Table 4.4: The conditions of the surface process. Based on pressure- and temperature- measurements from daily operations (22 April 2015).

It can be seen from Fig. 4.17b that the condensate from the gas producers are significantly higher then for the previous two cases. Compared to Fig. 4.17a, the condensate have increased with more than 20%. The surface oil from the oil wells have also increased somewhat, while the gas rate still remains at around zero deviation (the gas from oil wells is slightly reduced). This figure therefore indicate that the efficiency, and the total produced oil are very dependent on the separator conditions.

The last surface process that was studied is shown in **Fig. 4.17d**, which is based on a more complex train which includes the different scrubbers and the recycling of the condensate. How this process looks like is shown in **Fig. 4.18**, and the conditions used for the different separation vessels are those from Table 4.4. The first stage scrubber have the lowest pressure, and the pressures in the following scrubbers are gradually increasing. The dehydrator/glycol contractor scrubber has the highest pressure, but the last scrubber before the export compressors has the lowest temperature. Both high pressure and low temperatures promotes condensation, and these scrubbers will therefore have a considerable effect on the total produced oil.

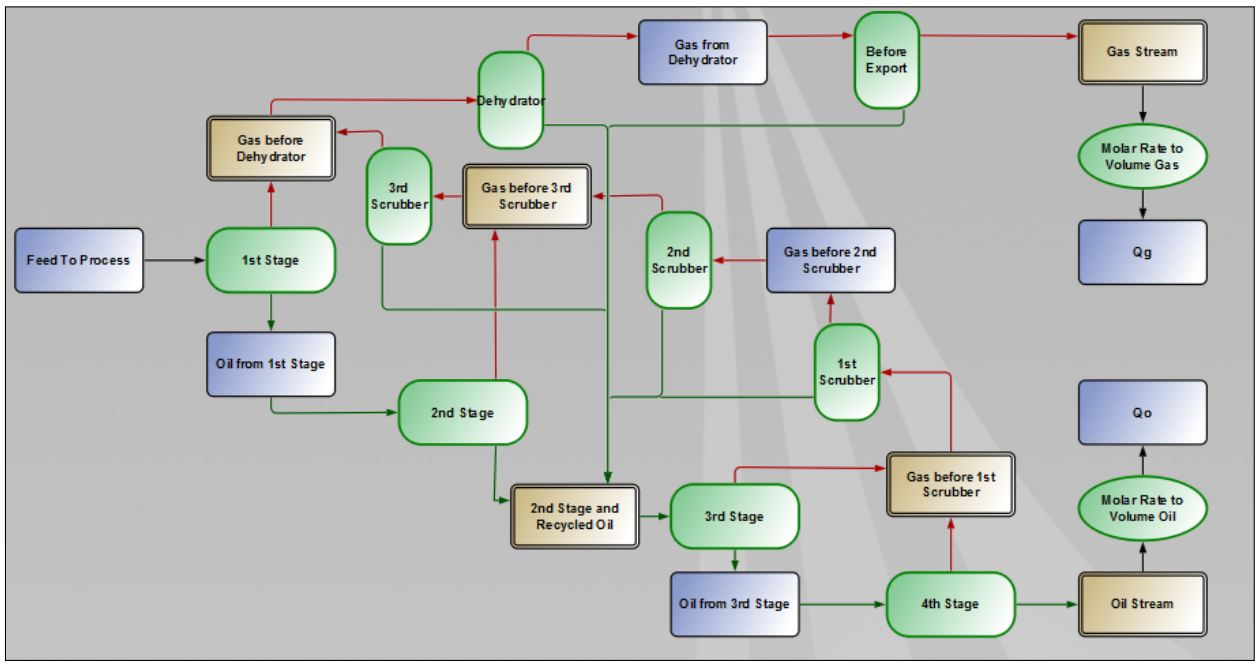

Figure 4.18: Implementation of a complex surface process, with scrubbers and recycling of condensate. This surface train is an iterative process, because the condensate from the scrubbers are commingled into the third stage separator. Should therefore check that the total amount of moles into the process is the same as the total amount of moles out. When the process have converged to a solution, the this means that the material balance is upheld. Also note that a process that includes recycled streams (as in this case), might require operator intervention in order to achieve a stable solution.

It can be seen from Fig. 4.17d that the condensate is significant higher then any of the other cases. The oil rate from the oil producers have also been shifted upwards with almost 5% compared with the black-oil properties. The gas rate from the gas producers have also been slightly reduced, but not very much (less then 1.5%).

4.5 Generating Lookup Tables

The previous section showed that the surface process have a significant impact on the calculated surface rates. This dependency on the process might also help explain the systematic deviation that was seen in the current allocation results (Section 3.3). It would therefore be interesting to compare the calculated surface rates based on one of the defined surface processes discussed in the previous section, against the meters measuring the rates out of facility. Before doing this comparison however, it is necessary to

1. Correct the daily theoretical rates (from the Integrated-Surveillance-Information-System) to match the rates from the multiphase meter tests.

2. Convert the corrected volumetric rates to daily molar compositional streams.

3. Add the individual molar streams together, and sending the resulting commingled stream through a defined surface process.

Note that the purpose of the last two steps is to capture the effect of commingling (instead of just adding the adjusted theoretical rates together). In the current allocation process, the multiphase tests are connected together with the daily rates by assigning appropriate correction factors and surface ratios in a manual fashion. This alternative allocation process is however based on an automatic procedure using lookup tables. One lookup table is needed to adjust the theoretical rates, whereas another lookup table is used to find the daily compositional streams.

Lookup Table for Correction Factors and Surface Ratios

Every single row in a lookup table consists of a unique key variable (or a set of variables), together with some associated reference data. The lookup table will in this case consist of two different key indexes, which are the well id and the well test date. Every single row in the table will therefore represent a specific MPFM test for a specific well. The reference data associated with the key variables are the correction factors and the surface ratios, and these values will depend on how the surface process in defined.

When one of the theoretical rates from the Integrated-Surveillance-Information-System matches one of the rows in the lookup table (have the same key indexes), then this theoretical rate will be assigned with the reference data from that lookup-row.

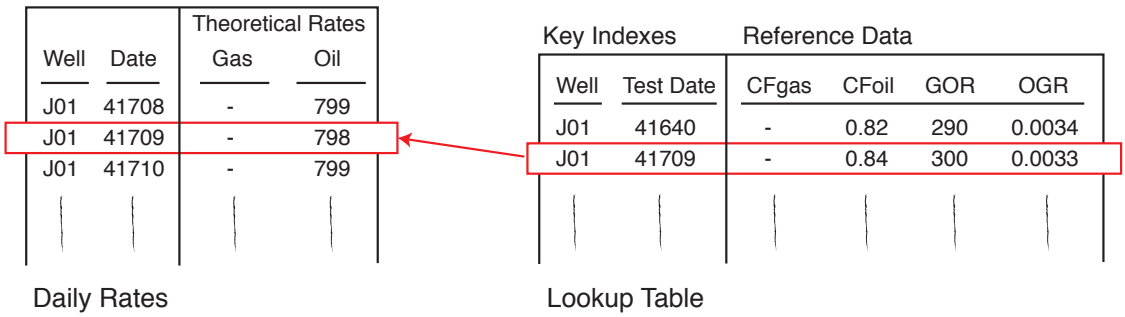

Figure 4.19: Illustration of lookup table for correction factors and surface ratios.

For the daily theoretical rates that falls in-between the well test dates, the correction factors and the surface ratios can be estimated by using interpolation. One typical interpolation method is to simply assume constant values from the latest well test **(Figs. 4.20a and 4.20b)**. This type of interpolation is the one chosen for the alternative allocation, as this is the method that closest resemble the way the correction factors are currently found at Skarv. The lookup table is created by using the AWK programming language, and this process is shown in **Appendix I**.

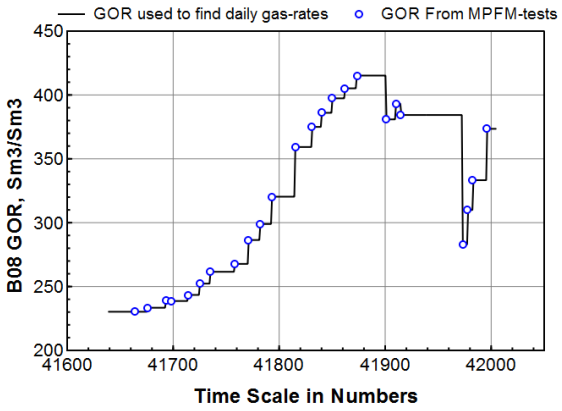

(a) Producing *GOR* used to find gas-rate from B08.

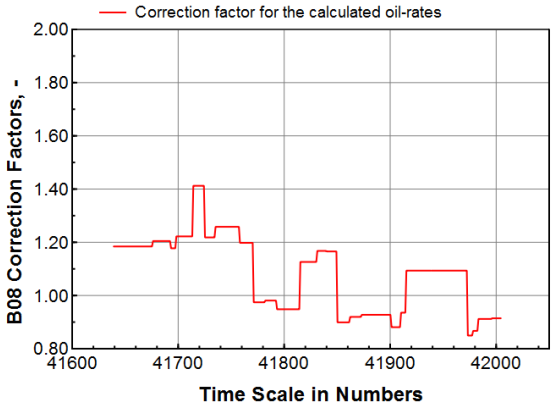

(b) Producing *GOR* used to find gas-rate from B08.

Figure 4.20: Show the GOR and the correction factors when using interpolation that assumes constant values from the latest well test.

Another typical method used is piecewise linear interpolation, which can be expressed as

$$f(x) \simeq f(x_1) + \frac{f(x_2) - f(x_1)}{x_2 - x_1} \cdot (x - x_2) \qquad (4.4)$$

This type of interpolation is shown in **Figs. 4.21a and 4.21b**. One of the advantages by finding

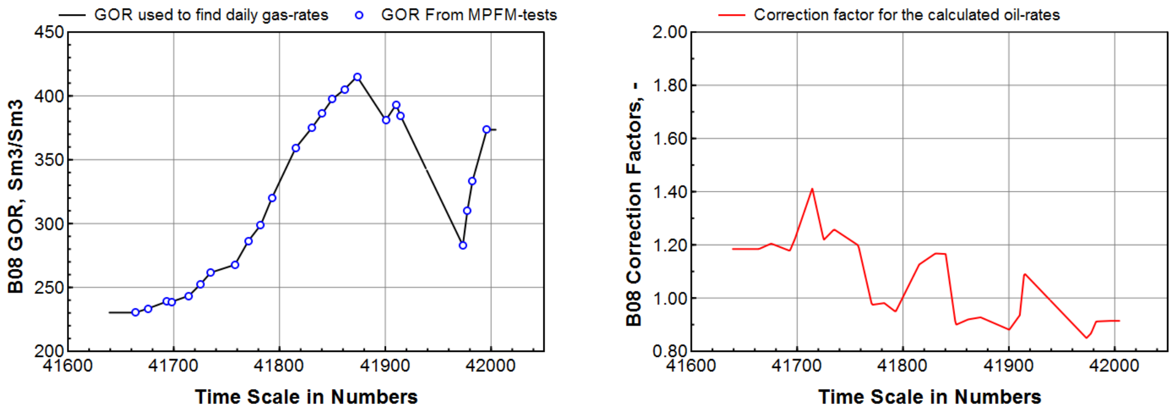

(a) Producing *GOR* used to find gas-rate from B08. (b) Producing *GOR* used to find gas-rate from B08.

Figure 4.21: Show the GOR and the correction factors when assuming linear interpolation.

the correction factors and surface ratios using lookup tables, is that the values are found in a consistent way following a specific pattern. It is therefore also easier to find anomalies, and strange behaviors. Another advantage is that it assures that every row in the table is unique, and that none of the well test dates overlap (ie. due to wrongly inputed data).

One disadvantages by using this automatic procedure, is that it becomes more difficult to make small changes that do not follow the specific pattern (for example to the correction factors). **Figs. 4.22a and 4.22b** show two different results from the adjusted theoretical rates, when using this automatic generated lookup table. In these figures there are two clear anomalies, which are developed as a result of dramatic changes in the calculated theoretical rates. These dramatic changes might for example occur if well performance models used to predict the daily rates are changed. The easiest way to correct for these anomalies, is to make specific changes to code (AWK programming language) that is used to create the tables, or optionally make changes to the table after it have been generated.

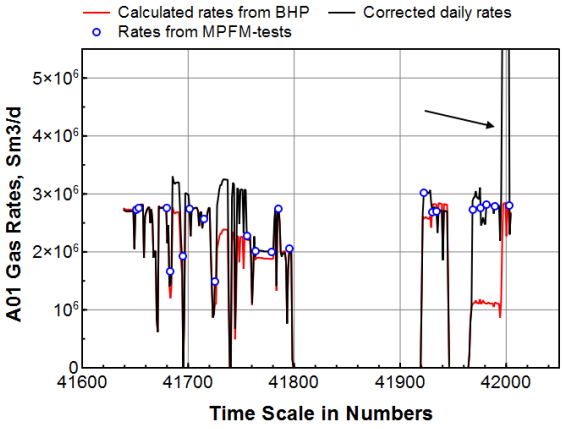

(a) Daily oil-rates for B08.

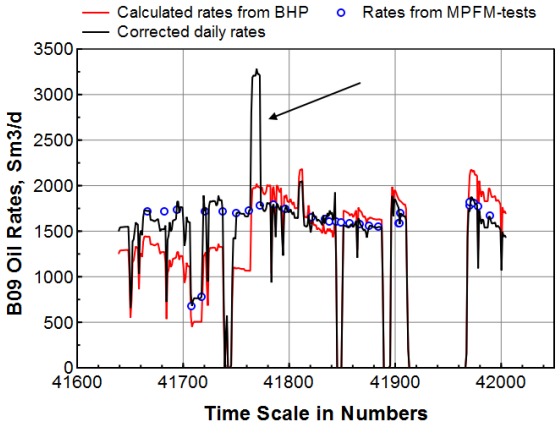

(b) Daily gas-rates for A06.

Figure 4.22: Resulting surface rates when using lookup tables (assuming constant interpolation).

Lookup Table for Normalized Compositions

The lookup table used for the compositions is not as intuitive as the one for the correction factors and the surface ratios. The reason is because this table is not actually used of distribute the compositional molar streams (n_i) to the daily rates. The molar streams that were found for the MPFM test (in Section 4.3) are only representative for the volumetric rates at these test, as they were the volumes that the seed feed were scaled to match. However, the estimated daily rates in-between test-periods will constantly fluctuate depending on the measured pressures. As a consequence, the compositional molar streams cannot simply be linear interpolated or assumed to be the same as the last well test (as was the case for the correction factors). If for example the compositional molar rates were to be linear interpolated, then this is equivalent to assuming that the volumetric rates are linear in-between the test, which we know is not true. If the compositional lookup table was used to assign the compositional molar streams to the daily time-basis directly; then these assigned molar streams would only give an accurate representation of volumetric rates at the test-periods (and not the period in between).

The compositions need to be normalized (z_i) before they can be used to generate the lookup table. After they are assigned to the daily basis, then they need to be rescaled to fit the adjusted daily rates (that are found from correcting the theoretical rates). This rescaling is done using the WTC method in a similar way that was done for the MPFM tests (in Section 4.3). This means that the normalized compositions in the lookup table will actually act as seed feed compositions, feeding this new WTC process. An important distinction between this new WTC and the one that was used for the MPFM tests, is that the new seed feeds are not flash at the MPFM line conditions. This is because the adjusted daily rates that is used for the scaling, are reported at

standard conditions, which means that the new seed feed also needs to be brought to standard conditions. Consequently, the flash that was used in the MPFM tests needs to be replaced by an equivalent process train that was used to convert the MPFM rates to surface condition. **Fig. 4.23** shows the procedure for scaling the compositions using the new WTC (in Pipe-It).

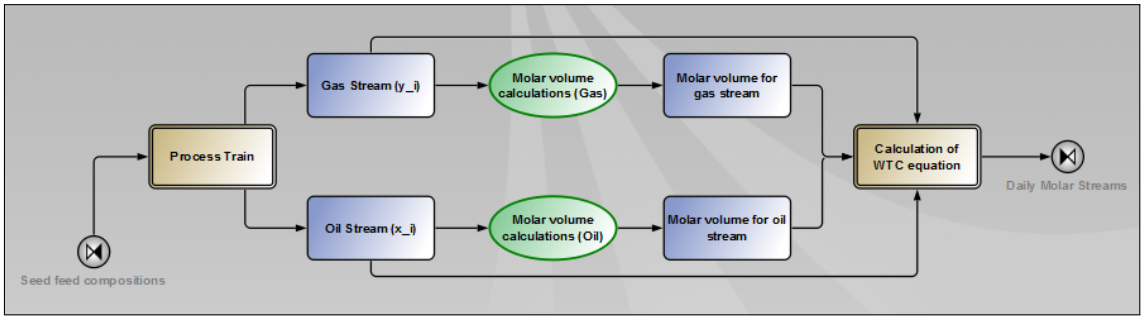

Figure 4.23: WTC method used to rescale compositions to match the corrected theoretical rates. The process train should be defined the same way as the one used to convert the MPFM rates to standard conditions.

The compositional lookup table is also created by using the AWK programming language, and the code can be found in **Appendix I**. An illustration that shows the overall process for connecting the multiphase meter data with the daily rates using lookup tables, is shown in **Fig. 4.24**.

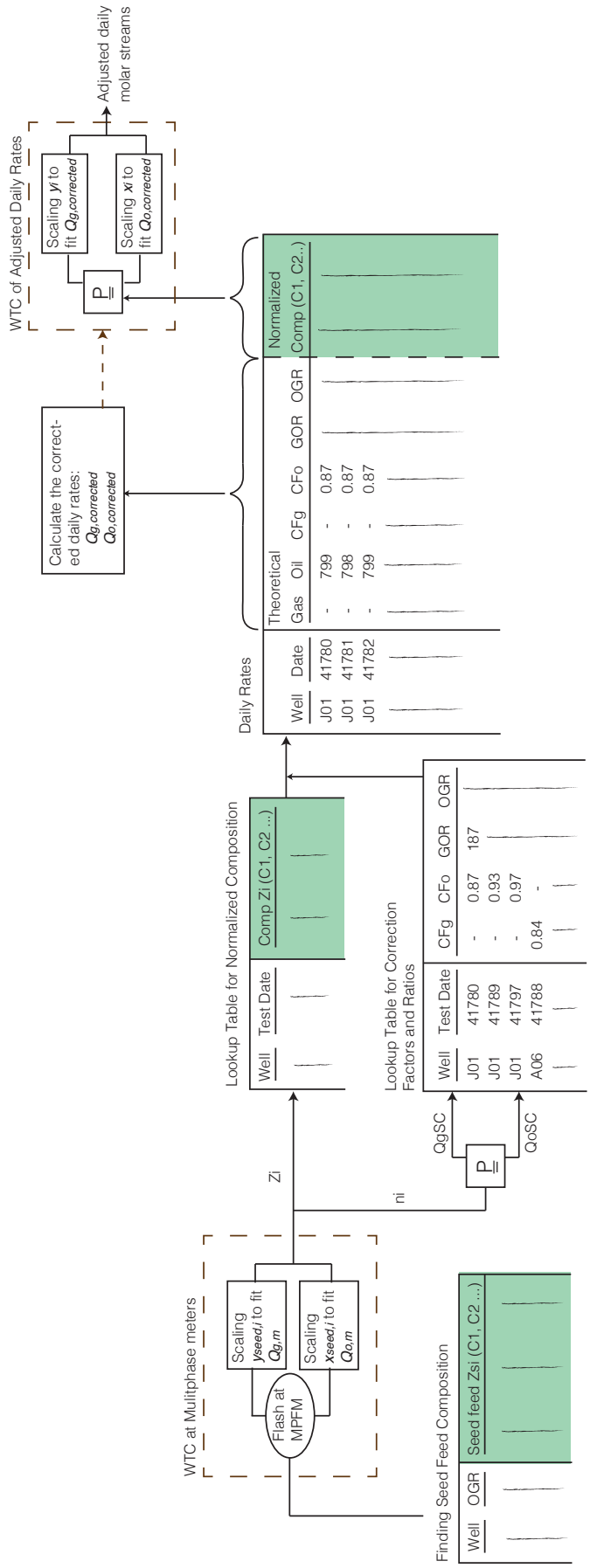

Figure 4.24: This illustration shows all the major steps that is used to find the lookup tables, and how the resulting tables are connected to the daily rates. The first step is to assign seed feed compositions to the wellstreams used for the MPFM tests. These seed feeds are then scaled to match the measured volumetric rates using the WTC method. The molar streams calculated from the WTC method is either normalized, and used to generate the compositional lookup table, or sent through a process train in order to find the surface rates. The surface rates out of the process train are used to generate a lookup table for the correction factors (calculated using Eqs. 2.12a and 2.12b), and the surface ratios. The key variables in both lookup tables are used to assign (or collect) all the information to the daily rates. The correction factors are used to adjust the theoretical gas rates (for gas wells), and the theoretical oil rates (for oil wells). The OGR is used to find the daily oil rates (for gas wells), and the GOR is used to find the daily gas rates (for oil wells). All of these corrected daily rates are then used to scale the normalized compositions (found from the compositional lookup table), by using a new WTC procedure. The normalized compositions need to go through an equivalent surface process as the surface rates from the MPFM data. The main result of going through all these steps is to find estimations of the daily molar rates.

4.6 Processing of Commingled Flow at the FPSO

The individual wellstreams are not processed exactly the same way when they are sent through the facility by themselves, and when they are sent through the facility as a commingled blend. This non-linearity is also known as the effect of commingling (EOC), and this effect will be greater if the fluid characterization for the individual wellstreams are very dissimilar. The final step in the alternative allocation process is therefore to collect the daily molar steams together, and reprocess them as a commingled wellstream.

This section will go through some of the results after doing the reprocessing, and compare the calculated product-rates against the meters measuring the rates out of facility. The different processes that will be looked at here, will be the same ones that were discussed in **Section 4.4** (when finding the surface rates for the MPFM tests). Note that when for example the detailed surface train have been used for the reprocessing, then this train have also been used in all other parts in the allocation system. This means that the same process have also been used to find the surface rates for the MPFM tests, and the surface equilibrium compositions needed in the second WTC procedure.

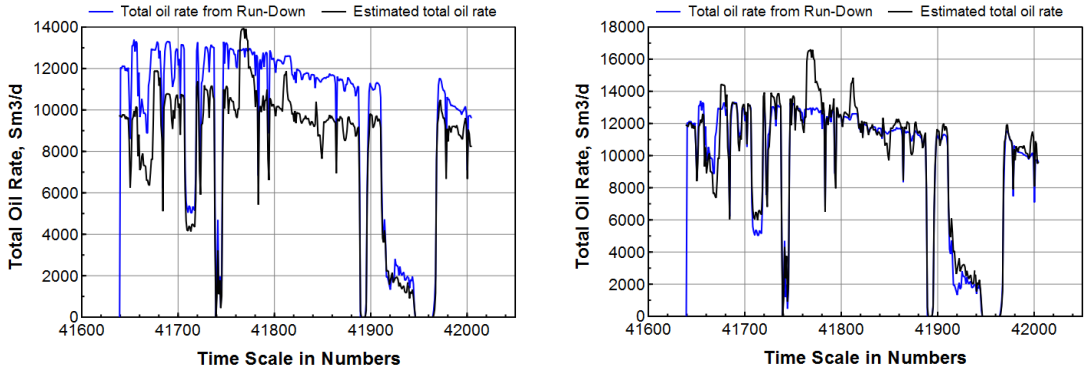

(a) Calculated oil rates based on the the same surface process as in the reservoir simulator.

(b) Calculated oil rates based on the complex surface process with scrubbers and recycling.

Figure 4.25: Comparison of product oil out of facility, when using the alternative allocation method. Blue lines represent the rates from meters measuring the total streams out of facility.

Figs. 4.25a and 4.25b show the calculated oil rates out facility for two different cases. Fig. 4.25a is based on the surface process defined in Nexus, whereas Fig. 4.25b is based on the detailed process train (that was given in Fig. 4.18). It can be seen that there is a considerably difference in the oil rates between these two cases, and most of this difference is due to the increased condensate from the produced gas stream. However even if the detailed process is predicting more oil, it is still not able to fill the gap between what is calculated and what is actually measured. Also notice the predicted oil rates in the time interval 41920 to 41940 (September 2014). In this period none of the

oil wells were producing, which means that the measured oil represents the condensate from the gas wells. The calculated oil rate in Fig. 4.25a is less than measured, which indicate underestimation of condensate. In Fig. 4.25b however, the calculated condensate seems to be somewhat above the measured, which might indicate overestimation of condensate. It is also important to understand that due to the shut-in of the oil producers, the production system and the surface facility will also be in a transient state (not steady flow). The duration and significance of this transient state is not know, but it will effect the calculated theoretical rates and the efficiency of the facility.

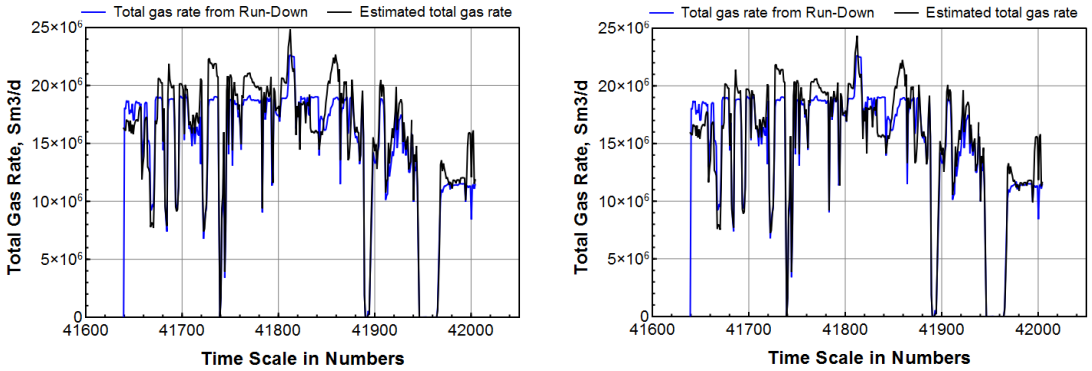

(a) Calculated gas rates based on the the same surface process as in the reservoir simulator.

(b) Calculated gas rates based on the complex surface process with scrubbers and recycling.

Figure 4.26: Comparison of product gas out of facility, when using the alternative allocation method. Blue lines represent the rates from meters measuring the total streams out of facility.

Figs. 4.26a and 4.26b show the calculated gas rates out facility for the same two cases. These two figures look almost identical, and there are only minute differences in the estimated surface gas. This insensitivity on the process train was also shown in Section 4.4, when surface rates from the MPFM tests were compared against the BO model.

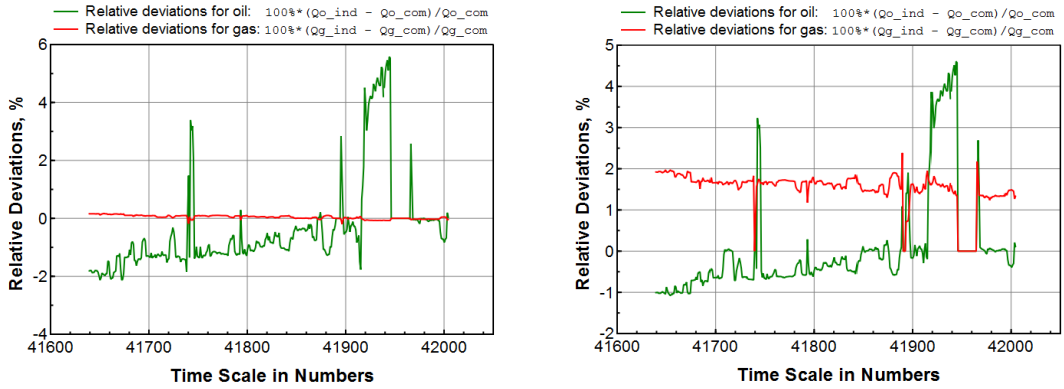

(a) EOC, surface process as in the reservoir simulator.

(b) EOC, detailed process with scrubbers and recycling.

Figure 4.27: Relative deviation between sum of individual wellstreams sent through process by independently, and the commingled flow.

Figs. 4.27a and 4.27b shows the difference in the total production, when sending the wellstreams through the surface process individually (adding them together afterwards), and when sending them through as a commingled stream. The relative deviation that in these figures are calculated as

$$RD_o^{EOC} = 100\% \cdot \frac{(Q_{o,individual} - Q_{o,commingled})}{Q_{o,commingled}} \quad (4.5)$$

$$RD_g^{EOC} = 100\% \cdot \frac{(Q_{g,individual} - Q_{g,commingled})}{Q_{g,commingled}} \quad (4.6)$$

where $Q_{o,individual}$ is the rates when streams are processed individually, and $Q_{commingled}$is the rates when processed as commingled stream. It can be seen from these figures that the effect of commingling is on the produced rates, and also how the surface train looks like. Fig. 4.27a shows that when the process is defined as in the reservoir simulator, then the EOC on the oil rates ranges from -2% to 6%. The EOC on the oil rates in the detailed process train is shown in Fig. 4.27b.

Figs. 4.28 and 4.29 show the relative deviations for the surface rates and the surface ratios, based on the same two cases as above. The relative deviations are calculated using Eqs. 3.3 through 3.6 that was defined in Section 3.3 (results from the current allocation process). Fig. 4.28 is based on the process used in Nexus, and it can be seen that this case have higher deviations than what were found using the black-oil tables in the current allocation method. This finding is not surprising, because we also found in Section 4.4 that this process estimated less surface oil from the MPFM tests compared with the black-oil model (see Fig. 4.17a). Fig. 4.29 is based on the detailed process, and it can be seen that the deviations in the oil rates have been improved compared to the four stage separation used in Nexus. The deviation in the gas rates are almost the same in both cases.

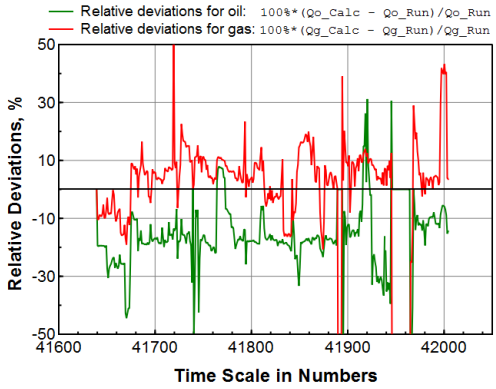

(a) Relative deviations between calculated surface rates and measured rates.

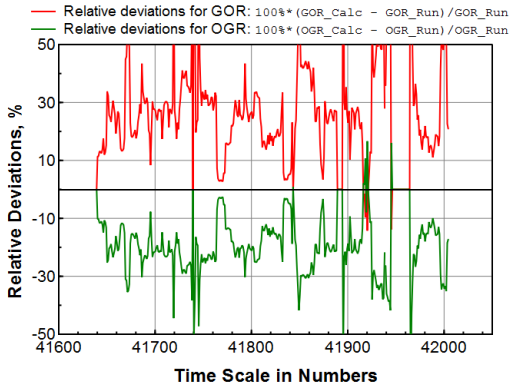

(b) Relative deviations between calculated surface ratios and measured ratios.

Figure 4.28: Relative deviations based on the the same surface process as in the reservoir simulator, and the same conditions (Table 3.1).

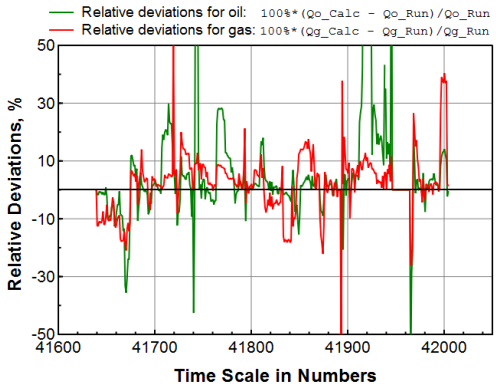

(a) Relative deviations between calculated surface rates and measured rates.

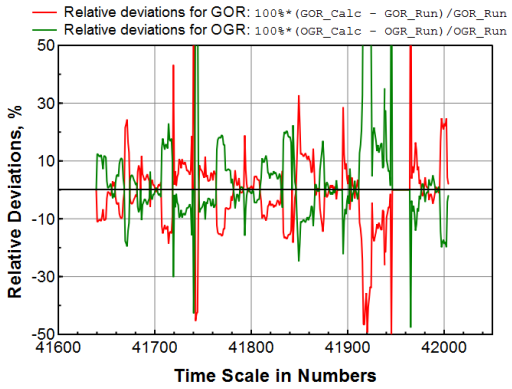

(b) Relative deviations between calculated surface ratios and measured ratios.

Figure 4.29: Relative deviations based on complex separation process with scrubbers and recycling. Conditions as defined in Table 4.4.

If comparing the deviations from either of these cases against the current allocation method, it is evident that the surface rates from the alternative allocation method fluctuates a great deal more. Part of these fluctuations is due to the correction factors found when using the automatically generated lookup tables. In the current allocation method, the engineer responsible can tune these factors to account for strange behaviors, or when the theoretical models (in the Integrated-Surveillance-Information-System) are updated.

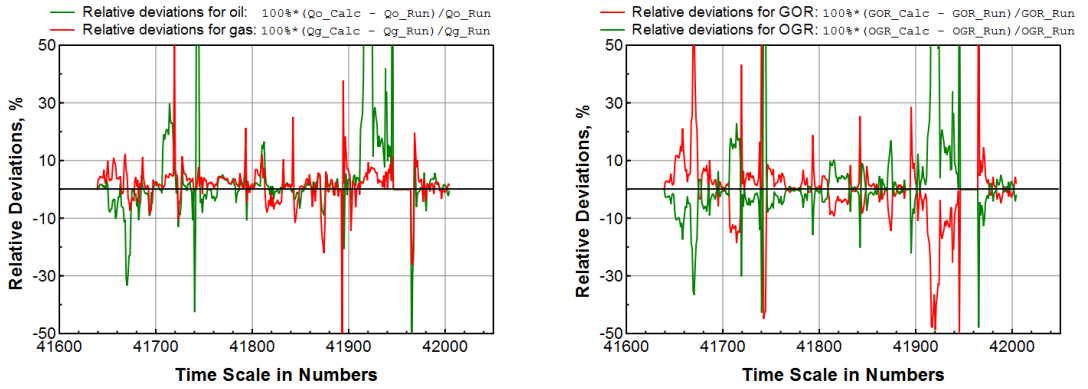

(a) Relative deviations between calculated surface rates and measured rates.

(b) Relative deviations between calculated surface ratios and measured ratios.

Figure 4.30: Relative deviations based on complex separation process with scrubbers and recycling. Conditions as defined in Table 4.4.

Fig. 4.30 shows an example of where the correction factors have also been tuned for the alternative allocation, in order to adjust for clear anomalies in the daily rates (ie. the peaks shown in Figs. 4.22a and 4.22b). It can be seen that this tuning of the correction factors will remove some of the fluctuations, but only to a certain extent.

The spike in the oil relative deviation around the time interval 41920 to 41940 is somewhat worrying. The oil rates in this period is very low, and small differences in the calculated and measured rates will have a big influence on the resulting relative deviation. However, if this spike is a result of overestimation in the condensate, then this might mean that

- The conditions used for the detailed process are not be representative of the conditions throughout the whole time interval.
- The lumped nine component EOS used in the alternative allocation method do not give an accurate description of the real fluids produced.
- The seed feed found from the WTC method is not able to predict the wellstream compositions accurate enough.

Another factor that might influenced the allocation, is the accuracy of the estimated theoretical

rates in between the MPFM tests. Also, if there is something wrong with the multiphase meter measurements themselves, then this will also have an impact.

Fig. 4.31 shows the calculated monthly oil rates compared with the fiscal meter, using the two cases discussed above (after tuning the correction factors). The relative deviations are calculated using Eqs. 3.9 and 3.10 that was defined in Section 3.3.

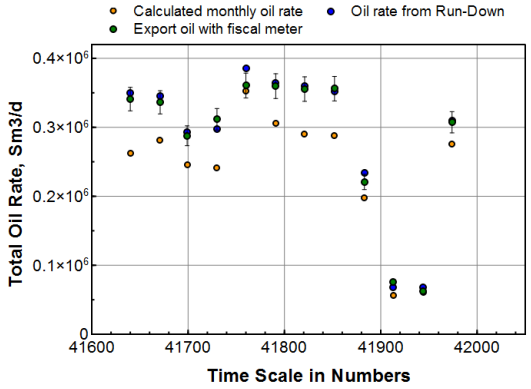

(a) Comparison of monthly oil rates. Topside process defined as in Nexus.

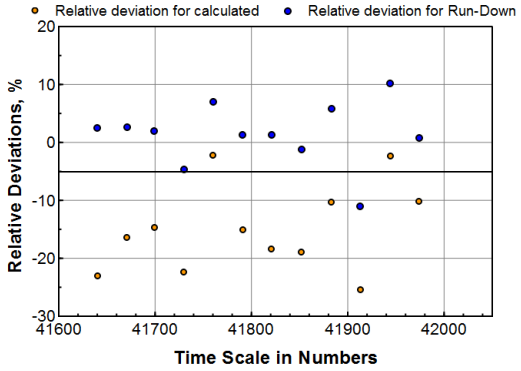

(b) Comparison with relative deviations, process defined as in Nexus.

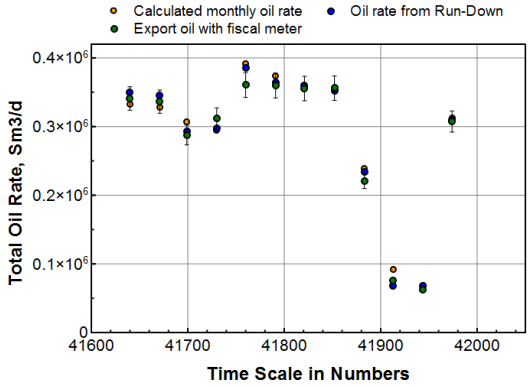

(c) Comparison of monthly oil rates, when using detailed process.

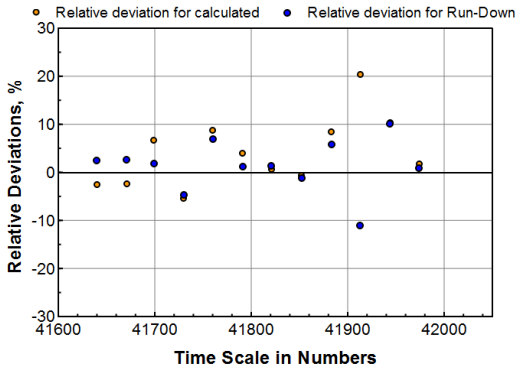

(d) Comparison with relative deviations, when using detailed process.

Figure 4.31: Comparisons of calculated monthly rates, when compared against the measured oil from storage into cargo. The error bars (when comparing rates) represents 5% deviation from fiscal.

4.7 Recommendation and Future Work

Doing the allocation in an automatic way has some benefits from doing it manually (as currently done at BP). It makes it much easier to change or manipulate the system as a whole, for example changing the topside process or the fluid model used. If the fluid model were to be changed in the current allocation method, then the engineer responsible would have to recalculate every single test and find the appropriate correction factors and surface ratios again. Doing the allocation automatically would save a lot of time, and it gives some assurance that all the calculated production rates are found in a consistent way.

However, it can be seen from the results from the alternative allocation method that there is still more work that can be done to improve the calculated surface rates. A considerable amount of the oil is produced from the condensate, and it is important to predict this condensate accurately. If an automatic allocation method were to be adapted, then on should also consider the following:

1. Estimate the wellstream compositions using the BOz method (instead of WTC method), and see if this have any impact on the final results.
2. Change the lumped nine component EOS used in the alternative allocation method to the 24 component EOS (used to find the black-oil tables in the current allocation). There are some differences between these models, and they will predict different amounts of surface volumes (which was seen in Appendix H).
3. Make a proxy model of the iterative recycled process, in order to simplify the train and save computation time.
4. Improve the daily theoretical rates estimated by Integrated-Surveillance-Information-System. Automatic updating of for example well deliverability models (ie. updating Prosper files) could also be integrated into Pipe-It.

In addition to this, the test separator at the Skarv has not been properly integrated into the alternative allocation system (nor the current allocation system). The test separator could be a very useful tool for validating the test measurements from the MPFM, and should therefore be included in the allocation system.

Chapter 5

Conclusions

- Results from the current allocation method used at Skarv show a systematic deviation between the calculated daily rates, and the rates measured out of facility. The total calculated gas rates appears to be overestimated, whereas the total oil rates are underestimated. The reason for this deviation could be a consequence of the fluid model used, and how the multiphase meters measurements are brought to standard conditions (using black-oil models).
- The proposed alternative allocation system is based on an automatic procedure, and calculate the surface rates based on compositional streams, a given EOS model, and a defined process. This system was used to do sensitivities of the topside process facility, and see the influence on the calculated surface rates. This analysis showed that the condensate from the gas wells are very dependent on how the separation train looks like, and the corresponding conditions of the separation vessels. By using a detailed surface process that includes scrubbers and recycling of the gas, then the condensate was increased by over 70% compared with using black-oil models with single-stage-flash to SC. This further indicate that the systematic deviation seen in the current allocation method is a result of how the MPFM test are brought to SC.
- The alternative allocation system was also used to process the wellstreams as a commingled flow, on a daily basis. This showed that the effect of commingling can be considerable. The total oil production when processing the commingled stream could differ up to 6% compared with sending the wellstreams through the facility individually (and adding them at SC after the processing). The resulting total calculated oils from the alternative allocation system (and using a detailed process train), do not see the same underestimation compared to the measured rates.

Definitions and Nomenclature

Abbreviations

BIP	–	binary interaction parameter
BO	–	black-oil
BOz	–	black-oil to compositional method
CCE	–	constant composition expansion
CF	–	correction factors
CGR	–	condensate gas ratio
EOC	–	effect of commingling
EOS	–	equation of state
FPSO	–	floating production, storage and offloading
GOR	–	gas oil ratio
I	–	systematic imbalance
IPR	–	inflow performance relationship
MPFM	–	multiphase flow meter
OGR	–	oil gas ratio
$\underline{\underline{\mathrm{P}}}$	–	a process
PI	–	productivity index
PR	–	Peng-Robinson equation of state
PVT	–	pressure/volume/temperature analysis
SC	–	standard conditions

SPK – Soave-Redlich-Kwong equation of state

STO – stock tank oil

VFP – vertical flow performance

WTC – well test conversion method

Nomenclature and Symbols

a = empirical constant used in equation of state (5.1)

A = empirical constant used in equation of state

b = empirical constant used in equation of state

B = empirical constant used in equation of state

B_{gd} = dry gas formation volume factor, m^3/Sm^3

b_{gd} = gas expansion factor, Sm^3/m^3

B_o = oil formation volume factor, m^3/Sm^3

b_o = oil shrinkage factor, Sm^3/m^3

CF = correction factor

f = fugacity

F_v = vapor mole fraction

I = system imbalance

J = productivity index

K_i = equilibrium ratio of component i

k_{ij} = binary interaction parameter of between the components i and j

$\dot{m}$ = mass flux

$\dot{n}$ = molar flux

N = total number of components

p = pressure, bar

p_c = critical pressure, bar

p_r = reduced pressure, bar

p_{sep} = pressure of separator, bar

p_{ST} = stock tank pressure, bar

p_{bi} = bubblepoint pressure, bar

p_{di} = dewpoint pressure, bar

$\bar{p}_r$ = average reservoir pressure, bar

p_{wf} = bottomhole flowing pressure, bar

Q = rate in volume, mass or moles

R = universal gas constant

R_p = producing gas oil ratio, Sm^3/Sm^3

R_s = solution gas oil ratio, Sm^3/Sm^3

r_p = producing oil gas ratio, Sm^3/Sm^3

r_s = solution oil gas ratio, Sm^3/Sm^3

s = volume shift factor

T = temperature, °C

T_c = critical temperature, °C

T_r = reduced temperature, °C

T_{sep} = temperature of separator, °C

$\dot{v}$ = volume flux

v = molar volume, m^3/mol

V_g = volume gas at given conditions, Sm^3

$V_{\bar{g}}$ = surface volume of gas, Sm^3

V_o = volume oil at given conditions, Sm^3

$V_{\bar{o}}$ = surface volume of oil, Sm^3

x_i = molar fraction of component i in the liquid phase, mol-%

y_i = molar fraction of component i in the vapor phase, mol-%

z_i = molar fraction of component i in the mixture, mol-%

Z = compressibility factor

α = allocation factor or reconciliation factor

δ_{RMS} = root mean square error

ϵ = error threshold

ρ = density, kg/m^3

σ = variance

ϕ = fugacity coefficient

ω = acentric factor

Ω_a = empirical constant used in equation of state

Ω_b = empirical constant used in equation of state

Bibliography

API RP 85, Use of Subsea Wet-gas Flowmeters in Allocation Measurement Systems, first edition. 2003. Washington, DC: API.

API RP 86, Measurement of Multiphase Flow, first edition. 2005. Washington, DC: API.

Corneliussen, S. , Couput, J. -P. , Dahl, E. et al. (2005). *Handbook of Multiphase Flow Metering*. Norwegian Society for Oil and Gas Measurement (NFOGM) and The Norwegian Society of Chartered Technical and Scientific Professionals (Tekna).

Eck, D. J. (2003). Production metering and well testing system. US Patent No. 6,561,041.

Economides, M. J. , Hill, A. D. , Ehlig-Economides, C. et al. (2013). *Petroleum Production Systems*, second edition. Westford, Massachusetts: Pearson Education, Inc.

Energy Institute Staff (2012). *Hydrocarbon management 96: Guidelines for the Allocation of Fluid Streams in Oil and Gas Production*, first edition. London: Energy Institute.

Golan, M. and Whitson, C. H. (1986). *Well Performance*, second edition. Englewood Cliffs, New Jersey: Prentice Hall, Inc.

Hoda, M. F. (2002). *The Engineering of Petroleum Streams*. Ph.D. Thesis, Norwegian University of Science and Technology, Trondheim (June 2002).

Hoda, M. F. and Whitson, C. H. (2013). Well test rate conversion to compositional wellstream. Paper SPE-164334-MS presented at the SPE Middle East Oil and Gas Show and Exhibition, Manama, Bahrain, 10–13 March. `http://dx.doi.org/10.2118/164334-MS`

Kappos, L. , Economids, M. J. , and Buscaglia, R. (2011). A holistic approach to back allocation of well production. Paper SPE-145431-MS presented at the SPE Reservoir Characterisation and Simulation Conference and Exhibition, Abu Dhabi, UAE, 9–11 October. `http://dx.doi.org/10.2118/145431-MS`

Kuntadi, A. (2012). *Stream Conversion Technology and Gas Condensate Field Developement*. Ph.D. Thesis, Norwegian University of Science and Technology, Trondheim (June 2012).

Lorentzen, R. J., Saevareid, O. , and Naevdal, G. (2010). Soft multiphase flow metering for accurate production allocation. Paper SPE-136026-MS presented at the 2010 SPE Russian Oil & Gas Technical Conference and Exhibition, Moscow, Russia, 26–28 October. http://dx.doi.org/10.2118/136026-MS

McCracken, M. and Chorneyko, D. M. (2006). Rate allocation using permanent downhole pressures. Paper SPE-103222-MS presented at the 2006 SPE Annual Technical Conference and Exhibition, San Antonio, Texas, 24–27 September. http://dx.doi.org/10.2118/103222-MS

Theuveny, B. C. and Mehdizadeh, P. (2002). Multiphase flowmeter applicaton for well and fiscal allocation. Paper SPE-76766-MS presented at the SPE Western Regional/AAPG Pacific Section Joint Meeting, Anchorage, Alaska, 20-22 May. http://dx.doi.org/10.2118/76766-MS

van der Geest, R., Broman, W.H. , Fleming, R. H. et al. (2001). Reliability through data reconciliation. Paper OTC-13000-MS presented at the 2001 Offshore Technology Conference held in Houston, Houston, Texas, 30 April–3 May. http://dx.doi.org/10.4043/13000-MS

Webb, R. A. (2008). Application of phase behavior models in production allocation systems. US Patent No. 7,373,285 B2.

Whitson, C. H., Brulé, M. R. (2000). *Phase Behavior*. Monograph Series, Richardson, Texas: Society of Petroleum Engineers Inc.

Appendices

Appendix A

Example Using Uncertainty-Based Allocation

A system consist of a reference Run-Down meter (Q_z) that measure the oil-rate out of facility into storage tank, and four individual wells measured by MPFMs.

$$Q_z = 4500\ Sm^3/d \pm 5\% \quad \text{(A.1)}$$

$$Q_{W1} = 1500\ Sm^3/d \pm 10\% \quad \text{(A.2)}$$

$$Q_{W2} = 500\ Sm^3/d \pm 7\% \quad \text{(A.3)}$$

$$Q_{W3} = 750\ Sm^3/d \pm 9\% \quad \text{(A.4)}$$

$$Q_{W4} = 1300\ Sm^3/d \pm 13\% \quad \text{(A.5)}$$

Because all the measurements are at reference conditions, the system imbalance can be found as

$$I = Q_z - \sum_{i=1}^{N=4} Q_i \quad \text{(A.6)}$$

$$= 4500 - (1500 + 500 + 750 + 1300) = 450\ Sm^3/d \quad \text{(A.7)}$$

The variance of the different meters can be found as

$$\begin{aligned}
\sigma_z^2 &= (Q_z \cdot 5\%)^2 = (4500 \cdot 5\%)^2 = 50625 \quad (Sm^3)^2 \\
\sigma_{W1}^2 &= (Q_{W1} \cdot 10\%)^2 = (1500 \cdot 10\%)^2 = 22500 \quad (Sm^3)^2 \\
\sigma_{W2}^2 &= (Q_{W2} \cdot 7\%)^2 = (500 \cdot 7\%)^2 = 1225 \quad (Sm^3)^2 \\
\sigma_{W3}^2 &= (Q_{W3} \cdot 9\%)^2 = (750 \cdot 9\%)^2 = 4556 \quad (Sm^3)^2 \\
\sigma_{W4}^2 &= (Q_{W4} \cdot 13\%)^2 = (1300 \cdot 13\%)^2 = 28561 \quad (Sm^3)^2
\end{aligned} \quad \text{(A.8)}$$

The total uncertainty in throughput variance

$$\sum_{j=1}^{N=4} \sigma_j^2 = 22500 + 1225 + 4556 + 28561 = 56842\ (Sm^3)^2 \quad \text{(A.9)}$$

The allocations factors can then be found as by using **Eq. 2.11** (from **Section 2.1.5**)

$$\alpha_{W1} = \frac{22500}{50625 + 56842} + \frac{1500}{4050} \cdot \frac{50625}{50625 + 56842} = 0.3838 \quad \text{(A.10)}$$

$$\alpha_{W2} = \frac{1225}{50625 + 56842} + \frac{500}{4050} \cdot \frac{50625}{50625 + 56842} = 0.0696 \quad \text{(A.11)}$$

$$\alpha_{W3} = \frac{4556}{50625+56842} + \frac{750}{4050} \cdot \frac{50625}{50625+56842} = 0.1296 \quad . . . . . \text{(A.12)}$$

$$\alpha_{W4} = \frac{28561}{50625+56842} + \frac{1300}{4050} \cdot \frac{50625}{50625+56842} = 0.4170 \quad . . . . . \text{(A.13)}$$

The adjusted rates for each well can then be calculated

$$Q_{W1}^{allocated} = Q_{W1} + I \cdot \alpha_{W1} = 1500 + 450 \cdot 0.3838 = 1673\ Sm^3/d \quad . . . . . \text{(A.14)}$$

$$Q_{W2}^{allocated} = Q_{W2} + I \cdot \alpha_{W2} = 500 + 450 \cdot 0.0696 = 531\ Sm^3/d \quad . . . . . \text{(A.15)}$$

$$Q_{W3}^{allocated} = Q_{W3} + I \cdot \alpha_{W3} = 750 + 450 \cdot 0.1296 = 808\ Sm^3/d \quad . . . . . \text{(A.16)}$$

$$Q_{W4}^{allocated} = Q_{W4} + I \cdot \alpha_{W4} = 1300 + 450 \cdot 0.4170 = 1488\ Sm^3/d \quad . . . . . \text{(A.17)}$$

And the sum of these allocated rates

$$\sum_{i=1}^{N=4} Q_i^{allocated} = 1673 + 531 + 808 + 1488 = 4500\ Sm^3/d = Q_z \quad . . . . . \text{(A.18)}$$

Appendix B

Derivation of Rachford-Rice Equation

Two-phase flash calculations are usually based on a component material balance constraint, which can be expressed as

$$n = n_v + n_L \quad \text{(B.1)}$$

$$nz_i = n_v y_i + n_L x_i \quad \text{(B.2)}$$

$$z_i = F_v y_i + (1 - F_v) x_i \; ; \qquad \text{where } F_v = \frac{n_v}{n_L + n_v} \quad \text{(B.3)}$$

where i represent the components, and F_v is the vapor mole fraction. Using the definition of the equilibrium ratio ($y_i = K_i x_i$), and rearranging **Eq. B.3** with respect to x_i gives

$$z_i = F_v \cdot (K_i x_i) + (1 - F_v) x_i \quad \text{(B.4)}$$

$$= x_i [F_v (K_i - 1) + 1] \quad \text{(B.5)}$$

$$x_i = \frac{z_i}{F_v (K_i - 1) + 1} \quad \text{(B.6)}$$

We also know that all mole fractions will by definition sum to one

$$\sum_{i=1}^{N} y_i = \sum_{i=1}^{N} x_i = \sum_{i=1}^{N} z_i = 1 \quad \text{(B.7)}$$

$$\sum_{i=1}^{N} (y_i - x_i) = 0 \quad \text{(B.8)}$$

The Rachford-Rice equation can then be derived by combining **Eq. B.6** and **Eq. B.8**

$$\sum_{i=1}^{N} (y_i - x_i) = \sum_{i=1}^{N} x_i \, (K_i - 1) \quad \text{(B.9)}$$

$$= \sum_{i=1}^{N} \frac{z_i (K_i - 1)}{1 + F_v (K_i - 1)} = 0 \quad \text{(B.10)}$$

$$= \sum_{i=1}^{N} \frac{z_i}{F_v + c_i} = 0 \; ; \qquad \text{where } c_i = \frac{1}{K_i - 1} \quad \text{(B.11)}$$

where **Eq. B.10** is the Rachford-Rice equation, and **Eq. B.11** is the Muskat and McDowell equation (computationally more efficient). Both of these equations can be solved iteratively by using for example Newton's method.

Appendix C

Inflow Performance Relationships

Production From Oil Reservoirs

Production of single-phase oil is given by

$$q_o = J \cdot \Delta p \quad \text{(C.1)}$$

$$= J_D \cdot \frac{kh}{\alpha_c^o B_o \mu_o} \cdot \Delta p \quad \text{(C.2)}$$

where k is the permeability, h is the net thickness of the reservoir, B_o is the oil FVF, μ_o is the oil viscosity, Δp is the drawdown, J_D is the dimensionless productivity index, and α_c^o is a constant depending on units used ($\alpha_c^o = 141.2$ for field units). The dimensionless productivity index is a variable that depends on the flow conditions, and is defined as

$$J_D = \left[\ln \frac{r_e}{r_w} + s\right]^{-1}; \quad \text{for steady state} \quad \text{(C.3)}$$

$$= \left[\ln \frac{0.472 r_e}{r_w} + s\right]^{-1}; \quad \text{for pseudosteady state} \quad \text{(C.4)}$$

$$= \left[1.15\left(\log \frac{kt}{\phi \mu c_t r_w^2} - 3.23 + 0.87s\right)\right]^{-1}; \quad \text{for transient state} \quad \text{(C.5)}$$

where r_e is the radius of outer boundary, r_w is the radius of the wellbore, s is the skin factor, ϕ is the porosity, and c_t is the total compressibility factor. Steady state means that means that all variables (including rate and pressures) are independent of time. This state will only hold true if the reservoir pressure is maintained constant, for example with natural water influx or water injection. Producing under pseudosteady state refers to when all the boundaries are felt, and the reservoir pressure have a constant decline with time. Transient state describe a system that is infinite-acting, meaning that the outer boundary is still not felt. This state is most often found at start of production, or reservoirs with very low permeability (ie. carbonate reservoirs).

If assuming that Darcy's equation is valid, then production of single-phase gas can be expressed as

$$q_g = \frac{kh \cdot [m(p_e) - m(p_{wf})]}{\alpha_c^g \cdot T \left[\ln \frac{r_i}{r_w} + s + Dq_g\right]}; \quad \text{steady} \quad \text{(C.6)}$$

$$= \frac{kh \cdot [m(\bar{p_R}) - m(p_{wf})]}{\alpha_c^g \cdot T \left[\ln \frac{0.472 r_e}{r_w} + s + Dq_g\right]}; \quad \text{pseudosteady} \quad \text{(C.7)}$$

$$= \frac{kh \cdot [m(p_i) - m(p_{wf})]}{1.15 \cdot \alpha_c^g \cdot T \left[\log \frac{kt}{\phi \mu_g c_t r_w^2} - 3.23 + 0.87(s + Dq_g)\right]}; \quad \text{transient} \quad \text{(C.8)}$$

where $m(p)$ is the real gas pseudopressure function, D is the non-Darcy coefficient, and α_c^g is a constant depending on units used ($\alpha_c^g = 1424$ for field units). The term Dq_g is often called the turbulent skin effect, and the D coefficient is typically in the order of 10^{-3}. For low gas rates, the turbulent skin effect will be negligible. The pseudopressure function is defined as

$$m(p) = 2\int_{p_0}^{p} \frac{p}{\mu_g Z} dp \quad \text{(C.9)}$$

$$\approx \frac{p^2 - p_0^2}{\mu Z}; \quad \text{pressures} < \sim 2000 \text{ psi} \quad \text{(C.10)}$$

$$\approx 2\frac{\bar{p}}{\bar{\mu}\bar{Z}} \cdot (p - p_0); \quad \text{pressures} > \sim 3000 \text{ psi} \quad \text{(C.11)}$$

where Z is the compressibility factor. Another common equation for the gas flow rate, is Fetkovich's approximation given as

$$q = C(\bar{p_R}^2 - \bar{p_{wt}}^2)^n \quad \text{(C.12)}$$

where C and n are empirical coefficient. This equation is also called the backpressure equation, and the value of n should be between 0.5 and 1. If the rate q is plotted against $(\bar{p_R}^2 - \bar{p_{wt}}^2)$ on a log-log plot, then this would show a straight line with slope $1/n$ and intercept C. Note that this equation could also be used this equation for oil reservoir, but this is not very common.

Two-Phase IPR

When producing from a saturated oil reservoir, then there will be two phases producted into the reservoir. Vogel (1968) proposed an empirical equation which can be used for such two-phase flow

$$\frac{q_o}{q_{o,\ max}} = 1 - 0.2\left(\frac{p_{wf}}{p_b}\right) - 0.8\left(\frac{p_{wf}}{p_b}\right)^2 \quad \text{(C.13)}$$

$$q_{o,\ max} = \left(\frac{1}{1.8}\right)\frac{k_o h \bar{p}_R}{141.2 B_o \mu_o \left[\ln\frac{0.472 r_e}{r_w} + s\right]} \quad \text{(C.14)}$$

where $q_{o,\ max}$ is referred to as the absolute open flow (the rate when $p_{wf} = 0$). Another empirical euation is the normalized form of Fetkovich's approximation proposed by Golan and Whitson

$$\frac{q_o}{q_{o,max}} = \left[1 - \left(\frac{p_{wf}}{\bar{p}_R}\right)^2\right]^n \quad \text{(C.15)}$$

where the exponent n is an empirical constant which accounts for the high-velocity effect (non-Darcy turbulent flow). Even if the reservoir pressure is above bubblepoint, the bottomhole flowing pressure might still be below ($p_{wf} < p_b$). If this is the case then one of the straigh-line equations given above can be used when the p_{wf} is above bubblepoint. If the p_{wf} is below bubblepoint, then

$$q_o = J(p_R - p_b) + \left(\frac{J}{2p_b}\right)\cdot(p_b^2 - p_{wf}^2) \quad \text{(C.16)}$$

which accounts for both the curvature area, and the straigh-line area of the IPR.

Appendix D

Beggs and Brill Method

The method that Beggs and Brill proposed in 1973 is a way to calculate the friction loss in Eq. 2.40 (mechanical energy balance). The method can be used for any pipe inclination, and it accounsts for the different flow regimes and the holdup behavior of the different phases. The friction factor is given as

$$\left(\frac{dp}{dz}\right)_F = \frac{2f_{tp}\rho_m u_m^2}{g_c D} \quad \text{(D.1)}$$

where f_{tp} is the two-pahse fricition factor, ρ_m is the mixture density, u_m is the mixture velocity, g_c is the standard gravity coefficient, D is the tubind diameter. The different mixture properties are given as

$$\rho_m = \rho_l\lambda_l + \rho_g\lambda_g \quad \text{(D.2)}$$

$$u_m = u_{sl} + u_{sg} = \frac{q_l + q_g}{A} \quad \text{(D.3)}$$

$$\mu_m = \mu_l\lambda_l + \mu_g\lambda_g \quad \text{(D.4)}$$

$$\lambda_l = \frac{q_l}{q_l + q_g} = 1 - \lambda_g \quad \text{(D.5)}$$

where λ_l and λ_g is the input fraction for the liquid and gas respectivly, u_{sl} and u_{sg} is the superficial velocity for the liquid and gas respectivly, μ_m is the mixture viscosity. The two-phase friction factor in **Eq. D.1** is an empirical parameter, and can be found as

$$f_{tp} = f_n e^S \quad \text{(D.6)}$$

where f_n is the non-slip friction factor, and the S is an empirical coefficient that accounts for the slipp effect. The non-slip friction factor can be found from moody's diagram using the actual pipe roughtness and the Reynolds number. the Reynolds number is given as

$$N_{RE_m} = \frac{\rho_m u_m D}{\mu_m} \quad \text{(D.7)}$$

The S-coefficient in **Eq. D.6** is given as

$$S = \begin{cases} \ln(2.2x - 1.2) & ; \text{if } 1 < x < 1.2 \\ \frac{\ln x}{-0.0523 + 3.182\ln x - 0.8725(\ln x)^2 + 0.01853(\ln x)^4} & ; \text{otherwise} \end{cases} \quad \text{(D.8)}$$

where the x-coefficient is dependent on the flow regime. This coefficient can be found as

$$x = \frac{\lambda_l}{y_l^2} \quad \text{(D.9)}$$

$$y_l = \frac{a\lambda_l^b}{N_{FR}^c} \cdot \psi \quad \text{(D.10)}$$

$$\psi = 1 + C\left[\sin(1.8\theta) - 0.333\sin^3(1.8\theta)\right] \quad \text{(D.11)}$$

$$C = (1-\lambda_l)\ln(d\lambda_l^e N_{vl}^f N_{FR}^h) \quad \text{(D.12)}$$

$$N_{FR} = \frac{u_m^2}{gD} \quad \text{(D.13)}$$

The constants a, b, c, d, e, f, and g are called the Beggs and Brill holdup constants, and can be found in **Table D.1**.

Flow Regime	**a**	**b**	**c**	
Segregated	0.980	0.4846	0.0868	
Intermittent	0.845	0.5351	0.0173	
Distributed	1.065	0.5824	0.0609	
	d	**e**	**f**	**h**
Segregated uphill	0.011	-3.7680	3.5390	-1.6140
Intermittent uphill	2.960	0.3950	-0.4473	0.0978
Distributed uphill	$C = 0$, $\psi = 1$ (no correction)			
All regimes downhill	4.700	-0.3692	0.1244	-0.5056

Table D.1: The empirical holdup constants given by Beggs and Brill.

Appendix E

Choke Models

A choke model tries to describe the relationship between the pressure drop across the choke, and the flow rate of the fluid passing through. The fluid that flows through a surface choke is rarely a single-phase liquid, because the pressures at the choke is typically below the bubblepoint. When considering a compressible fluid, the PVT properties and the expansion of the fluid will be major factors. The influence of these factors are especially difficult to describe when considering two-phase flow. In addition to this, if the fluid may also accelerate enough to reach sonic velocity through the choke throat, in which case the flow is considered critical. If the flow is critical, then the pressure drop across the choke is only dependent on the upstream pressure (and not the downstream pressure).

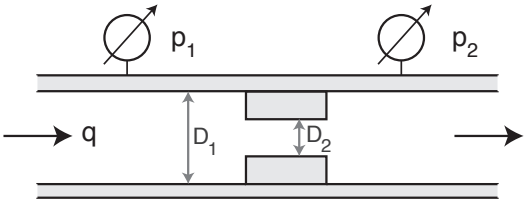

Figure E.1: Illustration of pressure drop across a choke.

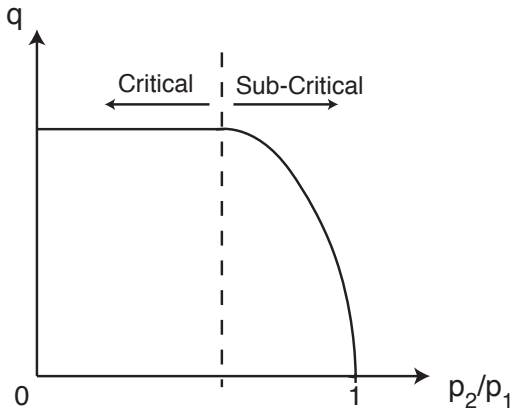

Figure E.2: Difference in critical and sub-critical flow.

To give an example of how a choke model might look like, lets consider a single-phase gas flow. By assuming an isotropic (and sub-critical) flow of an ideal gas, then the rate can be expressed with for example Szilas' (1975) equation

$$q_g = \frac{\pi}{4}\, D_2^2\, p_1 \frac{T_{sc}}{p_{sc}} \alpha \cdot \sqrt{\left(\frac{2 g_c R}{28.97 \gamma_g T_1}\right)\left(\frac{\gamma}{\gamma - 1}\right)\left[\left(\frac{p_2}{p_1}\right)^{2/\gamma} - \left(\frac{p_2}{p_1}\right)^{(\gamma+1)/\gamma}\right]} \quad \ldots \text{(E.1)}$$

where D_2 is the choke diameter, T_1 is the temperature upstream of the choke, p_1 and p_2 are the pressures upstream and downstream of the choke respectively, γ is the heat capacity ratio, α is the flow coefficient of the choke, γ_g is the gas gravity. If the flow was critical, then one should use the pressures and temperatures at the critical boundary (shown in **Fig. E.2**).

Extensive studies have also been conducted for two-phase flow, and the model are generally categorized on two groups; empirical and theoretical. The empirical models include Gilbert (1954), Ros (1960), Achong (1961), Pilehvari (1981), Ashford and Pierce (1975), Osman and Dokla (1990). The theoretical models are typically derived based on mass, momentum and energy balance. Some of these models was proposed by Sachdeva et al. (1986), Perkins (1993), Selmer-Olsen et al. (1995), and the Hydro model from Schüller et. al (2006).

Appendix F

Component Properties for the Topside Process

The reservoir simulator (Nexus) uses two different EOS models, one for modeling the reservoir (high pressure and temperature) and one for modeling the topside process. The only difference in these two models is a slight change in the volume-shift factors defined for the heavy components. Both models uses the Peng-Robinson method, with nine components, and the same binary interaction parameters. The component properties for the EOS when modeling the reservoir, was shown in Table 2.2. The component properties for the EOS when modeling the topside process is given below.

	Molecular Weight	Critical Constants			Acentric Factor	Volume Shift
Components	M (kg/kmol)	T_C (F)	P_C (psia)	Z_C	ω	s
C_1-N_2	16.19	-118.3	664.643	0.28626	0.0112	-0.1502
CO_2	44.01	87.746	1069.51	0.27433	0.2250	0.00191
C_2	30.07	89.906	706.624	0.27924	0.0990	-0.0628
C_3C_4	49.29	241.01	586.276	0.27619	0.1688	-0.0605
C_5C_6	77.57	415.76	483.865	0.27751	0.2457	-0.0302
C_7C_{10}	117.5	578.33	390.121	0.27324	0.3430	0.02715
$C_{11}C_{15}$	178.6	754.51	289.302	0.26121	0.5047	0.09623
$C_{16}C_{30}$	296.0	952.29	205.961	0.25845	0.7440	0.11786
C_{31+}	567.3	1218.4	133.773	0.28622	1.2031	0.12296

Table F.1: Component properties for the Skarv Field EOS (when modeling topside process).

Appendix G

Daily Rates Using Current Allocation Method

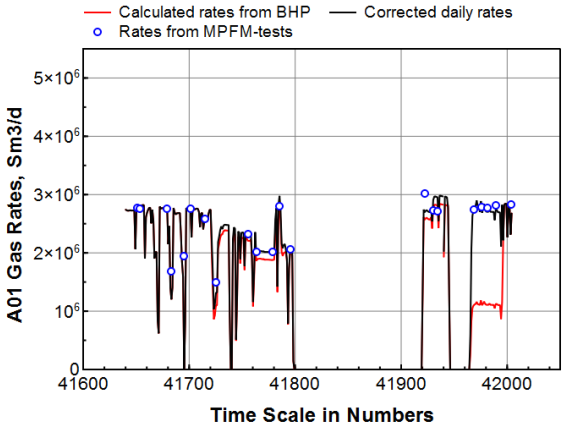

(a) Daily gas-rates for A01 (Snadd field).

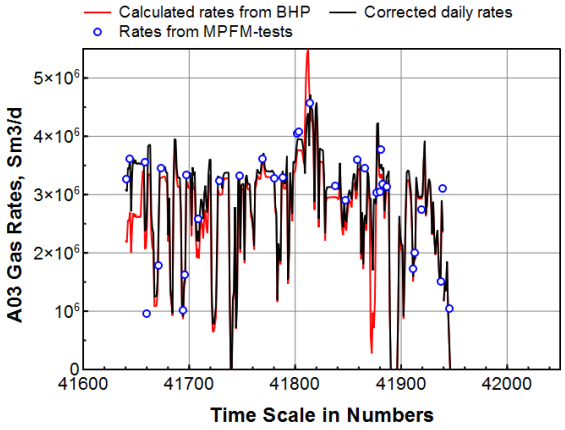

(b) Daily gas-rates for A03 (Skarv A field).

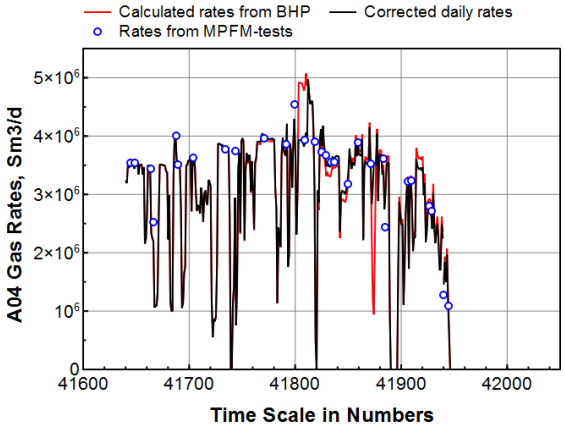

(c) Daily gas-rates for A04 (Skarv A field).

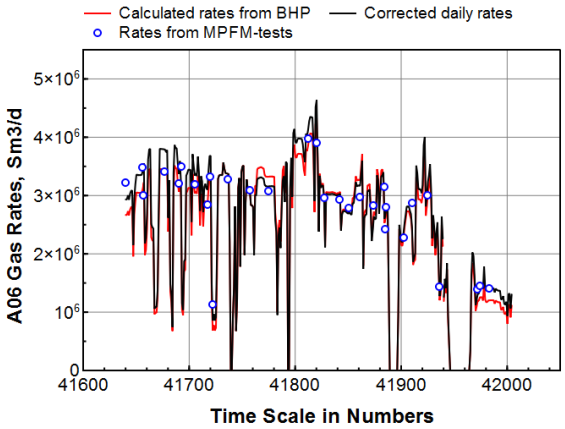

(d) Daily gas-rates for A06 (Skarv A field).

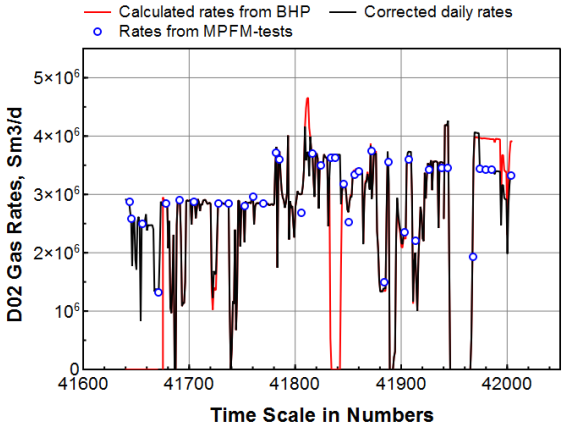

(e) Daily gas-rates for D02 (Idun field).

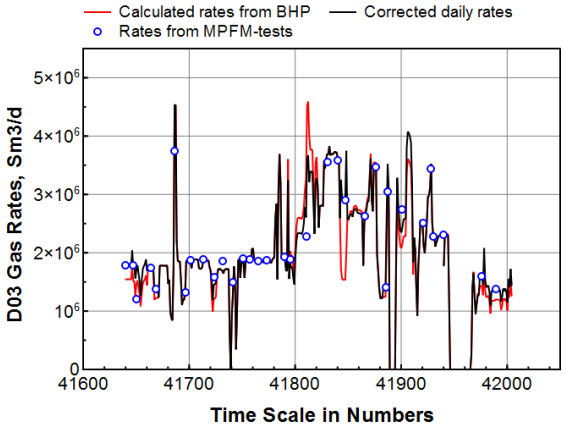

(f) Daily gas-rates for D03 (Idun field).

Figure G.1: Show the measured and calculated gas-rates for the gas-producers, when using current allocation.

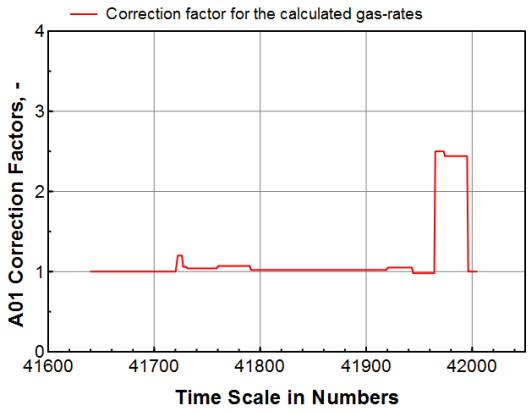

(a) Correction factors for A01 (Snadd field).

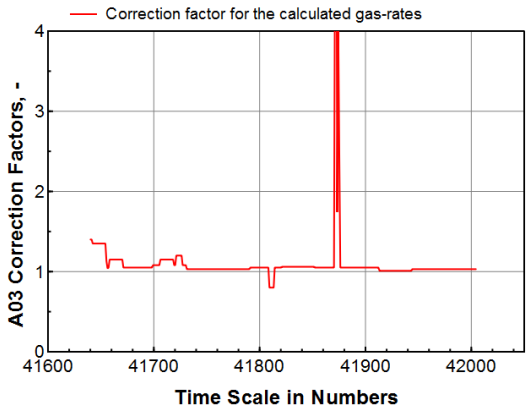

(b) Correction factors for A03 (Skarv A field).

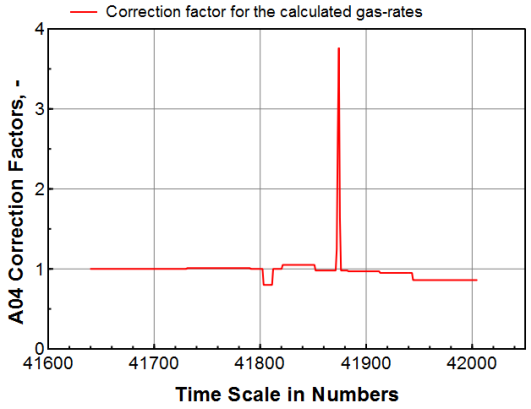

(c) Correction factors for A04 (Skarv A field).

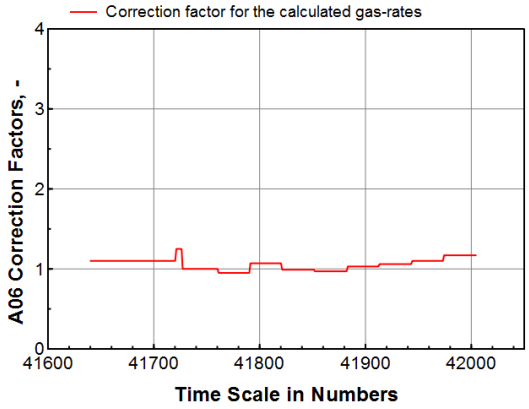

(d) Correction factors for A06 (Skarv A field).

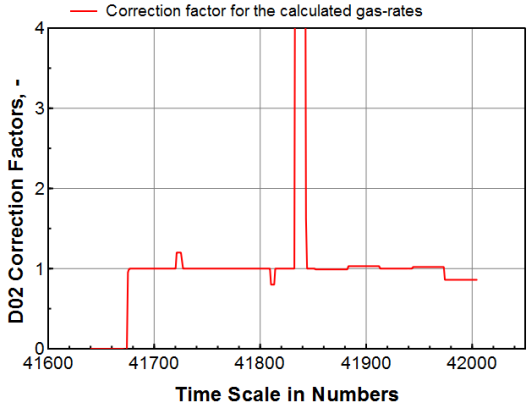

(e) Correction factors for D02 (Idun field).

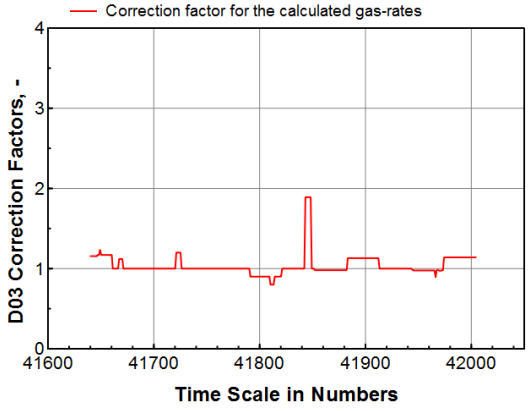

(f) Correction factors for D03 (Idun field).

Figure G.2: Show the correction factors used to adjust the theoretical gas-rates from gas-producers.

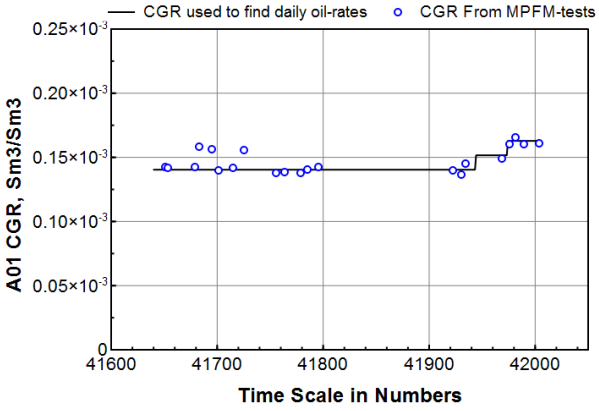

(a) Producing CGR used to find oil-rate from A01.

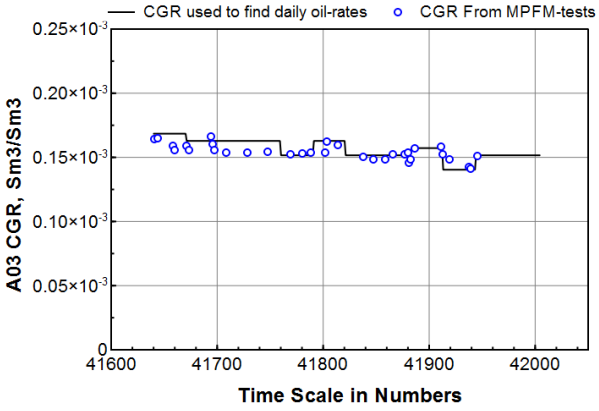

(b) Producing CGR used to find oil-rate from A03.

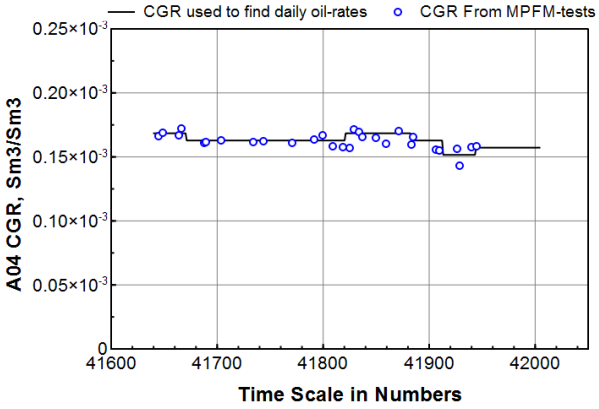

(c) Producing CGR used to find oil-rate from A04.

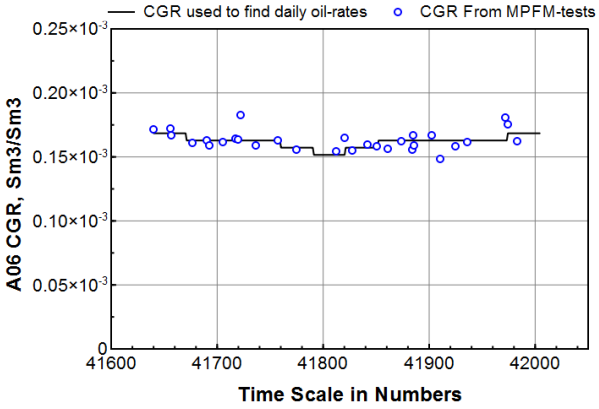

(d) Producing CGR used to find oil-rate from A06.

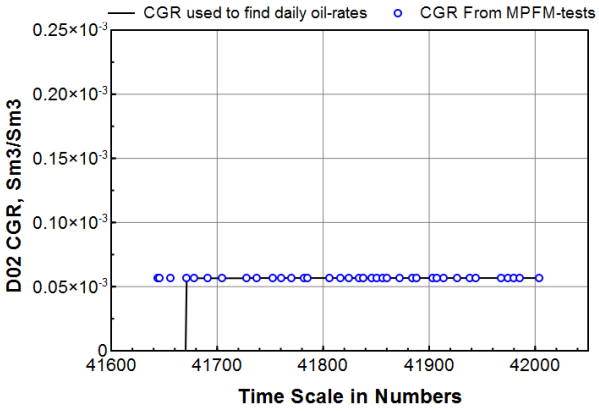

(e) Producing CGR used to find oil-rate from D02.

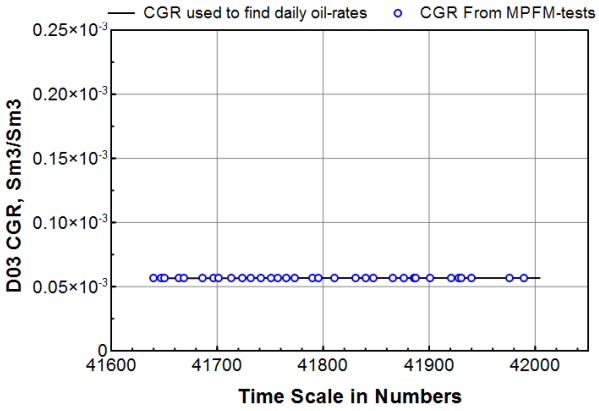

(f) Producing CGR used to find oil-rate from D03.

Figure G.3: Producing condensate gas ratio used in the current allocation process, in order to find the oil-rates from gas producers.

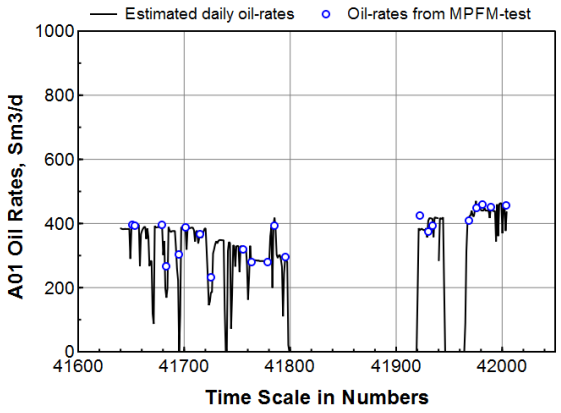

(a) Measured and calculated oil-rates for A01.

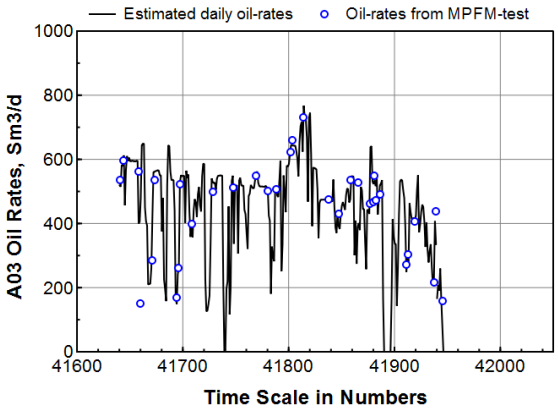

(b) Measured and calculated oil-rates for A03.

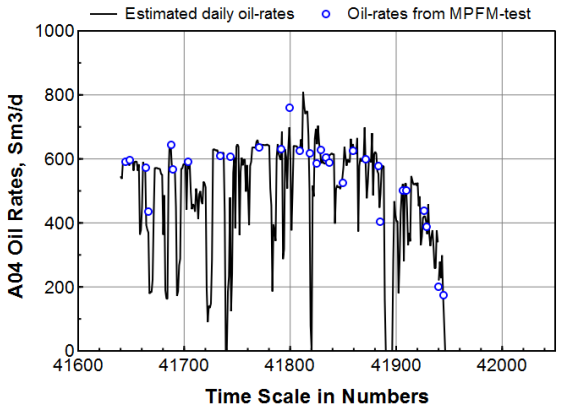

(c) Measured and calculated oil-rates for A04.

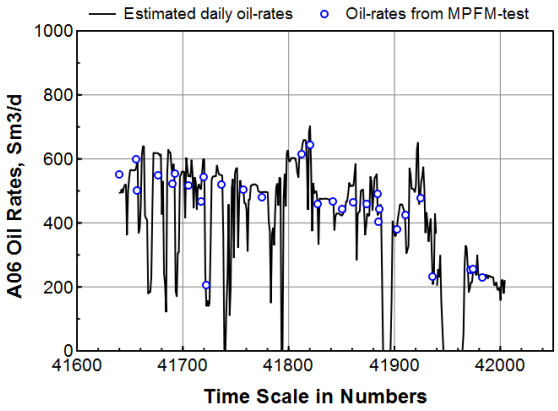

(d) Measured and calculated oil-rates for A06.

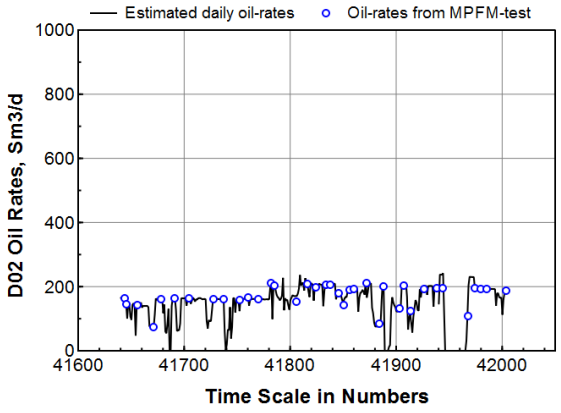

(e) Measured and calculated oil-rates for D02.

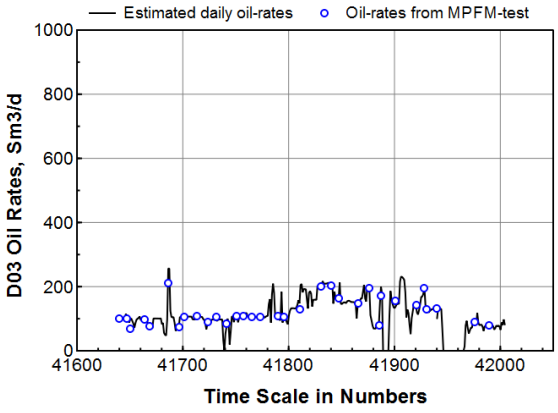

(f) Measured and calculated oil-rates for D03.

Figure G.4: Calculated daily oil-rates from gas-producers, by using the corrected theoretical gas-rates together with the appropriate producing CGR.

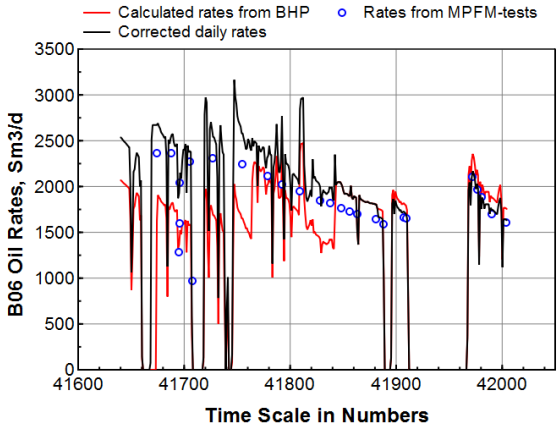

(a) Daily oil-rates for B06 (Skarv B field).

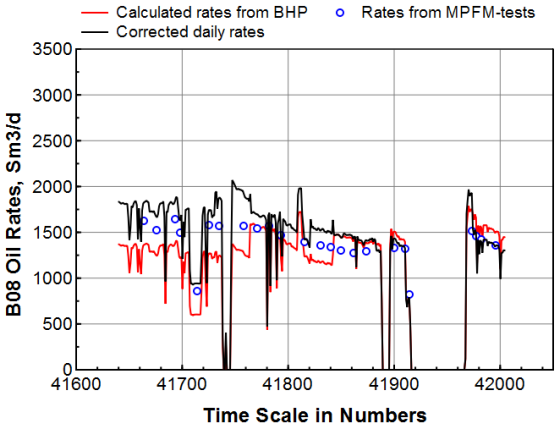

(b) Daily oil-rates for B08 (Skarv B field).

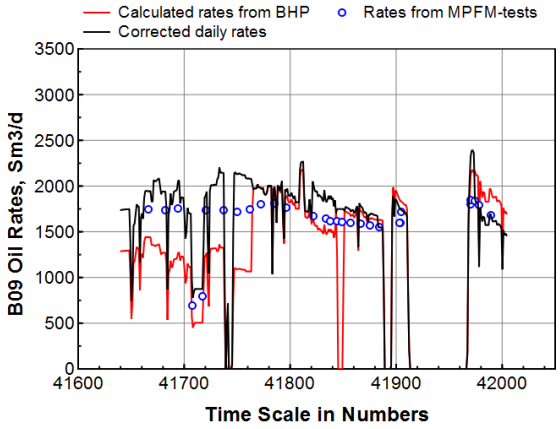

(c) Daily oil-rates for B09 (Skarv C field).

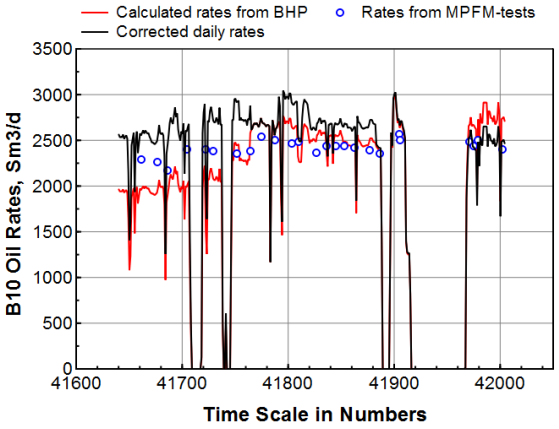

(d) Daily oil-rates for B10 (Skarv C field).

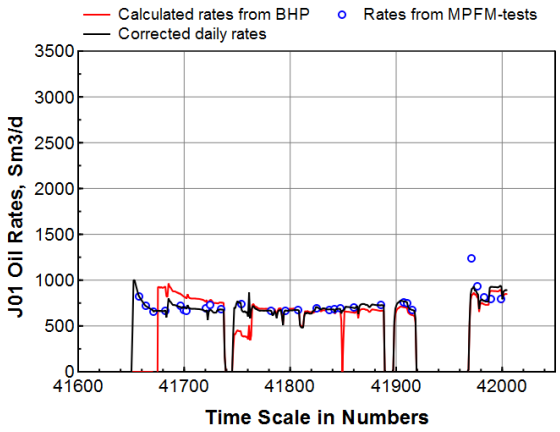

(e) Daily oil-rates for J01 (Tilje field).

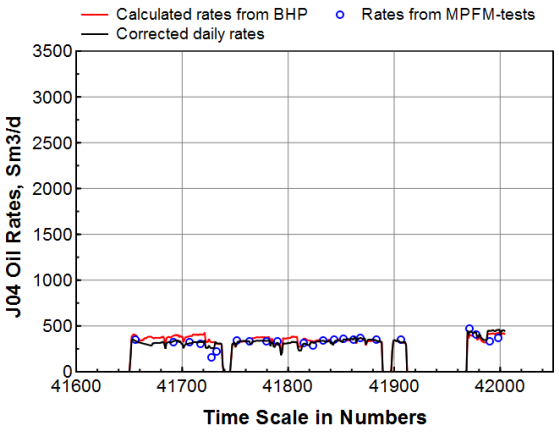

(f) Daily oil-rates for J04 (Tilje field).

Figure G.5: Show the measured and calculated oil-rates for the oil-producers, when using current allocation method. The red lines represent the theoretical oil-rates calculated for the oil-wells by using the pressure-measurements. Black line represent the adjusted theoretical rates when applying the correction factors to the theoretical rates. Blue circles are the oil-rates from the individual MPFM-tests.

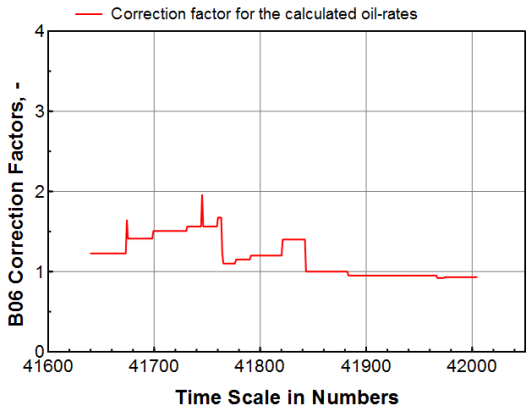

(a) Correction Factors for B06 (Skarv B field).

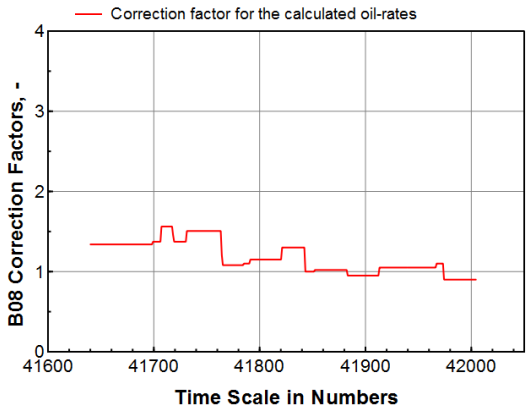

(b) Correction Factorsfor B08 (Skarv B field).

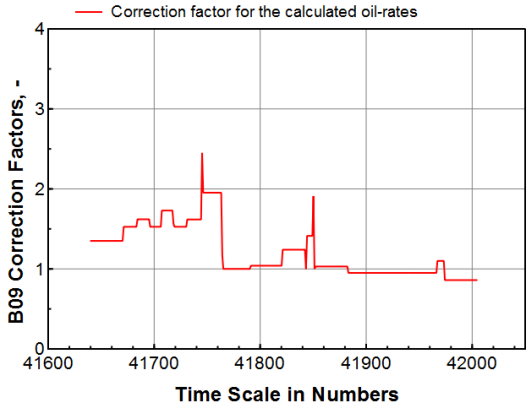

(c) Correction Factors for B09 (Skarv C field).

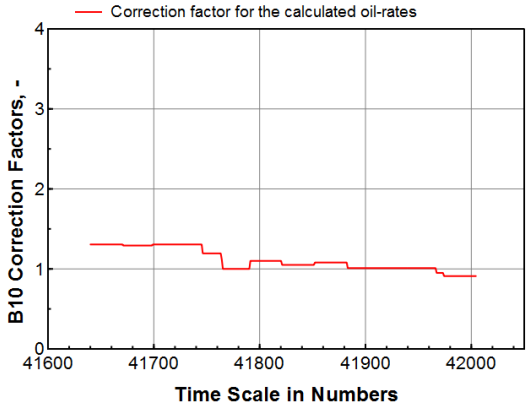

(d) Correction Factors for B10 (Skarv C field).

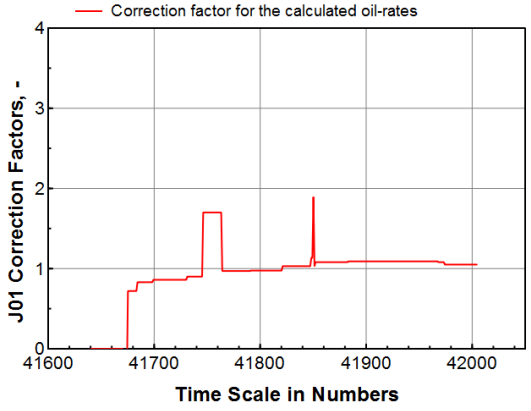

(e) Correction Factors for J01 (Tilje field).

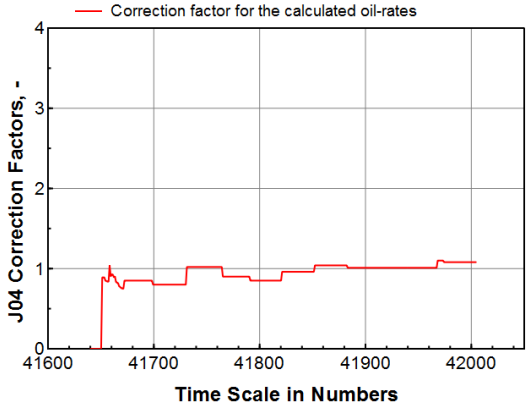

(f) Correction Factors for J04 (Tilje field).

Figure G.6: Show the correction factors used to adjust the theoretical oil-rates from oil-producers.

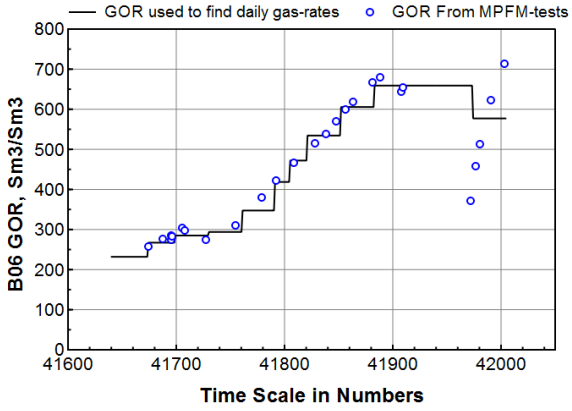

(a) Producing *GOR* used to find gas-rate from B06.

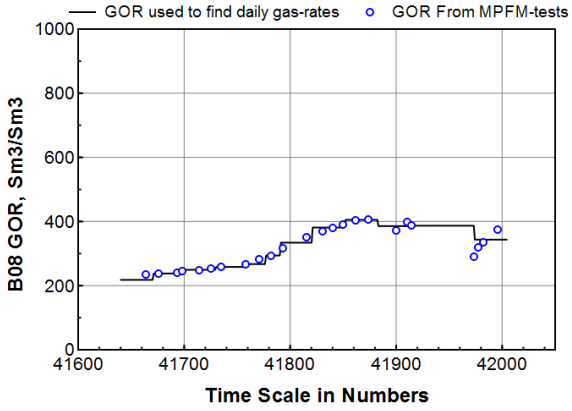

(b) Producing *GOR* used to find gas-rate from B08.

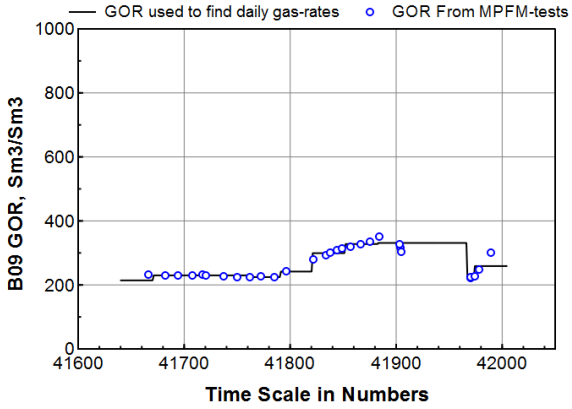

(c) Producing *GOR* used to find gas-rate from B09.

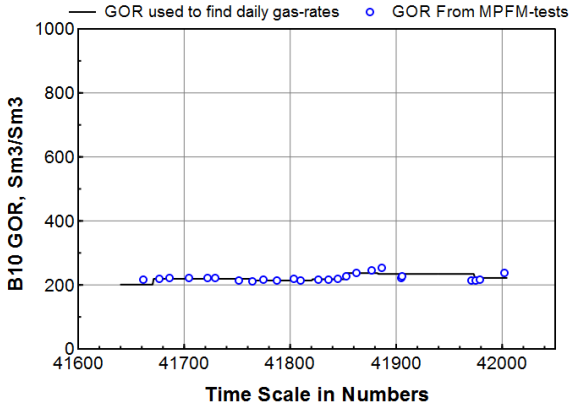

(d) Producing *GOR* used to find gas-rate from B10.

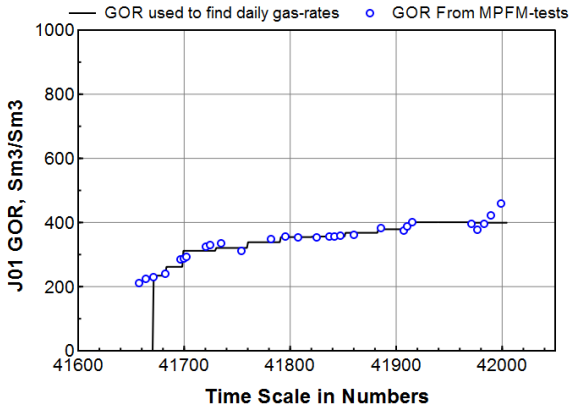

(e) Producing *GOR* used to find gas-rate from J01.

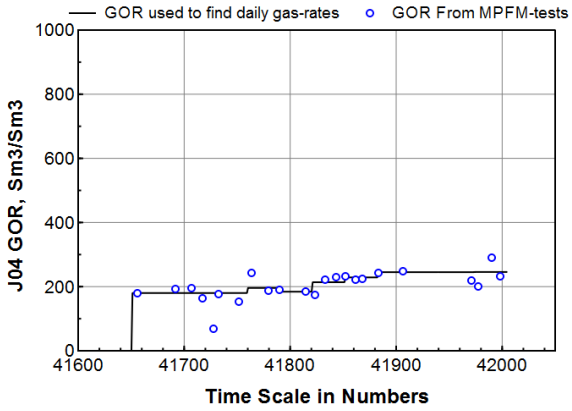

(f) Producing *GOR* used to find gas-rate from J04.

Figure G.7: Producing *GOR* used in the current allocation process, in order to find the gas-rates from oil-producers.

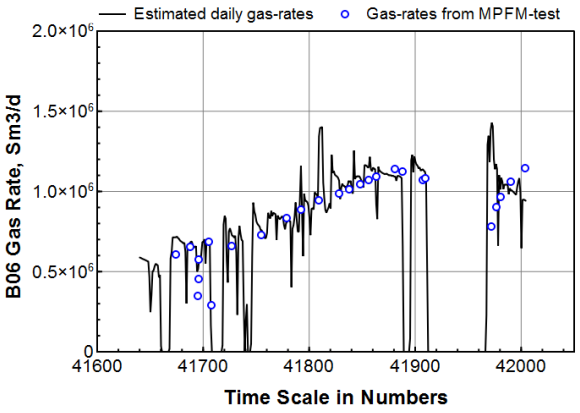

(a) Measured and calculated gas-rates from B06.

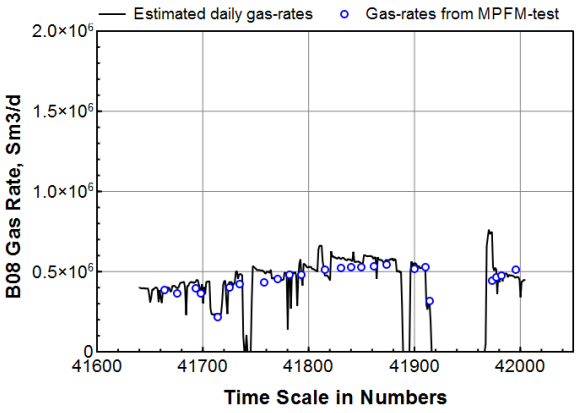

(b) Measured and calculated gas-rates from B08.

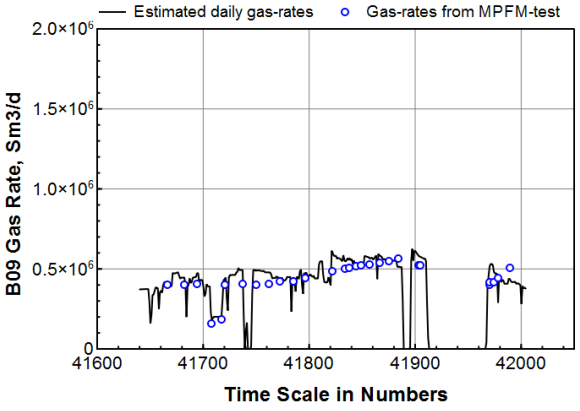

(c) Measured and calculated gas-rates from B09.

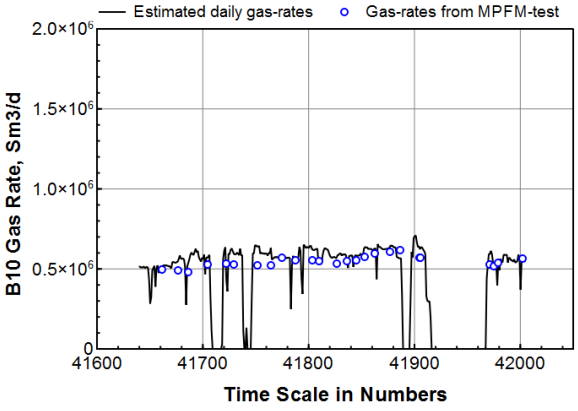

(d) Measured and calculated gas-rates from B10.

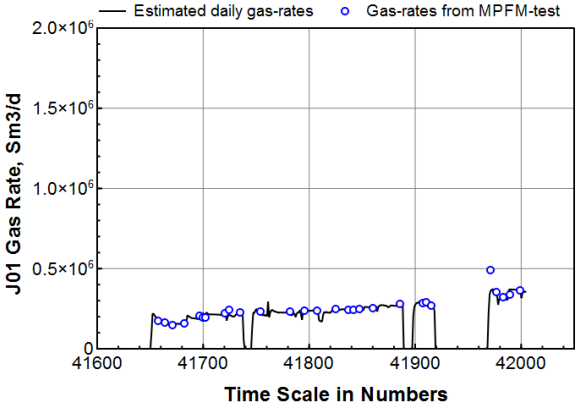

(e) Measured and calculated gas-rates from J01.

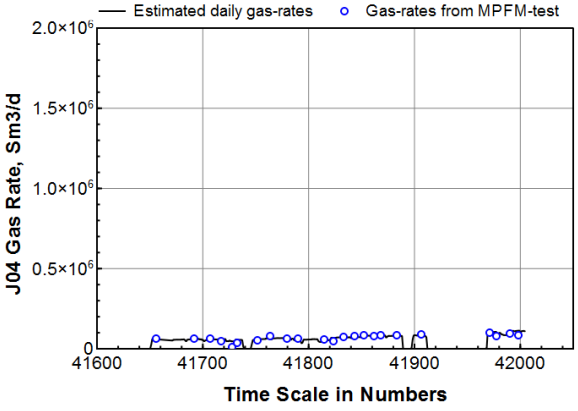

(f) Measured and calculated gas-rates from J04.

Figure G.8: Calculated daily gas-rates from oil-producers, by using the corrected theoretical oil-rates together with the appropriate producing GOR.

Appendix H

Comparison between BO-values generated from PVTp and those generated in Pipe-It

The black-oil tables used in the current allocation are generated from the PVTp software, and they are based on a 24 component EOS model. This 24 component EOS will predict the surface rates differently from the lumped nine component EOS. Consequently, the BO-values generated in Pipe-It (which are based on the nine component EOS) will also be different from the BO-tables generated from the PVTp software.

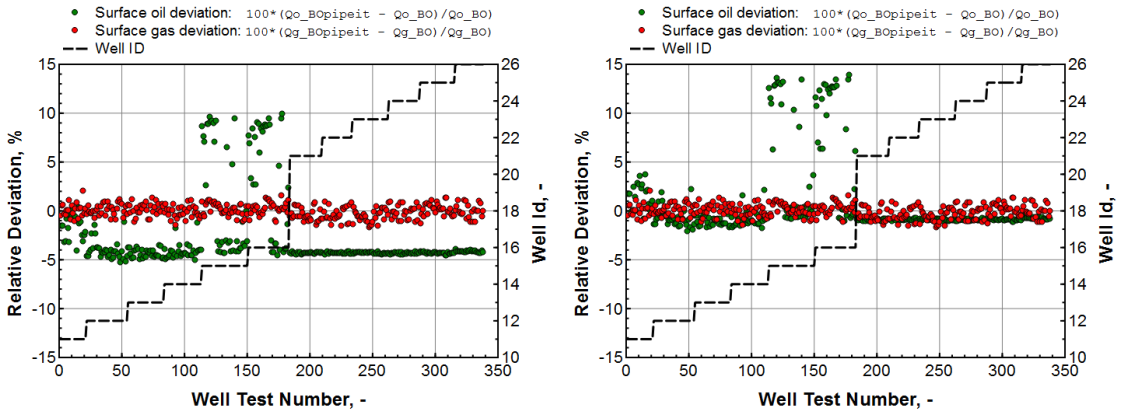

(a) BO-properties in Pipe-It are based on Table F.1 (9 component EOS for topside processing).

(b) BO-properties in Pipe-It are based on Table 2.2 (9 component EOS for reservoir modeling).

Figure H.1: Comparison between the surface rates based on the black-oil tables generated by BP, and the surface rates based on BO-values generated in Pipe-It.

Fig. H.1 shows a comparison between the surface rates based on the black-oil tables generated by BP ($Q^{PVTp\ BO}$), and the surface rates based on BO-values generated in Pipe-It ($Q^{PipeIt\ BO}$). The relative deviations in these figures are calculated as

$$RD_o = 100\% \cdot \frac{\left(Q_o^{PipeIt\ BO} - Q_o^{PVTp\ BO}\right)}{Q_o^{PVTp\ BO}} \quad \text{(H.1)}$$

$$RD_g = 100\% \cdot \frac{\left(Q_g^{PipeIt\ BO} - Q_g^{PVTp\ BO}\right)}{Q_g^{PVTp\ BO}} \quad \text{(H.2)}$$

Fig. H.0a is based on the nine component EOS used for topside processing (see Table F.1). It can be seen from this figure that there are some deviations in the calculated rates, and the surface oil rates from Pipe-It ($Q_o^{PipeIt\ BO}$) have been shifted ∼5% downwards. **Fig. H.0b** is based on the nine component EOS used for reservoir modeling (see Table F.1) at high pressure

and temperature. It actually appears that the 24 EOS model used in the PVTp is more similar to the nine component EOS used for reservoir modeling (then the one used for the topside processing).

Also notice the offbeat surface oil-rates for D02 and D03 (well ids 15 and 16). These data point are a result of a mistake/oversight in the BO-tables used for the current allocation method. In these tables the PVTp software have only calculated the CGR for a certain range of pressures and temperatures, and when the MPFM operates outside of these conditions, then the CGR will be assumed to be zero. The estimated surface rates $Q_o^{PipeIt\ BO}$ form Pipe-It will therefore be much higher (shift upwards), because the surface rates $Q_o^{PVTp\ BO}$ from PVTp do not include the CGR.

Appendix I

Automatic Procedure for Generating Lookup Tables Using AWK Script

Pipe-It has its own lookup system that uses a *conversion file* to connect two different tables together. This conversion file will tell Pipe-It how the data from the lookup table should be assigned to the other table. **Fig. I.1** shows how the conversion file is used to connect two different tables together, and **Listing 1** gives an example of how the conversion file might look like.

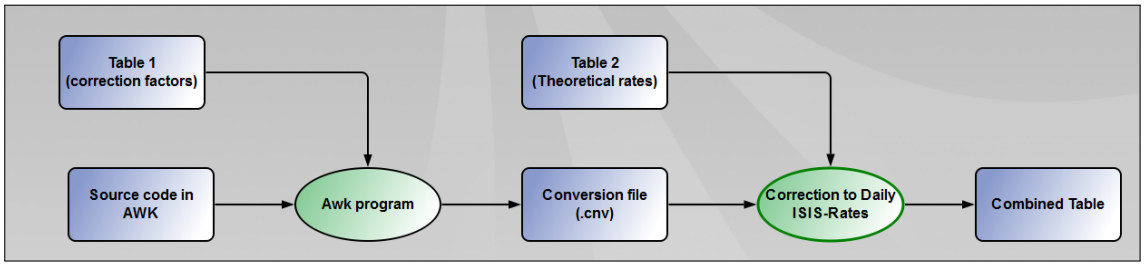

Figure I.1: How conversion file is used to connect two tables together.

Listing 1: Illustration of how a conversion file might look like.

```
RESTORE Daily_Theoretical_Rates
RESTORE Dummy
;-----------------------------
; Lookup Table
;-----------------------------
VARIABLE Well_id real
VARIABLE Start real

RESTORE Daily_Theoretical_Rates
CONVERT Dummy from Amount to Amount
SET Well_id 25 Start 41657.3
SPLIT Dummy Qo/ISIS_o 2.0585600 2.1475400 0.0045528 219.6460000
SET Well_id 25 Start 41682.2
SPLIT Dummy Qo/ISIS_o 2.0585600 2.1475400 0.0045528 219.6460000
SET Well_id 25 Start 41682.3
SPLIT Dummy Qo/ISIS_o 0.6811560 0.7173330 0.0039719 251.7660000
SET Well_id 25 Start 41696.2
```

```
SPLIT Dummy Qo/ISIS_o 0.6811560 0.7173330 0.0039719 251.7660000
SET Well_id 25 Start 41696.3
SPLIT Dummy Qo/ISIS_o 0.7901980 0.8461370 0.0032874 304.1870000
...
SET Well_id 24 Start 42002
SPLIT Dummy Qo/ISIS_o 0.8402230 0.8865750 0.0040111 249.3090000
END
```

The SET command Listing 1 is used to identify the control variables, and the SPLIT command is used to assign the data (from lookup table, or table 1 in Fig. I.1) when these control variables are found in table 2 (daily theoretical rates). If the control variables are not found, then the default in Pipe-It is to use linear interpolation between the two closest values. However, it is also possible to make Pipe-It interpolate by assuming a constant value from the latest MPFM test (which is the method used in the alternative allocation method).

Listings 2 and 3 show two different AWK codes used to automatically generate the conversion files that are needed. Listings 2 is a code that can be used together with the lookup table for correction factors and surface ratios. This code will generate a conversion file that uses linear interpolation. Listings 3 is a code that can be used together with the lookup table for the normalized compositions. That code will generate a conversion file will interpolate by assuming a constant value from the latest MPFM.

Listing 2: AWK code used to generate conversion file for correction factors and surface ratios.

```
BEGIN {
  FS="\t"
  print "RESTORE ISIS_Rates"
  print "RESTORE Dummy"
  print ";------------------------------"
  print "; Lookup Table"
  print ";------------------------------"
  print "VARIABLE Well_id real"
  print "VARIABLE Start real"
  print "RESTORE ISIS_Rates"
  print "CONVERT Dummy from Amount to Amount"
  status = 0
}

status == 0 && $0 == "DATA" {
  getline
```

```
    getline
    for (i=1; i<=NF; i++) header_index[$i]=i
    status = 1
    next
}

status == 1 {
    if($header_index["Amount Qo/ISIS_o"] != 0 || $header_index["Amount Qg/
        ISIS_g"] != 0 ){
    print "SET Well_id " $header_index["Well_id"] " Start " $header_index["
        Start"]
    printf ("SPLIT ISIS Qo/ISIS_o %5.7f %5.7f %5.7f %5.7f \n", $header_index["
        Amount Qo/ISIS_o"], $header_index["Amount Qg/ISIS_g"], $header_index["
        Amount OGR_pi"], $header_index["Amount GOR_pi"] )
}}

END {
    print "END"
}
```

Listing 3: AWK code used to generate the conversion file for the normalized compositions.

```
BEGIN {
    FS="\t"
    print "RESTORE EOS9_Res"
    print "RESTORE Dummy"
    print ";-------------------------------"
    print "; Lookup Table"
    print ";-------------------------------"
    print "VARIABLE Well_id integer"
    print "VARIABLE Start real"
    print "RESTORE EOS9_Res"
    print "CONVERT Dummy from Amount to Moles"
    status = 0
}

status == 0 && $0 == "DATA" {
    getline
    getline
    for (i=1; i<=NF; i++) header_index[$i]=i
```

```
19    status = 1
      next
21  }

23  status == 1 || status == 2{
      if(status == 2 && tmpA == $header_index["Well_id"]){
25      print "SET Well_id " tmpA " Start " $header_index["Start"] - 0.1
        printf ("SPLIT Dummy CO2 %5.7f %5.7f %5.7f %5.7f %5.7f %5.7f %5.7f %5.7f
            %5.7f \n", tmpB, tmpC, tmpD, tmpE, tmpF, tmpG, tmpH, tmpI, tmpJ )
27    }
      tmpA = $header_index["Well_id"]
29    tmpB = $header_index["Moles CO2"]
      tmpC = $header_index["Moles C1N2"]
31    tmpD = $header_index["Moles C2"]
      tmpE = $header_index["Moles C3C4"]
33    tmpF = $header_index["Moles C5C6"]
      tmpG = $header_index["Moles C7C10"]
35    tmpH = $header_index["Moles C11C15"]
      tmpI = $header_index["Moles C16C30"]
37    tmpJ = $header_index["Moles C31P"]
      print "SET Well_id " $header_index["Well_id"] " Start " $header_index["
          Start"]
39    printf ("SPLIT Dummy CO2 %5.7f %5.7f %5.7f %5.7f %5.7f %5.7f %5.7f %5.7f
          %5.7f \n", $header_index["Moles CO2"], $header_index["Moles C1N2"],
          $header_index["Moles C2"], $header_index["Moles C3C4"], $header_index["
          Moles C5C6"], $header_index["Moles C7C10"], $header_index["Moles C11C15
          "], $header_index["Moles C16C30"], $header_index["Moles C31P"] )
      status = 2
41  }

43  END {
      print "END"
45  }
```